ASSESSMENT OF SENESCENCE ON ORAL MUCOSAL MODEL TREATED WITH BISPHOSPHONATE

NUR BASHIRA BINTI SHAHARUDDIN

FACULTY OF DENTISTRY
UNIVERSITY OF MALAYA
KUALA LUMPUR

2017

ASSESSMENT OF SENESCENCE ON ORAL MUCOSAL TREATED WITH BISPHOSPHONATE

NUR BASHIRA BINTI SHAHARUDDIN

DISSERTATION SUBMITTED IN FULFILMENT OF THE REQUIREMENTS FOR THE DEGREE OF MASTER IN DENTAL SCIENCE

FACULTY OF DENTISTRY
UNIVERSITY OF MALAYA
KUALA LUMPUR

2017

UNIVERSITY OF MALAYA

ORIGINAL LITERARY WORK DECLARATION

Name of Candidate: Nur Bashira binti Shaharuddin

Matric No: DGC 120016

Name of Degree: Master of Dental Science

Title of Thesis : Assessment of Senescence on Oral Mucosal Model Treated with Bisphosphonate

Field of Study: Tissue Engineering

I do solemnly and sincerely declare that:

(1) I am the sole author/writer of this Work;
(2) This Work is original;
(3) Any use of any work in which copyright exists was done by way of fair dealing and for permitted purposes and any excerpt or extract from, or reference to or reproduction of any copyright work has been disclosed expressly and sufficiently and the title of the Work and its authorship have been acknowledged in this Work;
(4) I do not have any actual knowledge nor do I ought reasonably to know that the making of this work constitutes an infringement of any copyright work;
(5) I hereby assign all and every rights in the copyright to this Work to the University of Malaya ("UM"), who henceforth shall be owner of the copyright in this Work and that any reproduction or use in any form or by any means whatsoever is prohibited without the written consent of UM having been first had and obtained;
(6) I am fully aware that if in the course of making this Work I have infringed any copyright whether intentionally or otherwise, I may be subject to legal action or any other action as may be determined by UM.

Candidate's Signature   Date:

Subscribed and solemnly declared before,

Witness's Signature   Date:

Name:

Designation:

ABSTRACT

Osteonecrosis of the jaw (ONJ) has been associated with bisphosphonate (BP) treatment of Paget's disease of bone, bone metastases, as well as postmenopausal and steroid-induced osteoporosis. The inhibition of bone resorption has been effectively employed in bone-disease treatment, but bisphosphonate-specific toxicity on oral mucosa causes impaired soft tissue healing followed by the onset of inflammation. The modern generation of BPs that contain a nitrogen group (N-BPs) have been intravenously administered to improve the management and prevention of complications associated with bone cancer metastasis, but they are potent and accumulate in the bone. This study presents results of the construction of a three-dimensional model comprised of an air-liquid interface co-culture of normal immortalized oral keratinocytes (OKF 6/TERT 2) and normal human oral fibroblasts (NHOF). Co-culture of OKF 6/TERT 2 and NHOF in a tissue construct resulted in stratified epithelium and expression of differentiation-related protein such that the construct mimicked the histological appearance of normal oral mucosa. The goal of the project is to investigate the senescence effect of a commonly prescribed N-BP, zoledronic acid (ZOL), on the tissue model's histoarchitecture and inflammatory cytokine release. When each of the OKF 6/TERT 2 and NHOF monolayer cultures were exposed to zoledronic acid at increasing dosage, viability was reduced proportionally as measured by the MTT assay with NHOF more resistant to zoledronic acid. When exposed to ZOL at 12 µM, OKF 6/TERT 2, not NHOF underwent senescence based on a significant increase in expression of the ß-galactosidase enzyme. Our mucosal model further demonstrated that ZOL induced senescence and potentially impaired re-epithelialization of oral mucosa through overactivation of the senescence-associated inflammatory response that leads to SASP (senescence associated secretory phenotype). Analysis of histology further showed degradation of the basement membrane

accompanied by keratinocyte invasion towards the lamina propria and a significant release of senescence-associated inflammatory cytokines (MMP-3 and IL-8) upon treatment with zoledronic acid. This study therefore suggests that zoledronic acid may impair mucosal re-epithelialization by overactivation of the inflammation response due to senescence.

ABSTRAK

Osteonecrosis rahang (ONJ) yang telah dikaitkan dengan bisphosphonate (BP) rawatan penyakit Paget tulang, metastasis tulang, serta menopaus dan osteoporosis yang disebabkan steroid. Kaedah perencatan penyerapan semula kalsium pada tulang telah dibuktikan berkesan dalam rawatan penyakit berkaitan tulang, tetapi ketoksikan bisphosphonate khusus pada mukosa mulut menyebabkan terjejas penyembuhan tisu lembut diikuti oleh bermulanya keradangan. Jenis bisphosphonate yang baru mengandungi kumpulan nitrogen (N-BP) diberi kepada pesakit melalui intravensi terbukti dapat memperbaiki pengurusan dan pencegahan komplikasi yang dikaitkan dengan metastasis kanser tulang, tetapi jenis ini lebih stabil dan berkumpul di dalam tulang pada jangka yang lama. Kajian ini membentangkan pembentukan model tiga dimensi terdiri daripada sel 'keratinocyte' yang normal (OKF 6/TERT 2) dan normal fibroblas manusia (NHOF) dikulturkan semula membentuk tisu mukosa. Kultur OKF 6/TERT 2 dan NHOF berjaya membentuk epithelia berstrata dan menghasilkan protein bersamaan histologi mukosa mulut normal. Matlamat projek ini adalah untuk mengkaji kesan penuaan ('senescence') daripada pendedahan kepada asid zoledronic, pada histoarchitecture dan cytokine radang keluaran model tisu ini. Apabila OKF6 dan NHOF 'monolayer' didedahkan kepada asid zoledronic dalam penigkatan dos, sel mati secara berkadar seperti yang diukur oleh 'MTT assay' dimana NHOF lebih tahan berbanding OKF 6/TERT 2. Apabila terdedah kepada Zol pada 12 mikron, OKF 6/TERT 2, bukan NHOF menjalani penuaan berdasarkan peningkatan yang ketara dalam peningkatan ß-galactosidase enzim. Model mukosa kami menunjukkan bahawa ZOL menyebabkan 'senescence' (tua) dan mungkin menjejaskan pertumbuhan semula mukosa oral melalui overactivation tindak balas keradangan hal disebabkan peningkatan aktiviti 'senescence' yang membawa kepada SASP ('phenotype' yang dikenalpasti berkait dengan 'senescence'). Analisis histologi lanjut menunjukkan degradasi protein membran diiringi

oleh keratinosit pencerobohan ke arah lamina propria atas rawatan asid zoledronic, di samping dengan keluaran yang ketara hal menjadi tua cytokines berkaitan radang (MMP-3 dan IL-8). Oleh itu, kajian ini menunjukkan asid zoledronic mungkin menjejaskan pertumbuhan mukosa berlandaskan 'overactivation' tindak balas keradangan yang diransangkan oleh 'senescence'.

ACKNOWLEDGEMENTS

I would first like to thank my thesis supervisor Associate Professor Dr. Chai Wen Lin of The Department of Restorative Faculty of Dentistry at University Malaya, Malaysia. She consistently allowed this paper to be my own work, but steered me in right the direction whenever she thought I needed it. I would like to express equal gratitude to Prof. Dan Jones from the Department of Biology, Indiana Wesleyan University, United States as the second reader of this thesis, and I am gratefully indebted to him for his very valuable comments on this thesis. I am gratefully indebted to Prof. Dan Jones who consistently sprinkled positive encouragement from afar and shared his expertise on related subjects with an open hand. I would also like to take this opprtunity to thank Prof. Ian Paterson who always shared his professional opinion on any research and lab questions that I had, since the beginning of this project.

I would also like to thank research officers,medical lab technologists, and professional medical staff in the Department of Oral Surgery, Craniofacial & Molecular Biology Research Laboratory (CMBRL), Research Diagnostic Lab (RDL), Oral Pathology Diagnostic and Research Laboratory (OPDRL), and the Biomaterial Research Laboratory (BRL) at the University Malaya who consistently provide advice and guidelines on technical difficulties that I encountered during my study.

I would also like to thank the Ministry of Education (MOE) who provided a grant under High Impact Research (HIR) and a scholarship Graduate Research Assistant (GRAS) for two years. In addition, I would like to express gratitude to the administration staff in Department of Diagnostic & Intergrated Dental Practice, Restorative and Postgraduate Management Office at the Faculty of Dentistry who always offered help when needed.

I would also like to acknowledge my labmates and teammates from batch 2012/2013 of Faculty of Dentistry at University Malaya. Without their passionate input and encouragement, the study could not have been successfully conducted.

Finally, I must express my very profound gratitude to my family and to my spouse for providing me with unfailing support and continuous encouragement throughout my years of study and through the process of researching and writing this thesis. This accomplishment would not have been possible without them. Thank you.

TABLE OF CONTENTS

LIST OF FIGURES

LIST OF TABLES

LIST OF SYMBOLS AND ABBREVIATIONS

2D	:	2-dimensional
3D	:	3-dimensional
5 aza CDR	:	5-Aza-2′-deoxycytidine
ALI	:	Air liquid interface
ATP	:	Adenosine triphosphate
BP	:	Bisphosphonate
BrDU	:	Bromodeoxyuridine
BRONJ	:	Bisphosphonate-related osteonecrosis of jaw
CDK	:	Cyclin-dependent kinase
CXCL	:	CXC chemokine ligand
DAPI	:	4',6-diamidino-2-phenylindole
DDR	:	DNA damage response
DMEM	:	Dulbecco modified eagle medium
DNA	:	Deoxyribonucleic acid
DT	:	Doubling time
EBV	:	Epstein-barr virus
ECM	:	Extracellular matrix
EGF	:	Epidermal growth factor
ELISA	:	Enzyme linked immunosorbent assay
FAD media	:	Media containing 3:1 DMEM and Ham's F12 medium
FBS	:	Fetal bovine serum
FCS	:	Fetal calf serum
GGOH	:	Geranylgeraniol
GIO	:	Glucocorticoid-induced osteoporosis

H&E	:	Hematoxylin & eosin
HA	:	Hydroxyapatite
HGF	:	Human gingival fibroblast
IHC	:	Immunohistochemistry
IL	:	Interleukin
IV	:	Intravenous
KGF	:	Keratinocyte growth factor
LDH	:	Lactate dehydrogenase
MAPK	:	Mitogen-activated protein kinases
MMP	:	Matrix metalloproteinase
mRNA	:	Messenger ribonucleic acid
MTT	:	3-(4,5-Dimethylthiazol-2-yl)-2,5-diphenyltetrazolium bromide
NaOH	:	Sodium hydroxide
N-BP	:	Nitrogen containing bisphosphonate
NHOK	:	Normal human oral keratinocytes
NK	:	Natural killer
NN-BP	:	Non-nitrogen containing bisphosphonate
OIS	:	Oncogene-induced senescence
OMM	:	Oral mucosal model
ONJ	:	Osteonecrosis of jaw
OPG	:	Osteoprotegerin
PBS	:	Phosphate buffered saline
PCNA	:	Proliferating cell nuclear antigen
PI	:	Propidium iodide
PKC	:	Protein kinase C
PPi	:	Inorganic pyrophosphate

pRb	:	Retinoblasma protein
RANK	:	Receptor activator of nuclear factor kappa-B
RANKL	:	Receptor activator of nuclear factor kappa-B ligand
RB	:	Retinoblasma gene
RHOE	:	Reconstituted human oral epithelium
SAHF	:	Senescence associated heterochromatin foci
SASP	:	Senescence associated secretory phenotype
S-A-β gal	:	Senescence associated β galactosidase
SIPS	:	Stress induced premature senescence
SIR	:	Senescence inflammatory response
siRNA	:	Short interfering ribonucleic acid
TERT	:	Telomerase reverse transcription protein
TGF	:	Transforming growth factor
TIMP	:	Tissue inhibitor of metalloproteinases
TNF	:	Tumor necrosis factor
TNF	:	Tumor necrosis factor
TUNEL	:	Terminal deoxynucleotidyl transferase dUTP nick end labeling

LIST OF APPENDICES

CHAPTER 1: INTRODUCTION

Since the late 1970s, bisphosphonates (BP) have been widely prescribed to reduce bone pain in skeletal-related events (SRE) including osteoporosis, Paget disease, multiple myeloma and metastatic bone disease secondary to all cancer types (Drake, Clarke, & Khosla, 2008). Although the drug dosages are generally well tolerated, the increasing dependence on the more potent type of N-BP (nitrogen-containing bisphosphonate) in the oncogenic population has surfaced a critical adverse effect known as bisphosphonate-related osteonecrosis of the jaw (BRONJ) (Kennel & Drake, 2009; Marx, 2003; Marx, Sawatari, Fortin, & Broumand, 2005). It has been assumed that the primary lesion is occurring in the bone, but it is unclear why such a lesion is characterized by simultaneous nonhealing oral mucosa of up to 2 months (Reid, Bolland, & Grey, 2007). Over the past few years, *in vitro* studies have highlighted compromised cellular activity upon treatment with BP in both cell components of the oral mucosa (oral keratinocytes and fibroblasts) including decreased proliferation (Landesberg et al., 2008; Pabst et al., 2012; Saracino et al., 2012; Scheper, Badros, Chaisuparat, Cullen, & Meiller, 2009), decreased migration (Pabst et al., 2012) and increased apoptosis (Landesberg et al., 2008; Saracino et al., 2012). These compromised cellular activities possibly contribute to the impaired healing of mucosal tissues in BRONJ patients. However, not until recently have scientists begun to emphasize an increased senescence activity in keratinocytes as a key mechanism that contributes to degeneration of the oral mucosa in BRONJ patients (R. H. Kim et al., 2011a).

The main question of why BRONJ only occurs in the jaw and no other part of the body (Marx, 2003; H. Ohnuki et al., 2012) has triggered increasing *in vitro* and *in vivo* studies that explore the potential of oral mucosa tissues to assist the onset of this lesion. To address the main question, a few *in vivo* studies have strongly highlighted the presence of

impaired healing in oral mucosa tissues when introduced to clinical dosages of zoledronic acid (Aguirre et al., 2012; Allam, Allen, Chu, Ghoneima, & Jack Windsor, 2011). However, the complex microenvironment in organisms hindered the downstream study of the molecular progression that might assist the degeneration of oral mucosa. In contrast, the monolayer model can provide a more controlled microenvironment for study of cell- specific responses. However, it does not represent the functional model of stratified epithelium as a protective barrier to the damaging oral microenvironment. Three-dimensional oral mucosa models serve as functional models of stratified tissues and provide a more controlled experimental microenvironment compared to animal models. In fact, a few interesting studies have demonstrated the impaired healing of oral mucosa in BRONJ using oral mucosa models with histological analysis (R. H. Kim et al., 2011b; Hisashi Ohnuki et al., 2012; Saito et al., 2014) and detection of protein markers specific to tissue injury (Saito et al., 2014). Underscoring these potentials of oral mucosa models as study systems, Saito *et al.* managed to highlight a few proteins that might contribute to impaired cell migration at the onset of BRONJ, including down regulation of integrin αVβ6 and TGF-β (Saito et al., 2014). Recently, Kim et al. (2011) proved that bisphosphonates caused a cell type-specific senescence effect, supported by cell cycle arrest and DNA damage response in different oral mucosa models (Hisashi Ohnuki et al., 2012). However, these oral mucosa models are represented by primary normal oral keratinocytes that have intrinsic features of senescence (Dimri et al., 1995; Jang et al., 2015; Kang, Guo, & Park, 1998). Therefore, to mold the tissue reconstructs to specifically assess senescence activity, normal immortalized cell lines seeded onto acellular dermis can be used as an improvised oral mucosa model without compromising the stratification function of oral mucosa tissues.

The development of oral mucosa models (OMM) has evolved progressively in both the fields of regenerative medicine and *in vitro* assay studies. In the field of *in vitro* assay studies, despite the challenges of fabricating OMM to 1) achieve an optimal mimic native tissue and 2) to endure the exhaustive experimental assays in the laboratory, it has advanced remarkably to be a reliable and informative study model system, bridging the gap between cell-based discovery research and animal models. However, one of the subjects that interconnects both challenges is the exhaustive culture of primary normal oral keratinocytes that have a limited life span as a laboratory sample (Bart Vande Vannet 2007; Dongari-Bagtzoglou & Kashleva, 2006b; Roesch-Ely et al., 2006; Rouabhia et al., 2012). Underlying these challenges, few studies have started to establish OMM reconstructed from immortalized cell lines that are able to retain functional stratification without displaying any cancer-associated changes (Bao, Akguel, & Bostanci, 2014; Dickson et al., 2000; Roesch-Ely et al., 2006). Only TERT cells (human telomerase reverse transcriptase), specifically OKF 6/TERT 2 has been functionally tested to represent a disease model for oral candidiasis (Dongari-Bagtzoglou & Kashleva, 2006c). This breakthrough displays the huge potential that genetic manipulation has on the advance of tissue engineered disease simulation models for *in vitro* assay of toxicity during drug delivery.

The current guidelines for the treatment of BRONJ, especially in oncogenic patients, rely on drug holiday (Diab & Watts, 2013), a surgical approach (Vescovi et al., 2012), and strict monitoring of any dental invasive procedures while the patient is under BP administration. This has proven successful, but not advisable for high risk patients (Whitaker, Guo, Kehoe, & Benson, 2012). Therefore, scientists have begun to search for an alternative that is able to reverse the degeneration of oral mucosa in BRONJ (Goffinet et al., 2006; Goldstein & Brown, 1990; Nogawa et al., 2005; Suyama et al., 2007; Zhong, Liang, Wang, Chang, & Lee, 2005). The underlying principle is to preserve the protective

barrier of mucosa in the jaw from the damaging oral microenvironment that might intensify the progression of the lesion. In 1990, Goldstein & Brown (Goldstein & Brown, 1990) discovered a biomolecular agent known as geranylgeraniol (GGOH) that has potential to reverse the adverse effects of bisphosphonates, specifically on degeneration of oral epithelium. This finding has shed some light on the capacity of biomolecular agents to manage long-term treatment of BRONJ. Subsequently, few studies have been able to reverse the degeneration effect on oral mucosa *in vitro* monolayer models (Cozin et al., 2011; Ziebart et al., 2011). Further studies need to be conducted to clarify the plausible mechanisms of GGOH rescue in organotypic models. Even though using normal cell lines has been justified to be representative and not prone to any genetic modification, therefore avoiding misleading findings in the end of the experiment, they are not technically suitable candidates to address senescence activity that has been claimed previously to be enhanced by treatment with bisphosphonates. The purpose of this thesis study is to assess the senescence activity in a novel oral mucosa model upon treatment with zoledronic acid, and in the future, be used for the downstream study of GGOH or another potential drug.

Defined by ultimate and irreversible loss of proliferative capacity in primary somatic cell culture by Hayflick et al. (1961) (Hayflick & Moorhead, 1961), senescence has been recognized as a potential therapeutic approach in cancer (Ewald, Desotelle, Wilding, & Jarrard, 2010; Nardella, Clohessy, Alimonti, & Pandolfi, 2011) and has been widely studied ever since. However, it is rather challenging to capture senescence in the *in vitro* environment due to the lack of a specific detection assay (Dimri et al., 1995) and intrinsic features of somatic cells which are prone to undergo senescence over time (Hayflick & Moorhead, 1961). Nevertheless, the most established concept regarding the onset of senescence is the theory of uncapping telomeres (Blackburn, 2000) that trigger the pathway of DNA damage response, cell cycle arrest, DNA repair, and inactivation of

telomerase in somatic cells (Wellinger, 2010). In more recent studies, however, senescence has been widely deciphered as a toxicity/stress indicator due to the increasing evidence of stress-induced premature senescence (SIPS) upon drug treatment that is telomere-independent such as p16INK4A dependent growth arrest in optimal culture conditions, over-expression of oncogenes, and radiation treatment (Althubiti et al., 2014; Stampfer & Yaswen, 2003). In 2010, Freund et al.(2010) discussed the role of senescence-associated secretory phenotype (SASP) on chronic inflammation in most aging-related diseases (Freund, Orjalo, Desprez, & Campisi, 2010). The role of SASP has been claimed to change the tissue microenvironment by disrupting cellular function in a cell-specific manner (Freund et al., 2010). This cellular function disruption includes release of inflammatory cytokines (Campisi, 2005) as well as cell proliferation and invasion targeting both immune and non-immune cells. Therefore, the phenotypic marker of senescence from senescence-associated inflammatory cytokine release, and histoarchitecture changes could be profiled in this stratified tissue oral mucosa model (OMM) to elucidate the senescence activity upon bisphosphonate treatment.

PURPOSE OF STUDY

The purpose of this study was to investigate the effect of zoledronic acid on the senescence of a 3D OMM. This project was divided into three objectives:

1. To develop a reproducible oral mucosa reconstruct using co-culture technique on an acellular dermis.

2. To determine the optimum dosage of zoledronic acid in monolayer and 3D OMM based on the viability and the senescence assay prior to 3D OMM treatment.

3. To confirm the senescence effect of zoledronic acid on the 3D OMM.

CHAPTER 2:LITERATURE REVIEW

2.1   Basic Bisphosphonate Pharmacology as a Potent Bone Resorption Inhibitor

Since the first treatments with bisphosphonates (BP) in 1969 (Bassett et al., 1969), they have been widely used to treat an array of bone disorders including heritable skeletal disorders in children, postmenopausal and glucocorticoid-induced osteoporosis (GIO), and bone metastases in patients with malignancies (Cremers, Pillai, & Papapoulos, 2005; Ibrahim et al., 2003; Kanis, 1995; Mundy, 1987; Rogers, Watts, & Russell, 1997). In this literature review chapter, first we review the current understanding of bone biology and remodelling. Second, we discuss the basic pharmacology and mechanism of BP as a bone resorption inhibitor and the significant role of BP in clinical practice over the decades. In a subsequent chapter, we will discuss current views on the adverse effect of BP in high risk patients, especially on soft tissue toxicity associated with BRONJ lesions.

2.1.1   Impaired Bone Remodelling Leads to Bone Loss Disorder

Bone is a dynamic tissue that is maintained by the tightly coupled functions of osteoclasts and osteoblasts in a process known as bone remodelling. This is complex process involves multiple cell types orchestrated in a temporary anatomical structure known as the basic multicellular unit (BMU) (Jilka, 2003). This process involves the tight coupling of old/damaged bone removal by the osteoclast (bone resorption) and subsequent replacement with new bone tissues by the osteoblast (bone formation) (Figure 2.1) ((Feng & McDonald, 2011). However, imbalanced activity between bone resorption and formation may occur, under certain pathological conditions such as imbalanced hormonal change, age-related factors, changes in physical activity, drugs and secondary diseases such as cancer (Feng & McDonald, 2011) which leads to development of various bone disorders. However, despite intense research to elucidate the molecular drive

towards impairment of bone remodelling (Phan, Xu, & Zheng, 2004), it is universally accepted that defects in the cells or obstruction of the intercellular communication between cells impairs bone homeostasis, which leads to loss of bone mass and increasing risk of bone fractures as observed in glucocorticoid-induced osteoporosis, transplant-associated osteoporosis, immobility-induced osteoporosis, Paget disease of bone, periodontitis, multiple myeloma and hypercalcemia of malignancies. Despite the intertwined nature of interaction between osteoblast and osteoclast in causing impaired bone remodelling, effective inhibition of bone resorption has always been recognized as a crucial therapeutic strategy for bone loss disorders (Feng & McDonald, 2011) (Figure 2.2).

Several new hallmarks from investigations of the molecular and cellular mechanisms underlying the pathogenesis of impaired bone remodelling have been elucidated, especially from study of osteoporosis since the 1980s. Studies of post-menopausal osteoporosis (hormonal imbalance leading to critical reduction in estrogen) have highlighted the role of estrogen as a skeletal protector by regulating activity of the osteoclast (Jilka, 1998; Pacifici, 1998) through modulating cytokines, including interleukins IL-1, IL-6, IL-7, tumor necrosis factor (TNF), and granulocyte/macrophage colony stimulating factor secreted by monocytes, stromal cells, and osteoblasts. Based on several *in vitro* and *in vivo* studies, the downstream effect of these cytokines is to indirectly promote osteoclastogenesis, a process of blood cells differentiating into osteoclasts, which explains the plausible mechanism of excessive osteoclast activity observed in bone loss disorder.

The other underlying hallmark that was established in the late 1990s is discovery of the TNF receptor superfamily (RANKL/RANK/OPG).OPG, known as osteoprotegrin plays overlapping roles in multiple types of cells, but exerts a crucial role in bone sparing

via a distinct mechanism (Feng & McDonald, 2011). A few *in vitro* studies have shown that the RANKL/RANK/OPG axis regulates several biological processes including osteoclast formation and function (Lacey et al., 1998; Yasuda et al., 1998). For example, in Paget disease, in which both turnover (resorption and formation) abnormally accelerates, resulting in a weak and misshapen skeleton, unusually increased expression of RANKL mRNA transcripts have been detected in osteoblastic cell lines (Menaa et al., 2000) followed by a lower amount of OPG, which functions in inhibiting osteoclastogenesis (Buckley & Fraser, 2002). These phenomena strengthened the potential theory that defects in RANKL-OPG might play a role in abnormal osteoclast activity observed in Paget disease. On another note, the skeleton is the most common site of metastatic disease, and 90% or more of patients with advanced cancer develop skeletal lesions. Many cancers are described as osteotropic, which either 1) metastasize to the skeleton or 2) grow primarily within bone marrow (multiple myeloma). These always lead to a condition known as hypercalcemia that has been associated with severe bone pain, skeletal destruction and pathologic fractures (Body, 2006).

Despite different mechanisms that stimulate the excessive activity of osteoclasts, there are now four major classes of anti-resorptive drugs (i.e., agents that can inhibit osteoclast formation and function) on the market: estrogen receptor modulators (Stefanick, 2005), recombinant parathyroid hormone (PTH), bisphosphonates, and calcitonin (Gruber et al., 1984). However, the most widely used are bisphosphonates (BP) which generally shorten osteoclast life span and became available as an inexpensive generic (Feng & McDonald, 2011) compared to other therapeutic approaches, including development of a monoclonal antibody to RANKL (Lewiecki, 2009; Miller, 2009). Despite the effectiveness of BP as an anti-bone resorptive, there are only a few fundamental features of BP that allow them to be effective clinical agents. In the following chapter, we will review the basic

understanding of the chemical structure of BP that is perpetually being improved over the

decades.
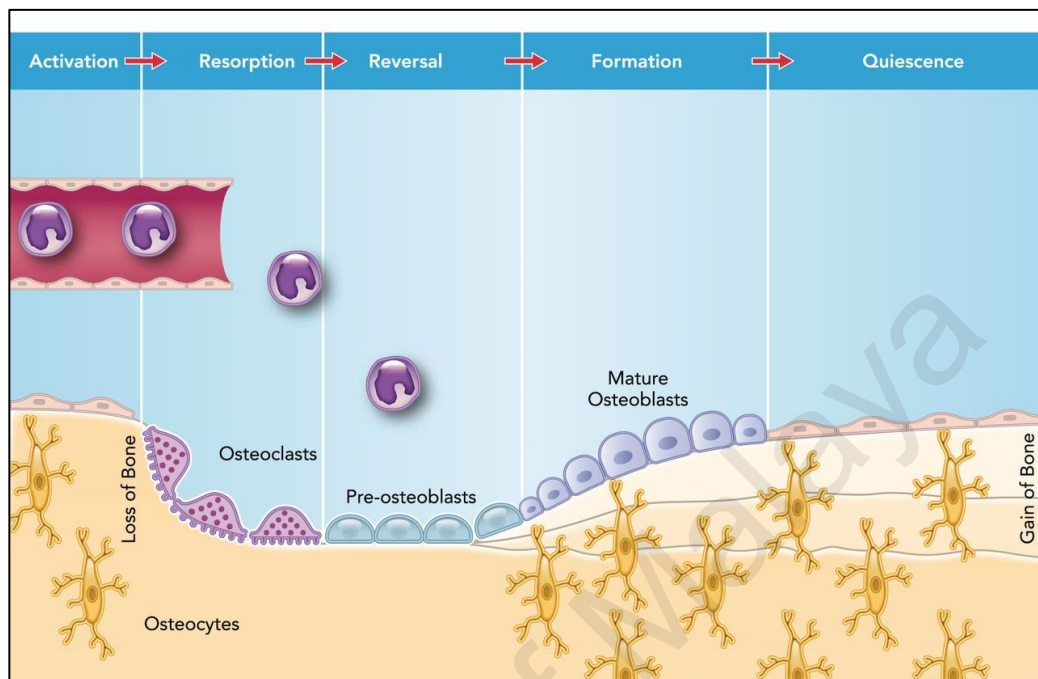
Figure 2.1: Remodeling is the replacement of old bone tissue by new bone tissue. This mainly occurs in the adult skeleton to maintain bone mass. This process involves the coupling of bone formation and bone resorption and consists of five phases. 1. Activation: Derived from the hematopoietic lineage, preosteoclasts are stimulated and differentiate under the influence of cytokines and growth factors into mature active osteoclasts 2. Resorption: osteoclasts digest mineral matrix (old bone) 3. Reversal: end of resorption 4. Formation: osteoblasts synthesize new bone matrix 5. Quiescence: osteoblasts become resting bone lining cells that become incorporated within the newly formed osteoid, which eventually becomes calcified bone.

(Siddiqui & Partridge, 2016)
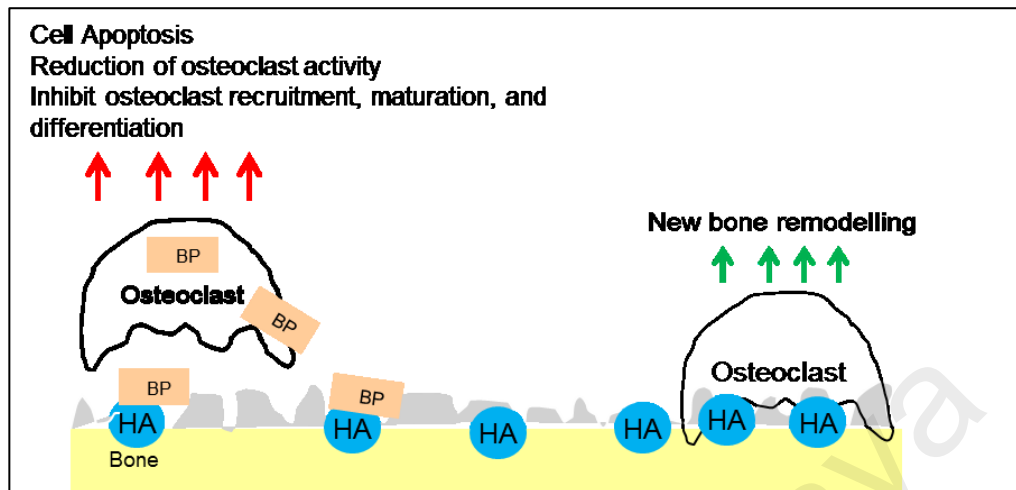
Figure 2.2: As they accumulate at sites of active bone remodelling (exposing increasing hydroxyapatite binding site), they can inhibit osteoclast activity and thereby inhibit breakdown of hydroxyapatite into calcium phosphate, calcium carbonate, calcium hydroxide and citrate. (Drake et al., 2008). Therefore, in this manner, bone mineral will be preserved and skeleton integrity will be maintained

2.1.2 Chemical Structures and Bisphosphonate Mechanism as Anti-Bone Resorptive

The profound effect of bisphosphonates (BP) on calcium metabolism was discovered in an early study of dental caries (Francis, Gray, & Griebstein, 1968) and has cultivated decades of research on drug development to manage bone loss disorders. This field of research development includes increasing the stability of BP in the bloodstream. To understand how BP helps to restore an impaired bone remodelling process, we will recapitulate the knowledge about bone mineral followed by how BP adsorbs to bone, not merely forming a protective barrier to bone but also modulates cellular function of multiple types of cells in the bone remodelling process. Equally important, in the 1990s the biochemical action of BP was established and helped further research on the advancement of BP in treating bone loss disorders and in time, in managing the complications of this treatment from a wider scope.

Matured bone is composed of organic matrix and mineral. The organic matrix is primarily composed of collagen type I that provides scaffolding before mineral is deposited. Bone mineral is composed of an insoluble salt of phosphorus and calcium known as hydroxyapatite (HA) that represents 65% of the total bone mass. Bisphosphonate has high binding affinity towards HA. Interestingly, the chemical structure of BP is analogous to a by-product generated from ATP hydrolysis in cells known to prevent calcification in soft tissues (Fleisch & Bisaz, 1962), inorganic pyrophosphate (PPi) (Figure 2.3) . BP are more chemically stable due to two phosphonate groups attached to a single carbon atom, forming a "P-C-P" structure (Russell, 2006). In the early stage of dental caries research, the high binding affinity of BP towards HA was physiochemically described as forming an ultra-thin, closely packed layer (1 to 5 nm), serving as a protective barrier to the enamel of teeth (Francis et al., 1968). On the surface, BP's basic function is to inhibit breakdown of HA during bone resorption into Ca^{2+}, H_3PO_4, H_2CO_3, water and other substances. This also means that BP's action depends on the availability of HA binding sites in the skeleton (Drake et al., 2008).

Over the years, numerous *in vitro* experiments have been conducted to elucidate the effect of BP on cellular function. During an accelerated bone remodelling phase (Drake et al., 2008), common in bone loss disorders, as BP accumulate at binding sites of the skeleton, they are not only forming a protective barrier, but also interfering with cellular morphology features of the osteoclast including disruption of the cytoskeleton. *In vitro* experiments have shown BP to be capable of inhibiting bone resorption in a variety of ways, including the inhibition of osteoclast recruitment, maturation, differentiation, resorptive activity and they may also induce apoptosis. In contrast to direct inhibition on resorption via the osteoclast, some experimental studies suggest that BP may also protect osteocytes and osteoblasts from apoptosis induced by glucocorticoids. Their specific mode of osteoclastic inhibition is unknown, but several mechanisms have been

highlighted by several investigations. These include inhibition of osteoclast development from monocytes (Hughes et al., 1995), increased osteoclast apoptosis (Hughes et al., 1995), stimulation of osteoclast inhibitory factor (Vitte, Fleisch, & Guenther, 1996), prevention of osteoclast development from bone marrow precursors (Hughes, MacDonald, Russell, & Gowen, 1989), reduction of osteoclast activity (Sato & Grasser, 1990) and down regulation of matrix metalloproteinase (Teronen et al., 1999). These advances in research of BP affecting cellular function, and not only in osteoclasts, has progressively driven the synthesis of more improved versions of BP and helped to elucidate the action of BP at the molecular level.

2.1.3   Classes of Bisphosphonates: Trends in Medical Practice

From a clinical aspect, there are early and late generations of BP that have emerged since their first development in 1897 by Von Baeyer and Hoffman (Francis & Valent, 2007). These different classes are due to the presence of a nitrogen bond in the late generation of the drug, accounting for the higher level of affinity to bone mineral (Kennel & Drake, 2009) and higher specificity for the osteoclast. BPs are commonly categorized into two classes: nitrogen (N-BPs) and non-nitrogen containing bisphosphonates (NN-BPs) (Table 2.1). To understand the trend of the alarming rise of adverse effects of BP treatment, we will review the biochemical mechanism that these types of drugs exert on cells and the use of these drugs in medical practice over decades. It is worth noting that the treatment mode is believed to exert multiple adverse effects on different types of tissues.

Early non–nitrogen-containing bisphosphonates (etidronate, clodronate, and tiludronate) (Figure 2.4) are considered the least potent since they are rapidly metabolized and do not accumulate in bone. Because of their close structural similarity to PPi, non–nitrogen-containing bisphosphonates (NN-BPs) become incorporated into molecules of

newly formed adenosine triphosphate (ATP) by the class II aminoacyl–transfer RNA synthetases after osteoclast-mediated uptake from the bone mineral surface (Russell, 2006). Therefore, intracellular accumulation of these non-hydrolyzable ATP analogues is believed to be cytotoxic to osteoclasts because they inhibit multiple ATP-dependent cellular processes, leading to osteoclast apoptosis (Figure 2.5).

Unlike early bisphosphonates, nitrogen-containing R^2 side chains (Figure 2.4) (Kennel & Drake, 2009) are able to increase the drug potency level by 10-10,000 fold relative to NN-BP. However, the mechanism by which N-BP (alendronate, risedronate, ibandronate, pamidronate, and zoledronic acid) promote osteoclast apoptosis is distinct from that of the NN-BP (Drake et al., 2008). At the cellular level, N-BPs inhibit the activity of farnesyl pyrophosphate synthase, a key regulatory enzyme in the mevalonate pathway critical to the production of cholesterol, other sterols, and isoprenoid lipids (Dunford et al., 2001; Kavanagh et al., 2006) (Figure 2.5), which serve as the basis for biosynthesis of molecules including post-translational modification (isoprenylation) of proteins (including the small guanosine triphosphate–binding proteins Rab, Rac, and Rho), the multiple step process of terpenoid synthesis, protein prenylation, cell membrane maintenance, hormone production, protein anchoring and N-glycosylation. (Luckman et al., 1998). Foundational to the discovery of this pathway, the specific activity of N-BP to bone tissue has been debated, due to increasing cases of adverse effects of N-BP in multiple tissues.

In the clinical setting, the treatment regimen of BP in patients varies depending on the severity of bone loss in the patient. More potent BP, such as pamidronate and zoledronate are taken intravenously due to the high dosage needed for the patient per treatment, commonly 4mg over a period of 15 minutes. This high dose regimen is needed to improve the management and prevention of complications associated with bone cancer

metastasis, such as pathological fractures, hypercalcemia, nerve root compression and spinal cord compression (Healey and Brown 2000). Suppression of resorption occurs even more rapidly after intravenous N-BP therapy (Kennel & Drake, 2009). In comparison with pamidronate, zoledronic acid was significantly more effective in controlling hypercalcemia of malignancy and reducing the overall number of skeletal-related events. If tolerated, it is not uncommon for these patients to be maintained on bisphosphonate therapy indefinitely (S. L. Ruggiero, Mehrotra, Rosenberg, & Engroff, 2004). Apart from that, oral bisphosphonates (alendronate and risedronate) are also potent osteoclast inhibitors, but they are not as efficacious in the treatment of malignant osteolytic disease and therefore are indicated only for the treatment of osteoporosis. Therefore, it is concluded that the diversity of BP treatment towards the management of bone loss disorders is highly effective, and it is needed for long term treatment
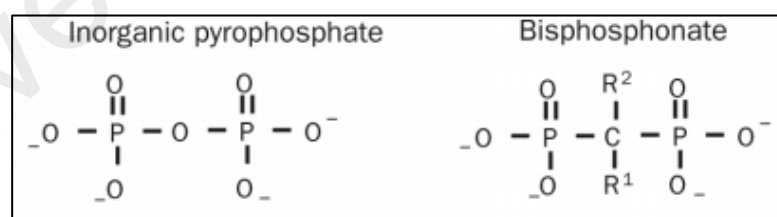
Figure 2.3: The basic chemical structure of bisphosphonate similar to pyrophosphate (PPi), a human by-product from body metabolism. The addition of 2 phosphate groups (R^1 and R^2), linked by esterification to the carbon, increases the bisphosphonate affinity for binding to hydroxyapatite (HA) crystal in bone. R^1 is an OH group and R^2 determines anti-resorptive potency biochemically, both R1 and R2 are capable of increasing binding affinity for HA. Adapted from "Adverse effects of bisphosphonates: implications for osteoporosis management," by Kennel,K.A and Drake, ,M.T, 2009, Mayo Clin Proceedings, vol 84, p. 632-7. Adapted [or Reprinted] with permission.(Kennel & Drake, 2009)

Table 2.1: The list of bisphosphonates available in the clinical setting and their respective mode of treatment.

Categories	Name of Drug	Method of Therapy
Non-Nitrogenous (NN-BP)	Etidronate	Oral
	Clodronate	Oral
	Tiludronate	Oral
Nitrogenous(N-BP)	Pamidronate /Aredia	Intravenous
	Alendronate / Fosamax	Intravenous
	Ibandronate / Boniva	Intravenous
	Risedronate / Actonel	Intravenous
	Zoledronate / Zometa	Intravenous
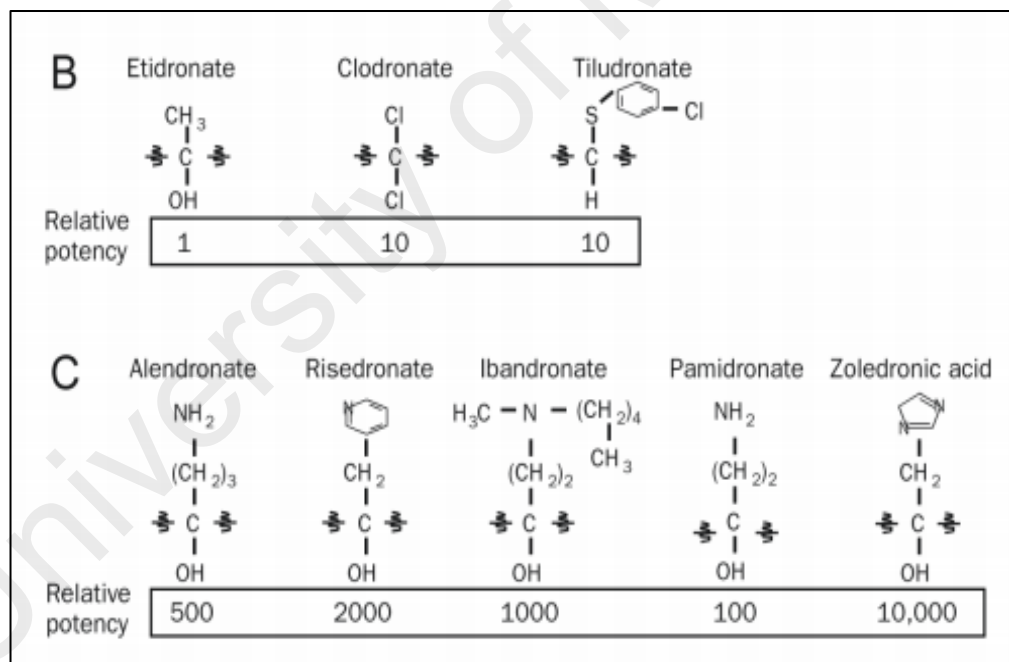
Figure 2.4: Bisphosphonate chemical structure and approximate relative potencies for osteoclast inhibition. Adapter from (Drake et al., 2008)
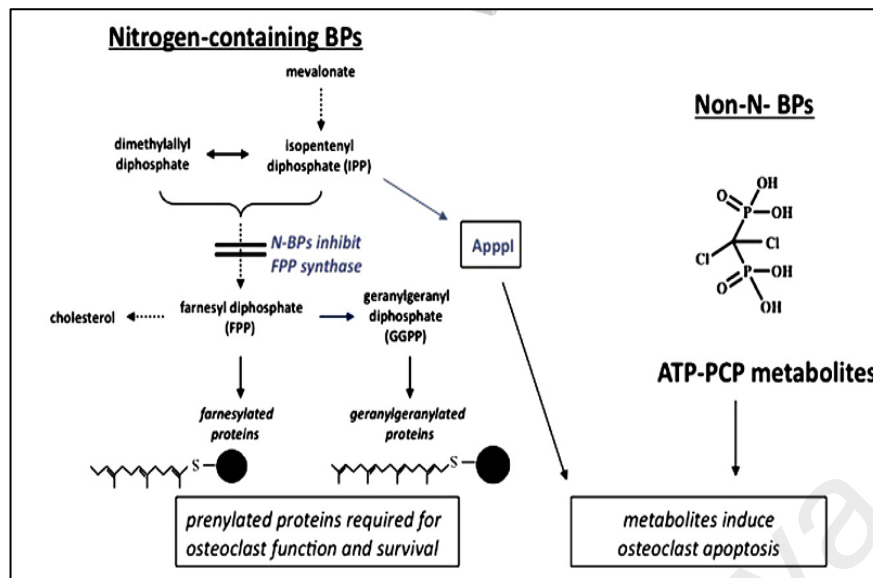
Figure 2.5: The diagram illustrates the mechanism of nitrogen-containing bisphosphonate inhibition of osteoclast activity by inhibiting the mevalonate in the mevalonate pathway and diversion to non- hydrolyzable ATP analogues that lead to apoptosis. Adapted from (Russell, 2011)

2.1.4 Adverse Effect of Bisphosphonates: Bisphosphonate-Related Osteonecrosis of the Jaw (BRONJ)

Bisphosphonates have been used in the treatment of various skeletal disorders for three decades, and it has also been recently discovered to promote osteointegration of dental implants (Borromeo, Tsao, Darby, & Ebeling, 2011; Meraw & Reeve, 1999; Meraw, Reeve, & Wollan, 1999; Yoshinari, Oda, Inoue, Matsuzaka, & Shimono, 2002). There are certain degrees of potency of these drugs that are not tolerated by some patients, depending on 3 factors: drug delivery route, duration of treatment, and risk profile of the patient. It has taken several years to elucidate the trend of adverse effects, since some of the trigger factors are correlated. Nevertheless, clinicians have categorized BP complications into 2 categories: short and long term effects (Kennel & Drake, 2009). The occurrence of adverse effects of BP can range from as short as 30

minutes to long term up to 10 years due to the long biologic half-life of bisphosphonates after a single-dose IV administration (Khan et al., 1997).

The short term effect of BP therapy that is most reported is ulcer and inflammation of the upper gastrointestinal tract (de Groen et al., 1996). The rest of the effects are complications from intolerance upon transient exposure to BP intravenously, such as acute phase reaction characterized by fever, myalgias, and arthralgias (Black et al., 2007), severe musculoskeletal pain ("Bisphosphonates (marketed as Actonel, Actonel+Ca, Aredia, Boniva, Didronel, Fosamax, Fosamax+D,Reclast, Skelid, and Zometa). ," 2009), ocular inflammation (Kennel & Drake, 2009), hypocalcemia (Kennel & Drake, 2009), and esophageal cancer (Drake et al., 2008). The long term effect of BP administration on the other hand, includes atrial fibrillation (Black et al., 2007), severe bone turnover suppression (Bone et al., 2004), subtrochanteric femoral fractures (Kennel & Drake, 2009; Kwek, Koh, & Howe, 2008; Lenart, Lorich, & Lane, 2008) and bisphosphonate related osteonecrosis of the jaw (BRONJ).

BRONJ has been described clinically based on 4 stages (Table 2.2) (S. L. Ruggiero et al., 2009) and has been formally defined by The American Society for Bone and Mineral Research (ASBMR) as "an area of exposed bone in the maxillofacial region that has not healed within 8 weeks in patients who have been exposed to BP therapy but not radiation therapy to the craniofacial region" (Silverman & Landesberg, 2009). Besides causing pain to the patient due to exposure of necrotic bone in the jaw, it is reported that BRONJ also shows a poor response towards preventive treatment such as resection of necrotized bone and antimicrobial drug treatment (Shirota et al., 2009).

Marx et al. (2003) was first to shed light on the correlation between BP and osteonecrosis of the jaw (Marx, 2003). The study described 36 cases of necrosis of the jaw patients receiving intravenous N-BP (Marx, 2003) as unreported, yet startling, and

should be taken into account. Since then, cases of BRONJ began to emerge, targeting primarily cancer patients who were taking N-BP intravenously (Vahtsevanos et al., 2009), followed by osteoporosis cases (C. Heng, Badner, Vakkas, Johnson, & Yeo, 2012; Marx et al., 2005). Similarly, the largest national cohort studies (n=958,126) were conducted in Taiwan and showed 73.5 per 100,000 person-years with strong associations. Trigger factors included delivery route, tooth extraction, and oral cancer with ONJ (hazard ratios = 51.4 for oral bisphosphonates, 153.3 for intravenous bisphosphonates, 5.3 for tooth extraction, and 278.1 for oral cancer) (Yuh et al., 2014). In addition, based on a sample of 4,000 cancer patients, 33 reported having ONJ with an overall occurrence rate of 0.8 %, with 2.8 % occurring in multiple myeloma patients and 1.2% in breast cancer patients (S. Ruggiero et al., 2006). In spite of the great number of patients receiving BP, ONJ is a rather rare complication (Bergmeister, 2012). The incidence of ONJ in patients with cancer has been estimated to be 1 to 10 per 100 patients (Woo, Hellstein, & Kalmar, 2006). This population typically received high doses of IV bisphosphonates including zoledronic acid (S. L. Ruggiero et al., 2004) (Durie, 2007) and pamidronate (Marx, 2003; S. L. Ruggiero et al., 2004) with a dosing schedule that is much more frequent than that used for other conditions.

Apart from that, there are also BRONJ cases reported related to oral treatment with BP (S. L. Ruggiero et al., 2004). On average, patients take oral bisphosphonates for 4.6 years (and a minimum of three years) before developing BRONJ. Current estimates of BRONJ related to oral BP therapy for osteoporosis are approximately 1 in 10,000 to 1 in 100,000 patient-years (Khosla et al., 2007). However, the prevalence in patients taking oral bisphosphonates is very low, ranging from 0.07 to 0.10 per cent compared to patients with cancer who are taking high-dose intravenous bisphosphonates. In conjunction, studies also suggested the presence of trigger factors for BRONJ lesions, which include poor oral hygiene (Woo et al., 2006), invasive dental procedures or denture use (Marx et

al., 2005), implants (Bell & Bell, 2008; Fugazzotto, Lightfoot, Jaffin, & Kumar, 2007; Grant, Amenedo, Freeman, & Kraut, 2008; Jeffcoat, 2006; Starck & Epker, 1995), and bacterial secondary infection (Abu-Id et al., 2008; Biasotto et al., 2006; Bisdas et al., 2008; Hansen, Kunkel, Weber, & James Kirkpatrick, 2006). Although BRONJ has been recognized as a rare incident (Bergmeister, 2012), it remains a distressing concern since there is no terminal treatment yet for this lesion in the long term, except for drug holiday (Diab & Watts, 2013) and surgical procedures to remove necrotic bone (S. Ruggiero et al., 2006).

The mechanism of BRONJ lesions is still uncertain; however, there are a few theories highlighted by literature review worldwide such as ischemia and toxicity to bone. However, this does not explain the occurrence of BRONJ in the limited area of the maxillofacial region instead of the entire skeleton (Reid, 2009). Also a study suggested that bacterial infection can increase bone resorption and inhibit bone formation as observed in necrotic bone (Reid, 2009). However, to date there is no data on specific bacteria that are responsible for triggering osteonecrosis of the jaw. Nevertheless, there is a study reporting the presence of biofilm formation from the species *Actinomyces* in a BRONJ patient and that the ONJ lesion was intensified due to the impenetrable feature of the biofilm towards antibacterial drugs and immune cells (Belibasakis et al., 2007).

Table 2.2: Clinical Descriptions of the Stages of BRONJ

(S. L. Ruggiero et al., 2009)

BRONJ Stage	Description
Stage 0/at risk	No apparent necrotic bone in patients who are taking either oral or IV BP
Stage 1	Exposed and necrotic bone in asymptomatic patients without evidence of infection
Stage 2	Exposed and necrotic bone associated with infection as evidenced by pain and erythema in a region of exposed bone with or without purulent drainage
Stage 3	Exposed and necrotic bone in patients with pain, infection, and one or more of the following: exposed and necrotic bone extending beyond the region of alveolar bone, resulting in pathologic fracture, extraoral fistula, oral antral/oral nasal communication, or osteolysis extending to the inferior border of the mandible or the sinus floor.

2.2 Bisphosphonate-Related Osteonecrosis of the Jaw (BRONJ): Towards Oral Mucosa Integrity

The pathophysiological role of BP in BRONJ remains undefined, as it is a multifactorial process governed by a combination of stresses in the oral microenvironment, anti-osteoclast activity of BP, anti-angiogenic effects caused by the depression of blood flow, and decreases of VEGF (Landesberg et al., 2008; S. L. Ruggiero, 2011; Sanna, Zampino, Pelosi, Nole, & Goldhirsch, 2005; Sarin, DeRossi, & Akintoye, 2008). An understanding of whether the lesion starts in the soft tissue or bone would be helpful in attempting to pinpoint the relative contribution of BP to the pathophysiology of ONJ. In 2007, Reid et al. (2007) suggested that delayed wound healing after dental intervention in patients taking N-BP treatment might be due to soft tissue toxicity and may be one of the underlying pathogenic mechanisms of BRONJ

lesions (Reid et al, 2007). After all, BP is no stranger to cases of epithelium toxicity, as numerous studies have explored the effect of BP on a variety of epithelial cells, including gastrointestinal cells, cervical epithelial cells, renal cells, and prostate epithelial cells. In widely known clinical cases, BP treatment is known to cause ulcer and irritation in epithelium lining the gastrointestinal tract, mostly from cases of oral bisphosphonate treatment. In addition, it has also been implied that the transition to intravenous treatment has managed to reduce the risk of ulcers in the gastrointestinal tract, but instead lead to increased cases of BRONJ that targeted oral epithelium (Reid, 2009). In the following chapter, we will review the chronology of soft tissue toxicity studies, studies ranging from monolayer to 3-dimensional model. Reviewing these studies also tracks the progress in our understanding of soft tissue toxicity's role in the pathophysiology of BRONJ.

2.2.1 Pathophysiology Studies Addressing Soft Tissue Toxicity

The significant fact that osteonecrosis lesions occur exclusively in the maxillofacial and mandibular region area has led to the plausible theory that N-BP somehow accumulates in the alveolar bone region and subsequently induces toxic concentrations in both soft and hard tissues. Therefore, it was suggested that the accumulation of N-BP in the alveolar bone reservoir from the intravenous route is due to the high rate of daily alveolar bone remodelling around the periodontal ligament due to high physiologic function (e.g mastication) (Marx et al., 2005) compared to other bone, potentially up to 10 times higher (Marx, Cillo, & Ulloa, 2007).

A series of experiments involving animal study (Aguirre et al., 2012; Allam et al., 2011) and osteomucosal tissue constructs (Bae et al., 2014) have been designed to prove whether BP released from bone towards a thin mucosal layer has the capacity to trigger a toxic concentration and subsequently will compromise wound healing in soft tissue (Table 2.3). The lesions were characterized by exposed necrotic alveolar bone followed

by the presence of bacterial colonies and periodontal tissue destruction. They were observed in mice after 18 and 24 weeks' intravenous treatment with a high dosage of zoledronic acid. BRONJ lesions were observed in N-BP (zoledronic acid) treated mice, and not in NN-BP (alendronate) treatment. (Aguirre et al., 2012). In another study, dogs were treated with zoledronic acid for 3 months intravenously and histology analysis of gingival tissues was performed based on a few protein markers for wound remodelling and apoptosis. The results showed the wound remodelling metalloproteinase protein MMP-9 was significantly reduced (Allam et al., 2011). Nevertheless, 5 out of 6 dogs showed unhealing gingival tissues over 3 weeks after tooth removal; however, no data was reported on bone necrosis. In another study using an oral osteomucosal tissue model, the direct contact effect of N-BP towards soft tissue was investigated. It was demonstrated that the N-BP was detected in soft tissue, even though the drug was introduced from a hard tissue representative (represented by dentin discs) (Bae et al., 2014). In addition, inhibition of keratinocyte growth has been documented when cultured in media exposed to N-BP-treated osteoblasts (Saracino et al., 2012). Apart from that, Saito T et al. (2014) also tested the capacity of a full thickness wound oral mucosa model to heal during treatment with 10μM zoledronic acid for 11 days. Based on the model, they reported that the primary mechanism that governs impairment of wound healing in zoledronic acid treatment is down regulation of proteins that are responsible for cell migration, including integrin αvß6 and TGF-ß as well as the downstream signaling molecule p-smad 3 (Saito et al., 2014).

While significant *in vitro* and *in vivo* studies have explained the contact of N-BP with soft tissue from intravenous treatment and from bone, the drug dosage responsible for inducing soft tissue toxicity clinically has not yet been elucidated because of confounding factors in the jaw such as dental intervention and long lasting treatment with the drug

(Landesberg et al., 2011; Reid, 2009) that might stimulate release of stored N-BP from bone towards the oral mucosa (Landesberg et al., 2011; Reid, 2009).

The *in vitro* research frontier (Table 2.3) of soft tissue toxicity as an inducing factor of BRONJ lesions began with multiple experiments to provide direct evidence relating features of impaired mucosa healing with N-BP treatment in terms of proliferation and apoptosis (Landesberg et al., 2008; Scheper et al., 2009). Increasingly, studies have compared N-BP and NN-BP on the basis of viability and migration with migration measured via a scratch wound assay (Pabst et al., 2012) utilizing monolayer models of the oral mucosa components: oral keratinocytes and fibroblasts. Growing evidence has shown that nitrogen containing bisphosphonate (N-BP) exert stronger negative effects toward oral mucosa cells (both keratinocytes and fibroblasts) compared to non-nitrogen containing bisphosphonate (NN-BP) (Pabst et al., 2012). Nevertheless, there are contradicting results regarding the underlying mechanism that drives N-BP's toxicity towards oral mucosa. Two studies based on human immortalized skin keratinocytes reported that zoledronic acid (N-BP) inhibited mucosa healing by inducing apoptosis (Saracino et al., 2012; Scheper et al., 2009). On the contrary, based on a mouse oral keratinocyte model, Landesberg et al.(2008) another study claimed that pamidronate (N-BP) inhibited keratinocyte growth, but not through an apoptotic mechanism (Landesberg et al., 2008). However, the contradicting results from these experiments might be due to an inconsistent cell type used in the study. Alternatively, related to the finding by Landesberg et al.(2008), Kim et al. (2011) further reaffirmed the potential of the senescence mechanism in human oral mucosa cells in a 3-dimensional model. The finding showed that soft tissue toxicity induced by pamidronate is driven by cell type-specific toxicity in which the keratinocytes undergo senescence, and the fibroblast undergo apoptosis (R. H. Kim et al., 2011b)

After Kim et al.(2011) first reported on evidence of N-BP-induced senescence in oral keratinocytes (R. H. Kim et al., 2011b), there are now many studies that have begun to analyse impaired healing of mucosa through a variety of assays other than apoptosis detection assays (DAPI staining, caspase-3 activity, TUNEL assay). In the following year, Ohnuki et al. (2012) reported that growth inhibition of oral keratinocytes treated with zoledronic acid was driven by a DNA damage protein. This finding is deduced from the result of cell cycle arrest in S phase and the detection of immunolabelling of the DNA damage protein histone H2A.X (H. Ohnuki et al., 2012). Saito et al. (2014) has further confirmed that impairment of healing in mucosa tissues was driven by attrition of migration capacity, explained by downregulation of the integrin αvß6 and TGF-ß downstream signaling molecules (p-smad 3) upon treatment with zoledronic acid (N-BP) in the 3-dimensional oral mucosa wound healing model (Saito et al., 2014). Prior to this confirmation, Kim et al.(2011) addressed pamidronate (N-BP) induced toxicity on oral mucosa cells by distinguishing a growth arrest mechanism exerted towards a cell-specific type (R. H. Kim et al., 2011b). However, most of these senescence markers were identified via *in vitro* studies carried out using primary normal cells, which are prone to senescence each time these normal somatic cells divide in the culture (Bodnar et al., 1998).

Table 2.3: A summary of studies on effect of BP on soft tissue toxicity using animal model, monolayer and 3D OMM

Authors(Year)	Model,Treatment Method	Evaluation Methods	Findings
Landesberg,R et al. (2008) (Pamidronate)	Mouse oral keratinocytes 0, 0.003, 0.01, 0.03 and 0.1 mM	• MTS assay at 24,48,72 and 168 hrs • Apoptosis assay • TUNEL assay • DAPI staining • Wounding assay	• Inhibit cell proliferation at 0.1mM • PAM does not cause apoptosis • Wound healing inhibited
Scheper et al. (2009) (Zoledronic Acid)	HaCat, HGF cell lines 0.25, 0.5,1,3uM up to 24 hours	• Apoptosis-Annexin V flow cytometry, PCR, Western blot, TUNEL assay • Proliferation- cell counter, MTS assay	• Confirmation effect of apoptosis in both of cell lines HGF and HaCat as dosage dependent • Reversal of proliferation effect of ZA by siRNA of caspase-3 and caspase-9 • Reduced proliferation by 30% in HGF and 72% in HaCat
Kobayashi (2010) (Zoledronic Acid)	Mice 6 weeks old treated with ZOL (250ug/kg/day) treatment for 7 days	• Histological analysis • Dorsal air sac assay • Matrigel network formation assay • Caspase assay • Wound healing assay • Hydroxyapatite adhesion assay • Colony formation assay for oral bacteria	• ZOL delayed wound healing by inhibiting osteogenesis and angiogenesis • ZOL increased caspase activity in endothelial cells and oral epithelial cells • ZOL increased oral bacteria adhesion
Eman Allam (2011) (Zoledronic Acid)	Dogs, 3 months intravenous treatment	• Cell proliferation-tissue assessed for PCNA. • Apoptosis-caspase 3 (IHC) and TUNEL • MMP expression	• No significant differences in proliferation, MMP-2 and MMP-14 and TUNEL positive cells • Significant increase in expression of caspase-3 cells and decrease in MMP-9 compared to non-treated

Table 2.4, continued

Authors (Year)	Model,Treatment Method	Evaluation Methods	Findings
Kim et al. (2011) (Pamidronte)	NHOK and NHOF, 10 and 50uM 96 hours Co-culture system-collagen based	• Flow cytometry-Cell Cycle analysis(PI staining) and apoptosis (Annexin V staining) • Western blot-caspase 3, p16INK4A, GADPH, ß-actin, phospho-p38, p38 • Senescence associated β-galactosidase staining • Organotypic raft culture to assess wound healing capacity • Immunohistochemistry-PCNA marker • qRT-PCR: expression of senescence-associated genes IL-8 and MMP-3	• Bisphosphonates induce toxicity in cell-type manner • Fibroblast undergo apoptosis based on WB analysis of cleaved caspase 3 • Apoptosis on fibroblasts and senescence in keratinocytes • Significant reversal of negative effect by GGOH treatment
J.I Aguirre, DVM et al. (2012) (Zoledronic Acid & Alendronate)	• Rice rat model of periodontitis, injection bi weekly (Alendronate), IV monthly with high and low dose of ZOL, treatment for 24 weeks	• Osteoclast analyses-osteomeasure system • Assessment of necrotic alveolar bone-LDH, TUNEL staining, fuchsin staining • Evaluation of angiogenesis/vascularity-IHC (anti CD 31) • MicroCT assessment • Peripheral quantitative computed tomography (pQCT)	• High doses of ZOL (80ug/kg) inhibit bone resorption in jaw • Anti-resorptive action of ZOL simultaneous with extensive ulceration of gingival epithelium, exposed necrotic bone, severe inflammatory cell infiltration and presence of bacterial biofilm

Note: ( ) Type of BP treatment in the study.

Table 2.4, continued

Authors (Year)	Model,Treatment Method	Evaluation Method	Finding
S.Saracino, (2012) (Zoledronic Acid)	• NCTC 2544 keratinocytes • MG-63 osteoblast cells • 5 or 50uM up to 48 hours	• Cell proliferation – cell counter • Cell viability-LDH assay • Cell cycle analysis-propidium iodide staining • Detect expression of functional cytokines that play role in inflammatory, osteogenic and osteoclastogenic: ELISA analysis and mRNA expression	• ZOL did not significantly induce necrosis in epithelial cells • ZOL significantly increased apoptotic cell percentage and expression of TNF-α at 5 and 50uM • In conditioned media, no significant increases in apoptotic and necrotic cells observed for osteoblast • Significant changes in cytokines involved in regulation of bone homeostasis after exposure to ZOL-conditioned media from epithelial cells
Hisashi Ohnuki et al. (2012) (Zoledronic Acid)	• NHOK , incubation 48 hours 0.1,0.3,1,3,10uM • Homotypic acellular dermis based (11d culture) 7d incubation with10uM ZOL	• Monolayer • Cell proliferation: BrDU ELISA and cell count • Apoptosis/Necrosis-Flow cytometry: Annexin V/ Propidium Iodide (PI) 10uM for 24, 48, 72 and 96 hrs • Western blot: cell cycle regulator protein (phosphor-protein), ubiquitin mediator regulator protein. • 3-D culture • Proliferation: Ki-67, • DNA replication negative regulator protein: Geminin • DNA damage protein: immunolabelling of histone H2A.X (γ-H2A.X)	• Increase cell percentage in S phase and decrease in G phase over time. However, no apoptosis peak was detected • S phase arrest due to decreased cell cycle protein regulator via increased expression ubiquitin mediator protein. • In 3D, ZA at 10uM for 7d decrease Ki-67 and Geminin marker for proliferation, thinner stratified epithelium, and increase DNA damage

Note: ( ) Type of BP treatment in the study.

Table 2.4, continued

Authors,Year,	Model,Treatment Method	Evaluation Method	Finding
Andreas M Pabst et al.,2012 (Clodronate,Ibandronate Pamidronate,Zoledronate)	HOK cells (Sciencell,USA)	• Cell viability- MTT assay • Cell migration-Boyden chamber and • Scratch wound assay • Apoptosis-TUNEL assay	• Nitrogenous bisphosphonate has stronger toxicity compared to non-nitrogenous bisphosphonate in cell viability, migration, and apoptosis
N Arai et al. 2013 (Zoledronic Acid)	Zoledronic Acid with media containing calcium 1.8mM and 4.8mM for 48 hrs	• Cell viability-MTT assay • Analyses of apoptosis-Annexin V-FITC • Direct microscopic observation	• Determine IC 50 of of ZA between 1 and 3uM • increased concentration of calcium increase the level of toxicity effect of ZA in viability, apoptosis • Data indicated the negative effects of high calcium and low serum on viability of HaCaT cells in the presence of ZA *in vitro*
Niall M.H Mc Leod,2014 (Alendronate, Zoledronate, Clodronate)	• HFFF(fetal foreskin fibroblasts) • OKF 6/TERT 2(Human oral keratinocytes) • Heterotypic culture -collagen based	• Cell proliferation-cell counter • Cell migration-transwell migration assay • Histology effect-organotypic culture	• BRONJ did not cause suppression of keratinocyte or fibroblast motility at subtoxic concentration

Note: ( ) Type of BP treatment in the study.

Table 2.4, continued

Authors, Year	Model, Treatment method	Evaluation Method	Finding
Susan Bae, 2014 (Zoledronic Acid)	• Zoledronic acid bound with fluorochrome • Treatment at 4uM for 1 week during air-lifting	• Cell proliferation-MTT • Detecting fluorochrome ZOL • Tissue processing and histological examination-H&E, IHC (K14)	• Development of 3-dimensional model (osteomucosal construct) that include both soft and hard tissues • First time evidence *in vitro* of localization of bisphosphonate in epithelium, onset potential mechanism for soft tissue toxicity. •
T Saito, 2014 (Zoledronic Acid)	• Zoledronic acid incubated for 11 days , after air-lifting for 3 days	• Histological and IHC examination-H&E, • Laminin, Ki-67, TGF-ß1, TGF-ß receptor I, TGF-ß receptor II, p-Smad2, p-smad3 (TGF-ß downstream signalling molecules) and intergrin αvß6 (increased in response to injury) • ELISA-Quantify TGF-ß1 in conditioned media	• Decreased Ki-67 proliferation cells in basal layer , thinner epithelium and continuity of epithelium maintained • Epithelium coverage delayed in wound model (even for 19d) • Weak expression of integrin αvß6in the newly formed epithelial layer of the ZA-treated model, resemble primary mechanism of the impairment of oral keratinocyte migration • TGF-ß1 signal transduction including its receptors and Smad3 were remarkably down-regulated by 10 uM of ZA treatment after wounding in a 3D *in vitro* oral mucosa model

Note: ( ) Type of BP treatment in the study

2.2.2   Senescence as a pathophysiology of an unhealing mucosa in BRONJ

Impairment of wound healing in mucosal tissues is observed in BRONJ patients, mostly from the precipitating factor of dental intervention (e.g. tooth extraction, mandibular exostoses, periodontal disease, and local trauma from ill-fitting dentures). This impairment has drawn researchers' attention to design experiments centered on the capacity of oral epithelium to re-epithelialize. In the previous chapter, we compiled various studies to clarify the current state of knowledge regarding soft tissue toxicity. These studies have shed light on a few effects of bisphosphonates on oral mucosal cells, including the DNA damage response, cell-specific senescence, and impairment of re-epithelialization through reduced cell migration. However, the causal relationship between senescence and impairment of re-epithelialization has remained elusive. Nonetheless, recent research has implied that senescence and inflammation might be overlapping factors that lead to tissue damage by either wounding or initiating cancer (Adams, 2009). Therefore, in this chapter, we will first review current perspectives on senescence followed by a more cohesive understanding of wound re-epithelialization.

2.2.2.1   Fundamentals of Senescence

Cellular senescence has been described as an ultimate and irreversible loss of replicative capacity occurring in primary somatic cell culture (Hayflick & Moorhead, 1961). Throughout the years, this intrinsic growth arrest has accounted for insufficient cell yield in routine cell culture procedures, despite ample nutrients, space, and growth factors supplied in culture. Nevertheless, the study of senescence mechanisms has become significant, mainly due to the therapeutic potential to inhibit cancer progression (Braig et al., 2005; Z. Chen et al., 2005; Collado et al., 2005; Courtois-Cox et al., 2006; Ewald et al., 2010; Michaloglou et al., 2005). However, as understanding of senescence responses grew, new insights were brought to the fields of wound healing (Ashcroft, Mills, & Ashworth, 2002) and aging-related diseases (Lasry & Ben-Neriah, 2015) which

involved inflammation mechanism. (Adams, 2009; Shelton, Chang, Whittier, Choi, & Funk, 1999).

Van Deursen, J.M. (van Deursen, 2014) has described senescence as a highly dynamic, multi-step process in which senescent cells continuously evolve and diversify, much like tumorigenesis, but without cell proliferation as a driver (De Cecco et al., 2013; Ivanov et al., 2013). Moreover, senescence has been identified to occur in a variety of mitotic cells including keratinocytes (Rheinwald & Green, 1975), melanocytes (Bandyopadhyay et al., 2001), endothelial cells (Thornton, Mueller, & Levine, 1983), epithelial cells (Shelton et al., 1999), glial cells (Blomquist, Westermark, & Ponten, 1980), adrenocortical cells (McAllister & Hornsby, 1987), T-lymphocytes (Effros & Walford, 1984) and even tissue stem cells (Oh, Lee, & Wagers, 2014) through various stimuli and pathway cascades. Further findings also revealed the presence of a senescence-like phenotype in post mitotic cells, including neurons (Jurk et al., 2012) and adipocytes of mice on a high fat diet (Minamino et al., 2009). The process of senescence is complex, and may occur through a variety of different mechanisms and be triggered by a variety of different stimuli. Therefore, to understand how cellular senescence can contribute to soft tissue toxicity induced by BP, it is important to understand the stimuli, senescence mechanism, and the consequences of senescence that might drive impairment of mucosal healing.

As currently defined, scientists have learned that DNA damage-initiated senescence has been manifested through a universal senescence cascade which can be triggered by several intrinsic and extrinsic stimuli (Adams, 2009) with telomere uncapping being the most established and most investigated stimulus (Blackburn, 1994). This is known as replicative senescence. Telomeres are essential structures that cap and protect the ends of linear chromosomes from chromosomal instability and tumorigenesis

(Bodnar et al., 1998; Hayflick & Moorhead, 1961). Due to the inability of polymerase to fully replicate the ends of linear DNA molecules and attrition of telomerase in maintaining the end sequences (Hug & Lingner, 2006; Verdun & Karlseder, 2007), they will accumulate an end-replication problem. Therefore, telomeres become progressively shorter with each round of cellular division. One of the severe problems due to telomere shortening is detrimental double strand break (DSB), in which cells will trigger classical DNA-damage initiated senescence. The DNA damage response (DDR) cascade will be engaged and lead to transient proliferation arrest, allowing cells to repair damage. However, if DNA damage reaches a certain threshold, cells are destined to undergo either apoptosis or senescence. The factors that determine the outcome remain largely elusive (d'Adda di Fagagna et al., 2003). Moreover, unlike stem cells and germline cells, dividing human somatic cells possess an absence (or minimal) telomerase activity to make up for losses incurred at the telomeres (Harley, Futcher, & Greider, 1990; Masutomi et al., 2003; Palm & de Lange, 2008; Wright, Piatyszek, Rainey, Byrd, & Shay, 1996).

However, scientists have learned that senescence can occur independent of telomere shortening, known as the stress-induced premature senescence response (SIPS). In 2000, Sherr et al.(2000) (Sherr & DePinho, 2000) described premature senescence occurring from stress exerted from inadequate culture conditions (Stampfer & Yaswen, 2003). Furthermore, in other studies, it was reported that mouse embryonic fibroblasts in culture undergo senescence after a number of passages (Loo, Fuquay, Rawson, & Barnes, 1987) despite retaining the expression of telomerase (Prowse & Greider, 1995) and the presence of long telomeres (Kipling & Cooke, 1990). This type of senescence can be induced by stress, with the nature of this stress still poorly understood (Campisi & d'Adda di Fagagna, 2007). However, increasing studies have started to reveal that strong mitogenic signals such as overexpression of activated oncogenes such as RAS or RAF and ectopic expression of tumor suppressors (Campisi & d'Adda di Fagagna, 2007; Q. M.

Chen, 2000; Q. M. Chen et al., 1998; Ramirez et al., 2001; Sedivy, Banumathy, & Adams, 2008; Serrano, Lin, McCurrach, Beach, & Lowe, 1997; Wright et al., 1996) induce senescence in primary mouse or human cells (Dimri et al., 1995; Ferbeyre et al., 2002; Lin et al., 1998). Studies also revealed some of the stimuli that induce DNA damage: various types of radiation (Herskind & Rodemann, 2000), drugs generating DSB (Robles & Adami, 1998), and different ways to generate oxidative stress, including increased oxygen tension (Balin, Goodman, Rasmussen, & Cristofalo, 1977; von Zglinicki, Saretzki, Docke, & Lotze, 1995) and treatment with hydrogen peroxide (Dumont et al., 2000).

The molecular pathways involved in triggering and/or maintaining the senescent phenotype are not fully understood (Salama, Sadaie, Hoare, & Narita, 2014). Nevertheless, up to this point, the senescence growth arrest mechanism is controlled by p53 and the p16INK4A-RB pathway (Figure 2.6). These pathways can interact, but can also initiate senescence independently. To some extent, these pathways are responding to different stimuli, cell-type-specific and species-specific (Michaloglou et al., 2005; Olsen, Gardie, Yaswen, & Stampfer, 2002). Stimuli that generate DDR (for example ionizing radiation and telomere dysfunction) induce senescence primarily through the p53 pathway and through its target p21 (Levine & Oren, 2009; Palm & de Lange, 2008). If the stress is not resolved by cellular repair mechanisms, this transient growth arrest can progress to senescence, via activation of p16INK4A. p16INK4A activation in turn will trigger growth arrest by inhibition of the kinases including CDK4 and CDK6, which phosphorylate the retinoblastoma protein (pRb). Unphosphorylated pRb binds the E2F transcription factor and inhibits it, thus arresting the cell in G1 phase (Chicas et al., 2010; W. Y. Kim & Sharpless, 2006). p16INK4A and p21 are both CDKIs; hence, both can keep pRb in an active, hypophosphorylated form, thereby preventing E2F from transcribing genes that are needed for proliferation (Sherr & McCormick, 2002). Stimuli

that produce a DDR can also engage the p16INK4A–RB pathway, but this usually occurs secondary to engagement of the p53 pathway (Jacobs & de Lange, 2004; Stein, Drullinger, Soulard, & Dulic, 1999). Nonetheless, some senescence inducing stimuli act primarily through the p16INK4A–RB pathway. This is particularly true of epithelial cells, which are more prone than fibroblasts to inducing p16INK4A and arresting proliferation, at least in culture. Furthermore, there are species-specific differences (Brenner, Stampfer, & Aldaz, 1998; Kiyono et al., 1998): for example, experimental disruption of telomeres primarily engages the p53 pathway in mouse cells but both the p53 and p16INK4A-RB pathways in human cells (Smogorzewska & de Lange, 2002). Therefore, scientists have claimed that activation of both p53 and p16INK4A pathways is crucial for induction of senescence in a variety of human cells (Kuilman, Michaloglou, Mooi, & Peeper, 2010). As a consequence, it has allowed scientists to use different senescence-induced mechanisms to transform cells, with the specific mechanism highly dependent on the cell strain (Kuilman et al., 2010).

The discovery of various senescence-induced mechanisms in cells has led to the establishment of immortalized cells through various strategies. Beside gaining extended proliferative capacity to circumvent inadequate supplies of cells, establishment of immortalized cells allows consistency in genotype or phenotype of the parental cells which is ideal for various *in vitro* experiments. The multiple strategies to circumvent senescence include exogenous expression of telomerase reverse transcription protein (TERT) by adenovirus transduction; viral oncogene expression such as simian virus 40 (SV40) T antigen transduction to induce telomerase activity (Jha, Banga, Palejwala, & Ozer, 1998; Kirchhoff et al., 2004); HPV16 E7 protein that can block pRB activation (Brenner et al., 1998; Kiyono et al., 1998), infection of EBV virus can reactivate telomerase (J. P. Liu, Cassar, Pinto, & Li, 2006). Likewise, overexpression of Ras *or* Myc T58A mutant has been identified to immortalize cells by silencing tumor suppressor genes

(p53, RB and others) (Kirchhoff et al., 2004). Another strategy is to knockdown p53 using siRNA to induce short term silencing of the p53 gene, which is commonly used as a secondary method to TERT exogenous expression (G. Yang et al., 2007). Some cells require more than one strategy of immortalization. For instance, immortalizing certain types of primary human cells, including keratinocytes and mammary epithelial cells, cannot be done by TERT alone (Kiyono et al. 1998). One immortalization method may yield low numbers of immortal cells or cause death of cells. Therefore, depending on the cell line, it may be beneficial to combine both suppression of a tumor suppressor (such as the cell cycle inhibitors mentioned above) and expression of TERT to immortalize a larger number of cells.

Recent studies have reported that transformed cells can still undergo senescence in response to oncogene activation (oncogene-induced senescence; OIS) or loss of tumor suppressors. This was first demonstrated in 1997 by a study reported on the activation of an oncogenic mutant rat sarcoma viral oncogene homolog (RAS) in cultured cells resulting in senescence (Serrano et al., 1997). Following that, more evidence of activation of oncogenes *in vivo*, or loss of tumor suppressors, lead to senescence in both mouse models and human premalignant lesions (Braig et al., 2005; Z. Chen et al., 2005; Collado et al., 2005; Courtois-Cox et al., 2006; Dhomen et al., 2009; Sarkisian et al., 2007). Senescence can be triggered by activated oncoproteins like BRAFE600 or RASV12, or by the loss of tumor suppressor proteins like PTEN or NF1 (Z. Chen et al., 2005; Courtois-Cox et al., 2006; Michaloglou et al., 2005) and occurs in a variety of cell types (Denoyelle et al., 2006; Lloyd et al., 1997; Nicke et al., 2005). One of the hallmarks shared by cells undergoing replicative senescence and OIS is the critical involvement of the p53 and p16INK4A–RB pathways, at least in certain settings (Kuilman et al., 2010). Compelling evidence has shown that OIS activates the inflammatory transcriptome (Kuilman et al., 2008). For instance, activation of v-raf murine sarcoma viral oncogene homolog B

(BRAF) also causes senescence but through a different mechanism involving p16INK4A induction, leading to upregulation of the inflammatory cytokines interleukin IL-6 and IL-8 (Kuilman et al., 2008). However in the current study, despite the limitations in technical aspects relating to identification and characterization of senescent cells in tissues (Childs, Durik, Baker, & van Deursen, 2015; Dimri et al., 1995), scientists suggest that inflammation (Lasry & Ben-Neriah, 2015) may be a potential marker to detect senescence, especially in 3-dimensional models devoid of immune cells. In conjunction with that senescent cells, especially fibroblasts and epithelial cells have been reported to secrete a striking increase of up to 40-80 factors that regulate various intercellular signalling phenotypes in tissue engineered oral mucosa (Coppe, Desprez, Krtolica, & Campisi, 2010; Coppe et al., 2008; Shelton et al., 1999; Young & Narita, 2009).

Moreover, it is also possible that the difficulty of identifying common, robust markers for senescent cells may imply senescence is a continuous process. Whereas senescence is often thought of as a binary state (cells are either senescent or non-senescent), it is likely that senescence does not occur instantly, but rather progresses as stress accumulates (Freund et al., 2010). The significance of cellular senescence as a mechanism for cancer therapeutics and as a contributor to age-related disease shows the need to establish a large variety of senescence markers. However, markers to detect senescent cells are limited and lack specificity (Althubiti et al., 2014). Moreover, populations of cells, either in tissues or in culture, will generally be a mixture of proliferating and senescent cells (Faragher & Kill, 2009), exacerbating quantitative measurement in any study. Scientists have agreed that a large variety of senescence markers simply represent different stages on the road to senescence, with some markers indicating early stages and others indicating late stages. This includes increased expression of intracellular/secreted protein p21, p16INK4A, macroH2A, IL-6, phosphorylated p38, MAPK, PPP1A, Smurf-2 or PGA. Apart from that, the p53 target

gene is critical for establishing senescence, whereas p16INK4A may be more involved in maintenance of the senescence phenotype. Some studies suggested that senescent cells display modification in chromatin organization. Hence, use of DNA staining on senescent cells will show a dot-like pattern known as senescence associated heterochromatic foci (SAHF) compared to a uniform stain outline on normal cells, and hence can be a specific senescence marker (Lawless et al., 2010). Since there is no cohesive senescence detection measurement yet, most studies utilize multiple markers, combinations of other markers such as proliferative (e.g. PCNA and KI-67), DNA damage markers (γH2A.X) and senescence associated heterochromatic foci (SAHF). However, this co-staining by multiple markers using immunohistochemistry or immunofluorescence serves as a technical challenge to measure senescent cells in tissues (Lawless et al., 2010).

The most established senescence measurement is detection of ß-galactosidase enzyme activity which involves enlargement of lysosomes in senescent cells (Althubiti et al., 2014). A major disadvantage of this measurement is that it requires fresh tissues as it is based on enzyme activity and limits the exploitation of the widely available formalin-fixed paraffin-embedded sample (Gorgoulis & Halazonetis, 2010). Further, confluent cells and treatment with hydrogen peroxide can also introduce false positive results. Indeed, there is a study that validates plasma membrane associated proteins that might serve as specific senescence markers (Althubiti et al., 2014). On the other hand, in order to generate reliable quantitative measurements, lipofuscin detection of oxidized proteins, lipids, and metals that accumulate in aged tissues has been validated as a novel senescence biomarker (Georgakopoulou et al., 2013). Senescent cells can also be characterized by unique inflammatory phenotypes, senescence associated secretory phenotype SASP (Coppe et al., 2008; Rodier et al., 2009) and senescence inflammatory response (SIR) (Pribluda et al., 2013), which are discussed extensively in the following section.
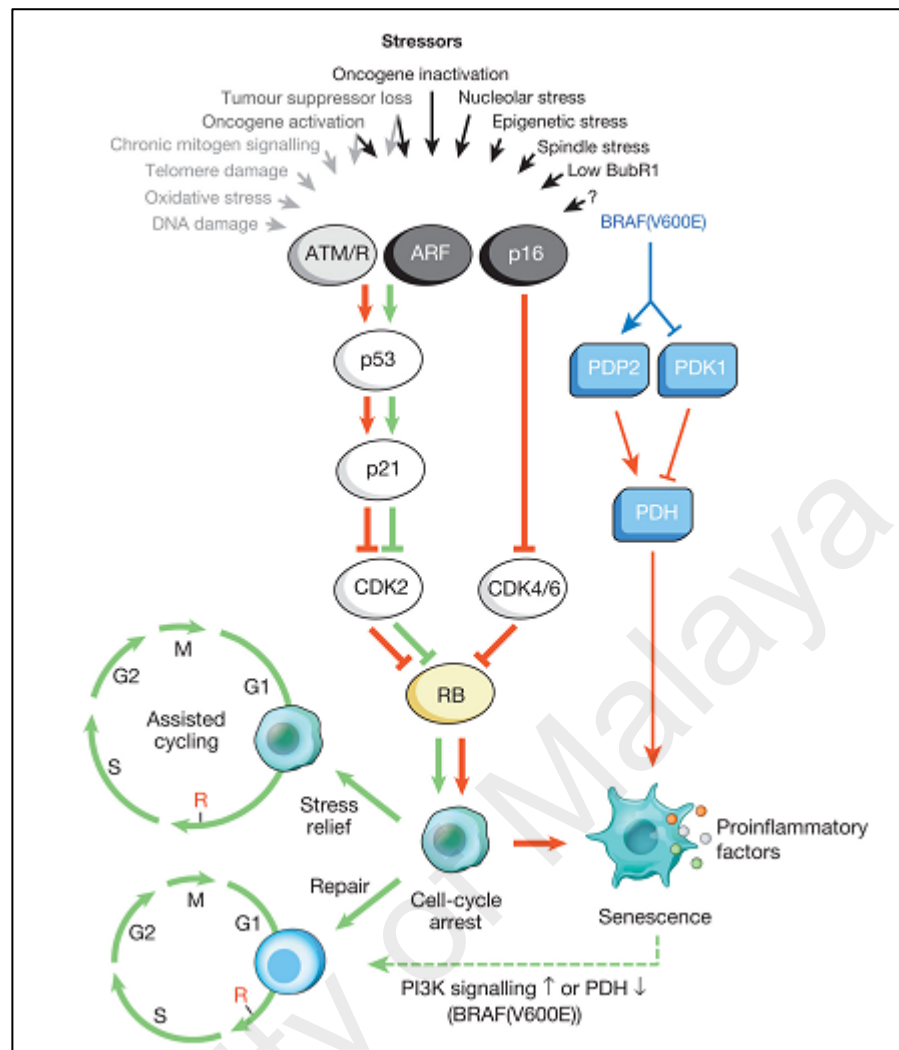
Figure 2.6: Variety of cell-intrinsic and extrinsic stimuli can activate cellular senescence mechanisms. These stimuli engage various signaling cascades but ultimately activate p53, p16, or both. Stimuli that activate p53 through DDR signaling are indicated in grey text and arrow. Activated p53 induces p21, which triggers temporal cell-cycle arrest by inhibiting E-Cdk2. On the other hand, p16 inhibit cell cycle progression by targeting cyclin D-Cdk4 and cyclin D-Cdk6 complexes. Both cascades ultimately inhibits activation of pRb thus resulting in continued repression of E2F target genes required for S-phase onset. Apart from that, cells that can be rescued will resume proliferation through stress support systems (green arrows). Cells undergoing senescence can induce inflammatory networks. Red and green connectors indicate 'senescence promoting' and 'senescence preventing' activities,respectively.

(van Deursen, 2014)

2.2.2.2   Consequences of Senescence

However, unlike apoptotic cells, scientists have learned that senescent cells are rather metabolically active, undergo widespread gene expression changes (Campisi & d'Adda di Fagagna, 2007) and secrete factors, collectively known as the senescence associated secretory phenotype (SASP). Through this secretion, senescent cells can alter their microenvironment, including positively or negatively influencing the neighboring tissue microenvironment and neighboring cells for as long as they persist, and has been discovered to exert effects on tissue-specific function in a variety of ways (Ashcroft et al., 2002; Freund et al., 2010; Lasry & Ben-Neriah, 2015). One of the hallmarks of SASP proven by some studies is that senescent cells rather than immune cells exert a striking increase in the secretion of pro-inflammatory cytokines that might be responsible for chronic inflammation (Freund et al., 2010). Chronic inflammation has been observed in aging-related diseases including heart disease, cancer, osteoporosis, Alzheimer's disease, diabetes, among others (Lasry & Ben-Neriah, 2015). *In vivo* SASP is part of a pathological cascade to recruit immune cells for the clearance of senescent cells in tumours; and prolonged SASP can trigger chronic tissue inflammation (Blackburn, 1994).

SASP varies in different tissues and is generally induced at the level of mRNA (Coppe et al., 2008) and includes a wide range of growth factors, proteases, chemokines, and cytokines. Proteins that are known to stimulate inflammation, including IL-1, IL-6, IL- 8, granulocyte macrophage colony stimulating factor (GM-CSF), growth regulated oncogene (GRO)α, monocyte chemotactic protein (MCP)-2, MCP-3, MMP-1, MMP-3, and many of the insulin-like growth factor (IGF) binding proteins (Coppe et al., 2008; Kumar, Millis, & Baglioni, 1992; S. Wang, Moerman, Jones, Thweatt, & Goldstein, 1996) are among the most robustly induced. To date SASP has not been widely studied but some studies have revealed the effects of SASP which are beneficial, while others are

deleterious if left unchecked (Tominaga, 2015). In general, SASP is part of an inflammatory response induced by senescent cells and plays a major role in wound healing, development, aging, tumor progression and tumor prevention (Lasry & Ben-Neriah, 2015).

It is still unclear what triggers the activation of other SASP factors, as well as what determines which SASP factors will be activated upon senescence in different settings (Lasry & Ben-Neriah, 2015). SASP is widely described in homeostatic control of wound healing by limiting ECM deposition and preventing fibrosis (Gurtner, Werner, Barrandon, & Longaker, 2008). Apart from that, studies have described evidence of SASP in response to persistent DNA damage (Rodier et al., 2009) by downregulating lamin B, a major component of the nuclear lamina that leads to depression of immune genes and activation of systemic inflammation (H. Chen, Zheng, & Zheng, 2014). During development, senescence has been described to play a major role in correct patterning of the embryo (Munoz-Espin et al., 2013; Storer et al., 2013). For instance, senescence of NK cells in the placenta is crucial for vascular remodelling during the early stages of pregnancy (Rajagopalan & Long, 2012). In contrast to the beneficial roles in development and wound healing, senescence and inflammation are deleterious in chronic inflammation occurring in age-related disorders.

It is worth noting that senescence exerts paracrine effects through SASP, thus propagating senescence within cells of tissues (Figure 2.8) (Lasry & Ben-Neriah, 2015). Moreover, it has been described *in vitro* that conditioned medium induces senescence in cultures of proliferating cells (Acosta et al., 2013; Hubackova, Krejcikova, Bartek, & Hodny, 2012). The most described effect of SASP is disruption of normal tissue histoarchitecture, mainly by its ability to degrade the tissue microenvironment (Campisi, 2005). Also, it was reported that SASP disrupts function in mammary gland culture

models (Parrinello, Coppe, Krtolica, & Campisi, 2005). Effects of SASP have been described *in vitro*, including acceleration of the invasion of transformed cells in a Boyden chamber assay via an epithelial to mesenchymal transition in the cells (Coppe et al., 2008); stimulation of both endothelial cell invasion in a Boyden chamber assay and angiogenesis in a xenograft model (D. Liu & Hornsby, 2007); and promotion of the proliferation of premalignant or malignant epithelial cells *in vitro* and *in vivo* (D. Liu & Hornsby, 2007). Further, senescence has been claimed to serve a role as a tumor promoter, as senescent endothelial cells and fibroblasts are sometimes found adjacent to malignant tumors in humans (Charalambous et al., 2007; Studebaker et al., 2008) and tumor cells themselves can senesce *in vivo* in human patients treated with DNA-damaging chemotherapy agents or in mice forced to express the potent tumor suppressor protein p53 (Xue et al., 2007; Zhong et al., 2005). The plasticity function of SASP is diverse, hence it is still an area requiring much further investigation.
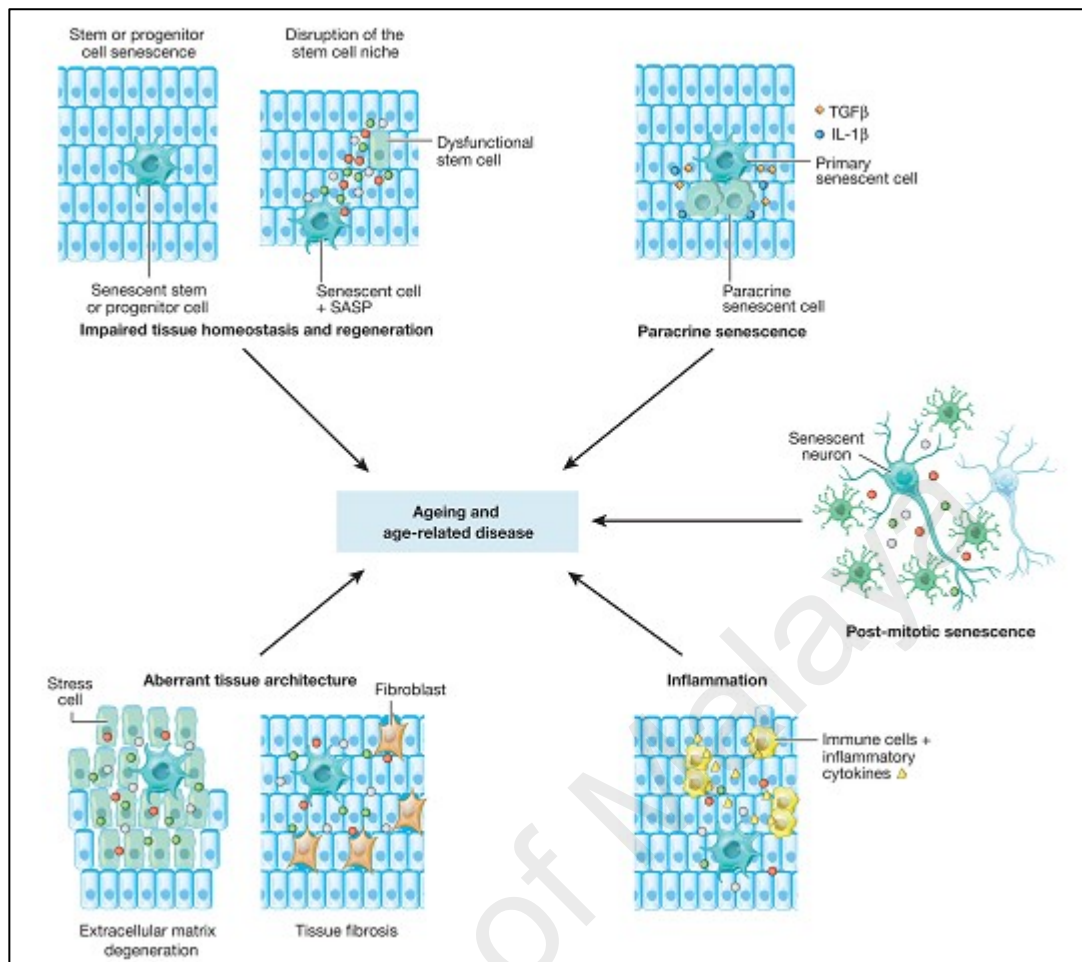
Figure 2.7:Senescence interferes with tissue homeostasis and regeneration, and lays the groundwork for its cell-non-autonomous detrimental actions involving the SASP. There are at least five distinct paracrine mechanisms by which senescent cells could promote tissue dysfunction, including perturbation of the stem cell niche (causing stem cell dysfunction), disruption of extracellular matrix, induction of aberrant cell differentiation (both creating abnormal tissue architecture), stimulation of sterile tissue inflammation, and induction of senescence in neighboring cells (paracrine senescence).

(van Deursen, 2014)
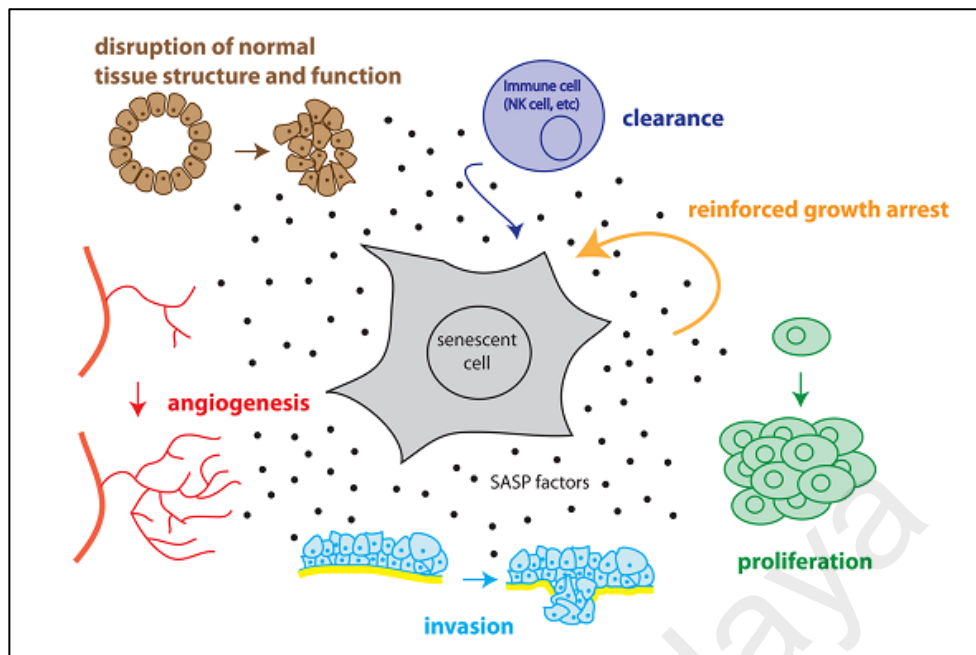
Figure 2.8: Response of cells to SASP depends on cell type. The SASP affects surrounding non-immune cells as well, increases proliferation of nearby epithelial and stromal cells, promotes invasion of any nearby preneoplastic or neoplastic cells via an epithelial to mesenchymal transition, stimulates angiogenesis by stimulating endothelial cells' migration and invasion, and disrupts normal tissue structure and function.

(Freund et al., 2010)

2.2.2.3   Wound Re-epithelialization Driven by Inflammation

Re-epithelialization is generally characterized as epithelial proliferation and migration over the provisional matrix within the wound (Guo & Dipietro, 2010) as a process of covering denuded epithelial surfaces (Pastar et al., 2014). This wound re-epithelialization is orchestrated by overlapping events including leukocyte recruitment, matrix deposition, epithelialization, and ultimately resolution of inflammation with the formation of a mature scar (Ashcroft et al., 2002). Although it becomes clear that wound healing processes employ a complex interaction among multiple different cells, 3-dimensional wound healing models as we currently know them are restricted to two key players: keratinocytes and fibroblasts. Keratinocytes play a function in immunity, especially in secretion of pro-inflammatory cytokines to recruit immune cells (e.g.

macrophages, T-lymphocytes, and neutrophils) and therefore protect cells from microbial pathogens (Pastar et al., 2014) as well as to facilitate re-epithelialization itself through a variety of physiologies. A better understanding of the re-epithelialization process may provide insights on the major mechanism behind the impairment of wound healing in BRONJ.

The surface of the re-epithelialization process employs migration and proliferation of basal cells towards the edge of the wound. The strength of the epithelium barrier depends on the outermost differentiated layer that has lost the capacity to proliferate; therefore, when an epithelium breach occurs, basal cells need to loosen the adhesion to each other and to the basal lamina to provide a flexible platform to migrate to the edge of the breach. This process is modulated by disassembly of cell-cell and cell-substratum contacts, maintained through desmosomes and hemidesmosomes, respectively (M. C. Heng, 2011). Underlying these mechanisms, however, are layered cascades of either paracrine and/or autocrine signaling that drive keratinocytes to cross-talk among other cells including fibroblasts, stem cells, and endothelial cells to facilitate migration of basal cells upward and trigger proliferation to ensure an adequate supply of cells to replace the compromised epithelium.

For the process of migration to begin, cell-cell interactions need to be dissolved by activation of PKCα, which decreases adhesion of desmosomes by triggering a transition from calcium-independent to calcium dependent desmosomes (Savagner et al., 2005) modulated by EGF and macrophage-stimulating protein (Santoro, Gaudino, & Marchisio, 2003). On the other hand, among multiple transcription factors involved in the process, transcription factor Slu allows for additional release of keratinocytes by heightening desmosomal disruption (M. C. Heng, 2011). As basal cells need to migrate upwards, basal cells adhering to the basement membrane need to be dislodged by

multiple proposed mechanisms targeting specific adhesion proteins expressed by basal cells known as α6β4 intergrins that bind to laminin-5 in the lamina densa of the basement membrane (Nguyen, Ryan, Gil, & Carter, 2000; Nikolopoulos et al., 2005).

Multiple regulators and modulators such as growth factors, cytokines, integrins, keratins, matrix metalloproteinases (MMPs), chemokines, and extracellular macromolecules modulate keratinocyte migration and proliferation. Among the most studied growth factors and receptors in modulating migration and proliferation of keratinocytes, is the family of epidermal growth factors (EGF) such as HB-EGF, EGF, and TGF-α that transactivate EGFR (Barrientos, Stojadinovic, Golinko, Brem, & Tomic-Canic, 2008). Some of the proteins even modulate expression of the cytokeratin proteins K6 and K16 (Lee et al., 2005) that have been claimed to increase viscoelastic properties of migrating cells (Freedberg, Tomic-Canic, Komine, & Blumenberg, 2001). Another group of growth factors, fibroblast growth factor (FGF)-2, FGF-7, FGF-10, and FGF-22 have also been shown to stimulate epithelialization mostly through paracrine effects. For instance, FGF2 (also known as KGF) is produced by fibroblasts and acts in paracrine fashion through KGF2IIIb receptor found exclusively on keratinocytes, resulting in increased migration and proliferation during wound healing (Werner et al., 1994).

On the other hand, cytokines such as IL-1, IL-6 and TNF-α have been shown to regulate migratory phenotypes of keratinocytes in a paracrine and/or autocrine manner. For instance, IL-1 secreted by keratinocytes triggers fibroblasts to secrete FGF-7 (Tang & Gilchrest, 1996) and KGF (Werner et al., 1994). Apart from that, IL-1 also has been shown to induce expression of K6 and K16 via an autocrine manner. Similar to IL-1, TNF-α also acts in an autocrine and paracrine fashion to promote fibroblast migration to an affected area and deposition of extracellular matrix (ECM) components, which increase keratinocyte motility during re-epithelialization (Sogabe, Abe, Yokoyama, &

Ishikawa, 2006). Another cytokine known as IL-6, which is secreted by neutrophils, acts as a chemoattractant to recruit immune cells to the site of the breach (Dovi, Szpaderska, & DiPietro, 2004; Werner et al., 1994) and at the same time regulates keratinocytes to respond to mitogenic factor and stimulate migration through a STAT3-dependent pathway (Gallucci, Sloan, Heck, Murray, & O'Dell, 2004).

Another crucial signaling molecule secreted by fibroblasts and keratinocytes is TGF-β1. Stimulation through TGF-β1 can promote migration through activation of MMPs (Jiang, Tomic-Canic, Lucas, Simon, & Blumenberg, 1995; Zambruno et al., 1995). The tight regulation of MMP activation is important to facilitate cell migration by providing a migration-conducive environment, consisting of fibrin and synthesized extracellular matrix (ECM). For instance, MMP-1, which is abundantly expressed at the wound edge, has been shown to sustain production of collagen type I during wound healing (Pilcher et al., 1999). In the re-epithelialization mechanism, proliferation of keratinocytes has been identified as equally important as migration. Studies have indicated that when basal cells migrate towards the wound area, the first layer of keratinocytes begin to proliferate (Pastar et al., 2014), depending on the availability of growth factors, degree of cell differentiation, and cell attachment to substrate (Pastar et al., 2014). The underlying proliferation process has shown an overlapping mechanism mode with migration through a network of a few growth factors including HB-EGF (heparin-binding), EGF, TGF-β1 and KGF (Gniadecki, 1998). Apart from that, cooperation between growth factors, MMPs, components of the ECM and integrins also promote keratinocyte proliferation (Pastar et al., 2014). For instance, the ECM will engage integrins to modulate the growth factor receptor pathway leading to increases of growth factor activity (Miranti & Brugge, 2002). Another finding reported is that insulin-like growth factor (IGF)-1 is also present in the wound, acting synergistically with HB-EGF in stimulating keratinocyte proliferation (Marikovsky et al., 1996). In addition note

that after keratinocytes have been activated to heal, cells will be deactivated, stop proliferating, and begin to stratify (Pastar et al., 2014).

Studies have shown that adverse effects of inflammation can lead to a non-healing wound. Inflammation is a normal part of the healing process and it is important in the removal of contaminating microorganisms. In the absence of effective decontamination, inflammation may be prolonged. Both bacteria and endotoxins can lead to the prolonged elevation of pro-inflammatory cytokines such as interleukin-1 (IL-1) and TNF-α and elongate the inflammatory phase. If this continues, the wound may enter a chronic state and fail to heal. This prolonged inflammation also leads to an increased level of MMPs, a family of proteases that can degrade the ECM.

Wound healing, as a normal biological process in the human body, is achieved through precisely and highly programmed events: 1) rapid homeostasis; 2) appropriate inflammation; 3) mesenchymal cell differentiation, proliferation, and migration to the wound site; 4) suitable angiogenesis; 5) prompt re-epithelialization; 6) proper synthesis, cross linking, and alignment of collagen to provide strength to the healing tissues (Gosain & DiPietro, 2004). Guo et al. (2010) reported that interruption, aberrancies, or prolongation in the process can lead to delayed wound healing or non-healing chronic wounds (Guo & Dipietro, 2010). However, often the delay in tissue repair results from disruption in the inflammatory phase of repair, with many different factors contributing to poor healing such as wound infection, foreign objects such as sutures, or the presence of debris and necrotic tissues. In addition, non-healing wounds have distinct characteristics. Among the characteristics are frequently high loads of bacterial contamination with growth factors, inflammatory mediators, and proteolytic enzymes imbalanced, favoring tissue degradation over repair. On the other hand, neutrophils and macrophages are abundant in these wounds and secrete many of the bioactive substances

that in high concentration exacerbate tissue damage (Dovi et al., 2004). Excess secretion of proteases such as MMPs are capable of degrading essentially all extracellular matrix components (ECM) and basement membrane proteins which can lead to substantial damage (Barrick, Campbell, & Owen, 1999; Gill & Parks, 2008).

2.2.2.4 Senescence and Impairment of Re-epithelialization

Studies have claimed that prolonged senescence through SASP can play a detrimental role in tissue function and repair. For example, proteases such as the matrix metalloproteinase family, which is chronically secreted by senescent cells may impair tissue structure by cleaving membrane-bound receptors, signaling ligands, extracellular matrix proteins or other compounds in the tissue microenvironment (Coppe et al., 2008; Parrinello et al., 2005). Other SASP components including IL-6 and IL-8 secreted by senescent fibroblasts may also stimulate tissue fibrosis in certain epithelial tissues by epithelial-mesenchymal interaction (EMT) (Coppe et al., 2008; Laberge, Awad, Campisi, & Desprez, 2012). There were also several studies reporting evidence in conjunction with impairment of re-epithelialization; including detection of senescent cells found in chronic non-healing wounds (Mendez et al., 1998; Stanley & Osler, 2001). Apart from that, the inhibition of senescence mechanism has been shown to increase activity of wound closure (Jun & Lau, 2010). More evidently, one study demonstrated reduced rate in re-epithelialization in mice after exhibiting premature aging and senescence. (L. Wang, Yang, Debidda, Witte, & Zheng, 2007). However, although senescent cell removal represents an attractive therapeutic avenue, there are many unknowns and potential pitfalls along this route. It was previously speculated that senescence through SASP has been facilitating wound-re-epithelization by limiting fibrosis during the final stages of wound healing (Jun & Lau, 2010; Krizhanovsky et al., 2008). Moreover, they also found that platelet-derived growth factor AA (PDGF-AA), which is also secreted during SASP from senescent cells at the injury site, accelerates skin repair by triggering differentiation

of non-senescent fibroblasts into myofibroblasts (Demaria et al., 2014). Despite many diverse studies on SASP in recent years, much remains unknown about the senescence associated inflammatory response, especially the difference between other types of inflammatory reactions and whether it is triggered or tissue specific (Lasry & Ben-Neriah, 2015).

2.3 The Current Trend of Oral Mucosal Models for *in vitro* Application Studies

Three-dimensional oral mucosa models (3D OMM) have been fabricated at many levels to achieve an optimal analogue that reflects the physical and functional characteristics of native epithelium tissue (Table 2.4). Begun as a tissue substitute to replace damaged/lost tissues in burn wounds, facial reconstructive surgery, chronic skin ulcers, cleft palate repair and carcinoma resection, they have advanced remarkably to be reliable and informative study model systems which potentially bridge the gap between cell-based discovery research and animal models (Table 2.5). Most of the *in vitro* application of tissue engineered oral mucosa has been adapted from the study of skin and oral squamous cancerous models.

There has been a shift of *in vitro* study models from two-dimensional (2D) keratinocyte monolayers to organotypic tissue engineered oral mucosa models that mimic morphological, geometrical and complexity features of *in vivo* tissues. In living organisms, development is well orchestrated by numerous regulatory factors that dynamically interact in the same type of cells, different types of cells, and between the cell and matrix at multiple levels. Therefore, the *in vitro* strategy of 3D OMM introduces approximate apical-basal polarity for cells to function innately in a co-culture system with an extracellular matrix protein blend, devoid of the unnatural geometric and single cell type constraints introduced by monolayer cell model systems.

The monolayer model system is not predictive of *in vivo* tissue response, especially towards the aim of reducing animal model testing. Indeed, there are *in vitro* studies using two types of model studies: monolayer and three dimensional in order to assess the potential of pharmaceutical agents in the oral mucosa, especially agents extracted from natural products (Khovidhunkit et al., 2011). On the other hand, these two model systems have been compared as a way to assess the potential of chemotherapeutic drugs and xenobiotic stress sources, which resulted in three-dimensional models displaying more resistance compared to monolayer model systems (Sun, Jackson, Haycock, & MacNeil, 2006). Sun et al. (2006) reported that keratinocytes, dermal fibroblasts and endothelial cells co-cultured under 3D conditions portrayed marked resistance to oxidative stress and heavy metal (silver) compared to monolayer (2D) and mono-culture (Sun et al., 2006).

In contrast, three dimensional cultures of oral keratinocytes exhibit new characteristics, which monolayer study systems failed to exhibit in terms of diversification of cell and tissue morphology, higher expression of certain stem cell markers, expression of metalloproteinases (MMP), pro-inflammatory cytokines (Dongari-Bagtzoglou & Kashleva, 2006b; Schaller, Mailhammer, & Korting, 2002), and most importantly the influence of epithelial-mesenchymal interaction (EMT). In addition, the three-dimensional models simulate an environment for cultured cells with an *in vivo*-like, but fully controllable environment, especially in terms of host-pathogen interaction. The full interaction of pathogen and multiple host cells provides a whole study system to assess the virulence factors of pathogens at multiple levels simultaneously, monitoring tissue damages and expression of certain fungal and host proteins (Korting, Patzak, Schaller, & Maibach, 1998; Schaller et al., 2002) and targeted genes for therapeutic application (Rouabhia et al., 2012).

The recruitment of endothelial cells in a three dimensional model of skin (Sun et al., 2006) for *in vitro* testing of cytotoxicity agents demonstrated how much complexity an *in vitro* model system could achieve. Interactions of multiple host cell types with pathogens or cytotoxicity agents could be assessed in multiple ways. The potential of 3D OMM as an *in vitro* study system has been further explored since. However, the culture strategies behind the establishment of these models remain to be explored in order to be accepted as a standardized three-dimensional model system that is able to approximate the tissue response of native tissues.

The concept of an organotypic model of oral mucosa has been exploited, depending on the study application, in conjunction with the advancement of biomaterials/and or synthetic scaffolds and cell cultureware in tissue engineering. The current viewpoint of the architecture of organotypic full thickness oral mucosa models constructed by a multi-layered cell system consisting of oral epithelial cells and underlying mesenchymal cells with a basement membrane in between is that they simulate the tissue environment and histological features of the oral epithelium. However, reviewing the literature shows, there are also studies that utilize 3D OMM without a connective tissue layer representative, hence lacking a lamina propria layer.

The establishment of well-organized three-dimensional architecture from cell lines and primary cells can be achieved through various detailed methodologies including the choice of scaffold, isolation and cell dissociation techniques, co-culture strategies, and culture media recipes, which all contribute to one aim, adaptation of tissues to the *in vitro* environment.

Table 2.4: A Summary of Studies on Oral Mucosal Models

Author (year)	Normal /Immortalized Cell Line Model	Scaffold	Construction of Model-Co-Culture, Submerge, ALI	Culture media	Application
Hai S Duong (2005)	Oral squamous carcinoma cell lines (SCC-9 and SCC 4)	Fibroblast populated collagen type I	Double seeding	FAD media supplemented with 10% FBS and hydrocortisone	*In vitro* model (cancer invasion)
Dongari-Bagtzoglou (2006)	Normal,OKF 6/TERT 2	Fibroblast populated collagen type I	Double seeding, Submerged (6 days) ALI (14 days)	Keratinocytes-SFM plus 5% FBS supplemented with $CaCl_2$ and glucose and keratinocyte additives	*In vitro* model (*Candidiasis* study)
M.C Sanchez (2007)	Normal	Fibroblast populated Fibrin-agarose	Double seeding, Submerged (10 days) ALI (21 days)	FAD media plus 10% FCS and keratinocyte additives	Transplantation
Mitchell Klausner (2007)	Normal	None	Submerged (4 days) ALI (7 days)	Serum-free DMEM:F12 (2:1) and keratinocyte additives	Toxicity
Moharamzadeh,K (2008)	TR 146	Fibroblast populated Collagen-GAG-chitosan porous scaffold	Double seeding Submerged (3 days) ALI (10 days)	FAD media supplemented with 10% FBS and keratinocyte additives	Toxicity
Locke M (2008)	Normal	Fibroblast populated collagen	Double seeding, Submerged (24 hr) ALI (14 days)	FAD media containing 10% FBS and keratinocyte additives	*In vitro* model (Epithelial-Mesenchyme interaction)
Hai S Duong (2005)	Oral squamous carcinoma cell lines (SCC-9 and SCC 4)	Fibroblast populated collagen type I	Double seeding	FAD media supplemented with 10% FBS and hydrocortisone	*In vitro* model (cancer invasion)

Table 2.4, continued

Author (year)	Normal /Immortalized Cell Line Model	Scaffold	Construction of model-co-culture, submerge, ALI	Culture media	Application
M.C Sanchez (2007)	Normal	Fibroblast populated Fibrin-agarose	Double seeding, Submerged (10 days) ALI (21 days)	FAD media plus 10% FCS and keratinocyte additives	Transplantation
Mitchell Klausner (2007)	Normal	None	Submerged (4 days) ALI (7 days)	Serum-free DMEM:F12 (2:1) and keratinocyte additives	Toxicity
Moharamzadeh,K (2008)	TR 146	Fibroblast populated Collagen-GAG-chitosan porous scaffold	Double seeding Submerged (3 days) ALI (10 days)	FAD media supplemented with 10% FBS and keratinocyte additives	Toxicity
Locke M (2008)	Normal	Fibroblast populated collagen	Double seeding, Submerged (24 hr) ALI (14 days)	FAD media containing 10% FBS and keratinocyte additives	*In vitro* model (Epithelial-Mesenchyme interaction)
Keerthi K Kulasekara (2009)	Normal, dysplastic human oral keratinocytes (DOK cell lines), neoplastic oral keratinocytes (PE/CA-PJ15 cell lines)	Fibroblast populated collagen type I	Double seeding, ALI (10 days)	FAD media –serum free supplemented with ascorbic acid and keratinocyte additives	*In vitro* model (cancer progression)
T.Tobita (2010)	Normal	AlloDerm coated with collagen type IV	Submerged (4 days) ALI (7 days)	EpiLife media supplemented with high calcium	*In vitro* model system (radiation-induced effect)
Pena et al. (2010)	Normal	Fibroblast populated fibrin-glue	Double seeding, Submerged (26-30 days)	FAD media plus 10% FBS and keratinocyte additives	Transplantation
Bayar G.R (2011)	Normal	AlloDerm-coated collagen type IV	Submerged (4 days) ALI (7 days)	EpiLife media supplemented with high calcium and EDGS (human keratinocyte growth factor) and keratinocyte additives	Evaluation

53

Table 2.4, continued

Author (year)	Normal /Immortalized Cell Line Model	Scaffold	Construction of model-co-culture, submerge, ALI	Culture media	Application
Yadev N.R (2011)	Normal	Fibroblast populated in de-epidermized dermis	Co-culture Submerged (3 days) ALI (14 days)	FAD media supplemented keratinocyte additives	*In vitro* model (oral candiadis)
E.L McGinley (2011)	Normal	AlloDerm populated with fibroblast	Co-culture Submerged (2 days) ALI (4 days)	FAD media supplemented keratinocyte additives	Biocompatibility Assessment (base-metal dental casting alloy)
Siribang-on Piboonniyo Khovidhunkit (2011)	Normal OKF 6/TERT 2	Fibroblast populated collagen	Double seeding	Keratinocyte-serum free media (K-SFM, Gibco USA)	*In vitro* model (Wound healing study)
Chai WL (2012)	TR 146	AlloDerm populated with fibroblast	Co-culture, Submerged (5 days) ALI (3-5 days)	FAD media and keratinocyte additives	*In vitro* model (implant-soft tissue interface)
Tra WM (2013)	Normal	De-epidermized dermis-fibroblast populated in agarose	Double seeding, Submerged (24 hrs) ALI (14 days)	FAD media plus 1% FCS supplemented with fatty acid cocktail and KGF (keratinocyte growth factor) and keratinocytes additives	*In vitro* model (ionizing radiation)

Table 2.5: List of *In Vitro* Application Studies Using Oral Mucosal Model

Type of In vitro Studies	Agent Tested /Drug/Disease Model	Cell Lines	Lamina Propria representatives	Analyses Techniques	Author (Year)
Biocompatibility	Base-metal dental alloys	Primary Oral Keratinocytes	AlloDerm™ (co-culture with fibroblast)	Inflammatory cytokines expression (IL-1α, IL8, prostaglandin E2 and TNF-α)	E.L Mc Ginley (2012)
	Orthodontics wires	TR 146 cell lines-Commercially available RHOE by SkinEthics	N/A	LDH assay	Vande Vannet, B (2007)
	Dental-composites resins	TR 146 cell lines	Cross-linked collagen-GAG-chitosan porous scaffold laminated with Matrigel populated with fibroblast	Inflammatory cytokines IL-1β	Moharamzadeh, Brook et al. (2008)
	Oral healthcare ingredients	TR 146 cell lines-Commercially available RHOE by SkinEthics	N/A	Differential release of inflammatory cytokines IL-1α, IL-8 via ELISA and qPCR, LDH release assay and MTT viability assay	(Hagi-Pavli, Williams, Rowland, Thornhill, & Cruchley, 2014)
	Effect of ethanol	Primary Oral Keratinocytes	Insert	H&E for histology and Alamar blue for viabiliry	K.Moharamzadeh (2015)

Table 2.5, continued

Type of In vitro Studies	Agent Tested /Drug/Disease Model	Cell Lines	Lamina Propria representatives	Analyses Techniques	Author (Year)
Therapeutic Treatment	Tacrolimus ointment - T-cell-mediated inflammatory oral mucosal diseases, including lichen planus	Primary Oral Keratinocytes	Collagen-populated fibroblast	Expression of EGF-R, TUNEL assay, adhesion test	(Rautava et al., 2012)
Pressure-loading Studies	Cyclic mechanical pressure mimicking denture wearers	Primary Oral Keratinocytes	Collagen-populated fibroblast	Immunohistochemistry of Ki-67, laminin, fillagrin, involucrin, integrin ß1 , MMP-9, type IV collagen	A Shiomi (2015)
Disease model	Oral *candidiasis*	Primary Oral Keratinocytes	Collagen-populated fibroblast	LDH assay, Apoptotic	(Rouabhia et al., 2012)
	Oral *candidiasis*	TR 146 cell lines	Porous Scaffold	Inflammatory cytokines TNF-α, IL-1β and CXCL8	Yadev N.R (2011)
	Oral *candidiasis*	OKF 6/TERT 2	Collagen-populated fibroblast	Inflammatory Cytokines	A.Dongari (2006)

Type of In vitro Studies	Agent Tested /Drug/Disease Model	Cell Lines	Lamina Propria representatives	Analyses Techniques	Author (Year)
Disease Model	Chronic Periodontitis	Primary Oral Keratinocytes	Unknown (no full text yet)	Expression of matrix metalloproteinase (MMP), tissue inhibitor matrix metalloproteinase (TIMP) via protein and mRNA level	(Andrian, Mostefaoui, Rouabhia, & Grenier, 2007)
	Oral *candidiasis*	Primary Oral Keratinocytes	Collagen-populated fibroblast	Expression of Toll-Like Receptor, human β defensins and pro-inflammatory cytokines IL-1β and IL-6	(Semlali, Leung, Curt, & Rouabhia, 2011)
	Radiotheraphy induced oral mucositis	Primary Oral Keratinocytes	Collagen-populated fibroblast	Post-radiation pro inflammatory cytokines (IL-1α and IL-8)- ELISA	T.Tobita (2010)
	Radiotheraphy induced oral mucositis	Primary Oral Keratinocytes	Acellular dermis (co-culture with fibroblast)	DNA damage and repair, Zymography for MMP-2 and MMP-9, IL-1ß, TGF-β, and tissue inhibitor of matrix metalloproteinase types 1 and 2 (TIMP-1 and TIMP-2) via ELISA, proliferation and apoptosis index	(Tra, Tuk, van Neck, Hovius, & Perez-Amodio, 2013)
	Oral *candidiasis*	Primary Oral Keratinocytes	Acellular dermis (co-culture with fibroblast)	Inflammatory cytokines TNF-α, IL-1β and CXCL8	(Yadev, Murdoch, Saville, & Thornhill, 2011)
	Bisphosphonate related osteonecrosis of jaw (BR-ONJ)	Primary Oral Keratinocytes	Acellular dermis (co-culture with fibroblast)	Expression of αvβ6	(Saito et al., 2014)

Table 2.5, continued

Type of In vitro Studies	Agent Tested /Drug/Disease Model	Cell Lines	Lamina Propria representatives	Analyses Techniques	Reference
Disease Model	*Porphyromonas Gingivalis* invasion	Primary Oral Keratinocytes and Cell Lines H357	Collagen populated with fibroblast	Immunodetection of specific P.Gingivalis antibody and chemokine array of inflammatory marker	Pinnock et al (2014)
Dental Implant System	n.a	TR 146	Acellular dermis (co-culture with fibroblast)	Attachment Test	Chai WL (2013)

2.3.1 Introduction of Normal Oral Mucosa Tissues

The moist lining of the oral cavity is called oral mucosa. It forms a continuous structure with the skin outside of the oral cavity but differs in appearance and structure, due to different environments exposed. The oral cavity is surrounded by saliva and moist all the time compared to skin. In the oral cavity, there are three types of mucosa depending on the function of either absorption or mastication, i.e. masticatory mucosa (hard palate and gingiva), specialized mucosa (tongue) and lining mucosa (buccal and the rest of the oral cavity). Regardless of the location of the cell; kidney, liver, gut, soft palate, gingival tissue, and skin, epithelial layers always serve to protect internal tissue from physical and chemical damage, infection, dehydration, heat loss, and mechanical stress (J. Liu, Bian, Kuijpers-Jagtman, & Von den Hoff, 2010; Presland & Jurevic, 2002) in their own way. In order to protect the underlying tissue, whether skin or oral mucosa, both have evolved defense mechanism that includes homeostasis between maturation and proliferation of the cell. This homeostasis serves the function of rapid clearing of the substrate to which many microorganisms adhere, so the microbes with are unable to produce toxic effects or to invade (Squier & Kremer, 2001).

Oral mucosa is built from stratified squamous epithelium; however, in the lining of the stomach and small and large intestine, the single layered lining of epithelium is useful for its special function of absorption and secretion. (Presland & Jurevic, 2002). Three different types of oral mucosa lining the oral cavity, differ in the keratinization pattern, generally dictated as keratinized and non-keratinized epithelium layers. Epithelial lining in skin and oral mucosa consists of multiple layer of cells with various stages of differentiation (maturation) from the deepest layer to the surface (Squier & Kremer, 2001). Generally, there are four layers of cells: basal layer, prickle-cell layer, granular

layer and keratinized layers. As for non-keratinized oral mucosa, the keratinized layer is absent. In contrast to the epidermis of skin, which is merely orthokeratinized, all three major differentiation patterns of keratinocytes occur in normal oral epithelia. In regions subject to mechanical forces associated with mastication such as the gingiva and the hard palate, a keratinized epithelium resembling that of the epidermis occurs. The pattern of maturation of keratinized epithelium mostly is orthokeratinization. Parts of these keratinized areas show a variation of keratinization, known as parakeratinization, in which the nuclei of the cornified layer are still recognizable. The floor of the mouth and the buccal regions, which require flexibility to accommodate chewing, speech, or swallowing, are covered with a lining mucosa with a non-keratinizing epithelium. The specialized mucosa on the dorsum of the tongue contains numerous papillae and is covered by an epithelium, which may be either keratinized or non-keratinized (J. Liu et al., 2010).

Apart from the keratinization pattern, the pattern of attachment to underlying tissue by connective tissue varies related to mastication. For example, the hard palate and gingiva tightly attached to underlying tissue by collagenous connective tissue in contrary to buccal and floor of the mouth, which require the flexible connective tissue to accommodate the chewing and speech. Apart from attachment to underlying structure, connective tissue also provides nutrients to epithelium layers.

For keratinized lining like skin and hard palate, the epithelial cell undergoes terminal differentiation and produces a predominant structural protein known as cytokeratin besides other structural proteins such as profillagerin, involcurin and loricrin to form the envelope protein barrier. Non-keratinized epithelia also express cytokeratin but do not aggregate to form bundles. (Squier & Kremer, 2001). As keratinocytes differentiate, the cell loses the organelles and fills the space with cytokeratin and lipid lamellae on the

surface while non-keratinized epithelium retains the organelles and extrudes short stacks of lipid lamellae (Squier & Kremer, 2001). Cytokeratin belongs to the intermediate filament superfamily. There are two types of families of keratin; Type I and type II which will have paired accordingly based on stage of differentiation. Cytokeratin is expressed a tissue-and cell-specific manner and often is used as the tissue specific-identification marker in a study. In order to maintain the cell and tissue integrity, cytokeratin will be produced and extend out to the cell surface from the nucleus, by being glued to adjacent cells by desmosomes. Cells will be cornified and the plasma membrane will be replaced by inter-linking proteins and will produce membrane coating granules containing lipid. As cells migrate superficially, keratinocytes undergo differentiation expressing different pairs of keratins. However, in certain circumstances like wound healing and cancer, keratinocytes, even in the upper layer will switch from differentiation to proliferation mode, aided by inflammatory cytokines and growth factors.

Oral mucosa equivalent consists of a portion of epidermis that contains keratinocytes and a deeper portion of dermis separated by a basal membrane (Sarper, 2011). Connective tissue forming the support structure includes lamina propria and submucosa for attachment. The term called non-keratinocytes includes Langerhan's cells, Merkel cells and melanocytes that lack desmosomal attachments intercellularly. Melanin pigments produced by melanocytes in the basal cell layer are injected into cytoplasm of adjacent keratinocytes, contribute the red color of oral mucosa (Squier & Kremer, 2001). Langerhan's cell is identified to serve as immunogenic function to help T-lympocytes in combating foreign material from environment. The constituent of in vivo oral mucosa is crucial to guide the scientist in producing reliable and reproducible three-dimensional models of the oral mucosa. The different layers of keratinocytes must be mimicked and generated on the dermal substitute with a proliferating basal cell layer as the foundation

layer. In future research endeavors, the importance of non-keratinocytes as part of the microenvironment toward regenerating the oral mucosa should not be neglected.

2.3.2 Three Dimensional Oral Mucosa Model (OMM)

For *in vitro* studies, organotypic oral mucosa models can be distinguished into two types: primary and immortalized cell line oral mucosal models (OMM), in which the source of epithelial cells are obtained from normal or tumor biopsies or established immortalized epithelial cell lines respectively (Dongari-Bagtzoglou & Kashleva, 2006a). The source of normal tissues has been from the biopsies of different sites of the oral cavity, i.e. masticatory mucosa such as gingiva (Bart Vande Vannet 2007; Chai et al., 2010; Dongari-Bagtzoglou & Kashleva, 2006a; Moharamzadeh, Brook, Scutt, Thornhill, & Van Noort, 2008; Moharamzadeh, Brook, Van Noort, et al., 2008) or non-keratinized oral mucosa area such as buccal (Dongari-Bagtzoglou & Kashleva, 2003a, 2003c; Dongari-Bagtzoglou, Wen, & Lamster, 1999) and alveolar mucosa (Devalia, Bayram, Abdelaziz, Sapsford, & Davies, 1999). The primary oral keratinocytes from the normal biopsies used in the construction of primary OMM more closely mimics the native tissue. However, one of the main constraints in culturing the primary oral keratinocytes is the limited *in vitro* life span of oral keratinocytes. It could normally subculture up to a fourth time (Rouabhia et al., 2012) due to senescence-based growth arrest (Dongari-Bagtzoglou & Kashleva, 2006b) and irreversible commitment of keratinocyte proliferation to differentiation (Bart Vande Vannet 2007). This feature may restrain the researchers to be able to grow enough cells for the number required in the OMM of the experiment. Primary cell lines have a limited life span in vitro and can be inconsistent in their contribution to 3D architecture due to donor variation(Bart Vande Vannet 2007) and from one donor to another there is variable constitutive and inducible expression of proteins (Cox, Gauldie, & Jordana, 1992; Devalia et al., 1999; Dongari-Bagtzoglou & Kashleva, 2003a, 2003c; Dongari-Bagtzoglou, Kashleva, & Villar, 2004; Dongari-Bagtzoglou et al., 1999; Feucht,

DeSanti, & Weinberg, 2003). The inconsistency of growth rate and protein expression introduced by a population of oral keratinocytes derived from normal tissues will hinder construction of reproducible and homogenous organotypic oral mucosa for *in vitro* experimental study.

Alternatively, immortalized cell lines of keratinocytes have been established to be more competent as a component of oral mucosa model testing for *in vitro* experiments, especially for repeated analysis which requires bigger sample sizes and standardized models. In order to overcome culture challenges of primary cell lines and normal-deviated immortalized cell lines, some studies reported on establishing both types of model to assess different parameters. Chai et al. developed organotypic oral mucosa derived from primary oral epithelial cells for qualitative analysis of the implant-soft tissue interface (Chai et al., 2011) but established a TR146 cell line 3D OMM for quantitative analysis of the biological seal of the implant-soft tissue interface (Chai, Brook, Palmquist, van Noort, & Moharamzadeh, 2012)

Epithelial cells could either be obtained from normal or tumor biopsies (primary cells) and from established immortalized epithelial cell lines (expressing E6/E7 gene from human papillomavirus type 16) in which telomerase was overexpressed (OKF6/TERT2) immortalized epithelial cell lines by E6/E7 gene of human papillomavirus type 16 (HPV 16) (Roesch-Ely et al., 2006) and forced expression of telomerase (OKF6/TERT-2)(Dongari-Bagtzoglou & Kashleva, 2006a). The switching pattern of using immortalized cell lines to replace primary cell lines is limited to studies involving biocompatibliity (Bart Vande Vannet 2007; Moharamzadeh, Brook, Van Noort, et al., 2008), toxicity, (Moharamzadeh, Brook, Scutt, et al., 2008) and clinical translation studies (Chai et al., 2010). Regardless there is evidence that OMM's constructed from immortalized cell lines are associated with aberrant chromosomal profiles (Boukamp et al., 1997) and different

keratin expression compared to normal organotypic oral mucosa models (Kulkarni et al., 1995). On the other hand, in cancer morphogenesis studies, scientist develop in house organotypic models derived from tumor tissues (Duong, Le, Zhang, & Messadi, 2005; Kulasekara et al., 2009) with normal cell line models as controls. However for in vivo studies, organotypic co-culture systems use primary cell lines derived from normal tissues to avoid recipient rejection during transplantation (Bhargava, Chapple, Bullock, Layton, & MacNeil, 2004; Boukamp et al., 1988).

Several studies have successfully used immortalized cell lines OKF 6/TERT 2 space here and in successive, similar situations (Dongari-Bagtzoglou & Kashleva, 2006c), IHGK (Roesch-Ely et al., 2006) and TR 146(Chai et al., 2012) to be constructs three dimensional settings without introducing aberrant changes in keratin expression (Dongari-Bagtzoglou & Kashleva, 2006b; Jha et al., 1998; Okuyama, LeFort, & Dotto, 2004; Rheinwald et al., 2002; Roesch-Ely et al., 2006). The immortalized cell line oral mucosal model constructed with the TR146 cell line, cultured on a polycarbonate insert with or without either scaffold or mesenchymal cell, formed a stratified squamous epithelial layer, sharing many morphological and functional characteristics of normal mucosa (Nielsen & Rassing, 2000; Sander, Nielsen, & Jacobsen, 2013; Vande Vannet & Hanssens, 2007). Besides similar morphological and functional characteristics, the TR146 cell line cultured model has been claimed to be compatible as an *in vitro* testing model for drug permeability and delivery systems (Nielsen & Rassing, 2000; Sander et al., 2013), biocompatibility of dental biomaterials (Bart Vande Vannet 2007; Moharamzadeh, Brook, Scutt, et al., 2008; Moharamzadeh, Brook, Van Noort, et al., 2008) and clinical testing for implant-soft tissue interface studies (Chai et al., 2010). In other studies, various primary cell lines isolated from oral-origin cancer tissues managed to be cultured into three dimensional models especially in collagen embedded fibroblasts (Che et al., 2006; Duong et al., 2005; Kulasekara et al., 2009). These models have served

as models for different stages of cancer invasion analysis (Colley, 2009), study of the function of basement membrane proteins in cancer cell invasion, (Kulasekara et al., 2009), the interaction of cancer and stromal cells such as fibroblasts (Berndt, Hyckel, Konneker, & Kosmehl, 1998; Che et al., 2006), and the invasion by malignant oral epithelial stem cells normal oral epithelial cells(Mackenzie, 2004). In addition, organotypic models derived from TR146 cell lines have been commercially available from SkinEthic Laboratory (Nice, France) and have been reported in several *in vitro* studies for toxicity of soldered and welded wire(Bart Vande Vannet 2007) and as well as for a candidiasis model(Dongari-Bagtzoglou & Kashleva, 2006b; Yadev et al., 2011), despite lacking a mesenchymal component (Dongari-Bagtzoglou & Kashleva, 2006c).

Although immortalized cell lines are stable compared to primary cells lines, they do not accurately reflect the responses of normal epithelial cells and should be confirmed further with other cell lines(Dongari-Bagtzoglou & Kashleva, 2006b). Therefore, the 'normal' oral epithelial cell line named OKF6/TERT-2, which was immortalized by forced expression of telomerase from normal tissue instead of cancer tissue, has been established to fulfill the analogue requirement to normal oral keratinocytes, OKF6/TERT2 are relatively devoid of "donor to donor" variation during primary isolation (Dongari-Bagtzoglou & Kashleva, 2006c). The 'normal' OKF6/TERT-2 oral mucosal model has been used to study oral *Candida* infection (Dongari-Bagtzoglou & Kashleva, 2006c) and the relationship between mesenchymal-epithelial transition (MET) and epithelial-mesenchymal transition (EMT) for maintenance of stem cell properties (Qiao et al., 2012).

CHAPTER 3:METHODOLOGY

3.1   Procurement of oral mucosa samples, isolation, and culture of primary normal human oral fibroblast cultures (NHOF)

In this study, the oral mucosa model was composed multilayer of OKF 6/TERT 2 cells and submucosa consisted of normal human oral fibroblast embedded in an acellular dermis. The normal human oral fibroblasts were isolated from gingival tissues retrieved from minor oral surgery procedures. Gingival tissues were taken from healthy individuals, males and females, aged 20-45 years old upon approval by the Medical Ethics Committee (No.DFDP1406/0061(L). Half of the biopsies were formalin-fixed paraffin embedded (FFPE). The remaining biopsies were rinsed 3 times for 5 mins per wash with Dulbecco Modified Eagle Media (DMEM) supplemented with Gibco® antibiotic-antimycotic, which contains 100 units/ml penicillin, 100 ug/ml streptomycin and 0.25ug/ml of Amphotericin B. The connective tissue was separated from epidermis by overnight incubation in 0.4mg/ml dispase solution (Sigma Aldrich Company, Ayrshire, UK) at 4°C (Figure 3.1). The separated connective tissue was then subjected to 0.05% (w/v) collagenase type I (Gibco, Thermo Fischer Scientific Company, Waltham, USA) at 37°C for overnight. After 24 hours' incubation, the tissue suspension was centrifuged at 1000 rpm for 5 minutes before being resuspended in complete Dulbecco Modified Eagle Medium (cDMEM) and plated at 6,000 cells /cm^2.

OKF 6/TERT 2 cell lines were thawed and resuspended in 10ml serum free media (Keratinocyte Serum FreeMedia, Gibco, Invitrogen) (see Appendix A 2)and centrifuged at 1000 rpm for 5 mins to remove remaining dimethyl sulfoxide (DMSO) in suspension. Cells were plated at 10,000 cells/cm^2 in T75 flasks until confluence in approximately 5-6 days. All media were changed every 2 days until confluent.
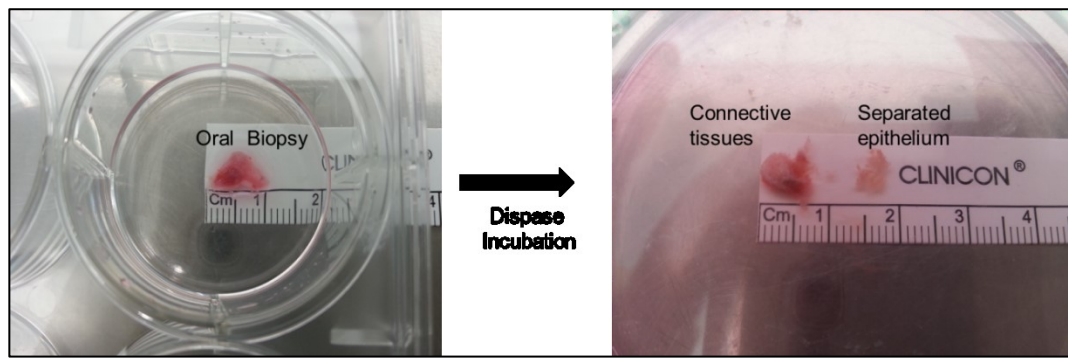
Figure 3.1: Separated layers of the oral mucosal biopsy after overnight incubation in Dispase I at 4°C.

3.2 Cell Culture and Maintenance

This model is composed of a multilayer of OKF 6/TERT 2. These cells represent normal oral mucosa epithelium immortalized by forced expression of telomerase via retroviral transduction (Dickson et al., 2000) and was kindly provided by Professor Ian Paterson (University of Malaya). Cells were grown in Keratinocyte Serum Free Media (K-SFM) supplemented with 1ng/ml epidermal growth factor (EGF), 100 units/ml Penicillin and 100 ug/ml Streptomycin, 30ug/ml Bovine Pituitary Extract (BPE) and 0.4mM dihyrated calcium chloride ($CaCl_2$). Primary normal human oral fibroblast (NHOF) was maintained in complete high glucose (4.5g/l) Dulbecco modified Eagle medium (DMEM) contain 10% fetal bovine serum, 2mM Glutamax and 100 units/ml penicillin and 100 ug/ml streptomycin. Both cells were maintained at 37°C, 5% CO_2 and 95% air in a humidified incubator, followed by media changing every 2 days and routine passage at 70% confluency.

Upon reaching the desired confluency of 70%, cells were detached for subculture or actual plating for experiment. Briefly, culture media was removed and 3ml of 0.25% Trypsin-EDTA was added to T-75 flask for 20-25 minutes (OKF 6/TERT 2 cells) and 3-5 minutes for NHOF. Flasks were visualized under light microscopy for presence of

floating cells. If cellular attachment was observed, flasks were tapped gently to facilitate the detachment of cells. Culture media containing 10% FBS was gently added to each flask to stop trypsinization activity. The cell suspensions were collected and transferred to a 20ml universal vial and centrifuged at 1000rpm for 5 minutes. The cell pellet was resuspended in 1ml culture media. For the cell count, 10ul of the homogenous sample was mixed with 10ul of trypan blue stain. The cell suspension was loaded onto a Luna™ Cell Counting Slide (Logos Biosystems, Dongan-gu Anyang-si, Gyeonggi, Korea). Cell count and viability was automatically measured after the slide was inserted into the instrument. Depending on the number of cells calculated, sufficient culture media was added to resuspend the cells at 1×10^6 cells per ml. The suspension was gently mixed thoroughly to break up the cell pellet and evenly distribute the cells throughout the mixture. OKF 6/TERT 2 and normal human oral fibroblasts were seeded at 16,000 cells/cm^2 and 5,000 cells/cm^2, respectively for all experiments including routine passaging. All experiments were performed on cells seeded 24-48 hours in advance, allowing cells to attach to the surface of the tissue culture ware and reach 70% confluency for the experiment.

3.3 Assay of Growth Characteristics of Cell Lines-Seeding Density and Cell Proliferation

Isolated primary normal human oral fibroblast (NHOF) cells from gingival tissues from two donors were first analyzed for 1) growth curve analysis within passages and multiple passages, and 2) optimization of seeding density using trypan blue dye exclusion tests of cell viability using 0.4% trypan blue solution and 3-(4,5-dimethylthiazol-2-yl)-2,5-diphenyl tetrazolium bromide (MTT) colorimetric assay (Sigma Aldrich Company, Ayrshire, UK), respectively (see Appendix B 4)70% confluency by placement of 100,000 cells per flask regardless of cell yield. The total number of cells was calculated based on

the assumption that all cells from the previous passage had been replated. Cell number was counted using a trypan blue exclusion test using automated Luna™ Cell Counting (Logos Biosystems, Dongan-gu Anyang-si, Gyeonggi, Korea), and plotted against days of culture. Cell-doubling time (DT) was calculated for every passage according to this formula (Rainaldi et al., 1991):

$$DT = \frac{CT}{\ln(N_f/N_i)/(\ln(2))}$$

where DT is the cell-doubling time, CT the cell culture time, N_f the final number of cells, and N_i the initial number of cells. This assessment was to determine the quality of cells isolated from mucosa tissues and to avoid using unhealthy cells during construction of 3D OMM.

Optimization of seeding density was performed for both cell types to determine the most efficient seeding density for experiments of the monolayer and construction of the 3D OMM. Experiments of seeding density were performed based on 2-fold dilution series with different starting cell numbers for OKF 6/TERT 2 and NHOF. For NHOF, a total of 50,000 cells was added directly into the first well (triplicate) of a 96 well plate containing 100ul media. Following that, 100ul of culture media was then added into each of the remaining wells. A two-fold dilution series was performed, and each well was mixed thoroughly before transfer (Figure 3.2). For OKF 6/TERT 2 cells, the dilution series established corresponded to 250,000; 125,000; 62,500; 31,250; 15,625; 7,813 cells/cm^2, and for NHOF cells corresponded to 10,000; 5,000; 2,500; 1,250; 625; 313 cells/cm^2 was established using serial dilution in 96 well plates. Each triplicate cell number was assayed every 24 hours up to 120 hours with a change of media every 48

hours. Optical density was measured at 570 nm with a reference wavelength of 690 nm using a multi-plate reader (Thermo Fisher Scientific, Waltham, MA, USA).
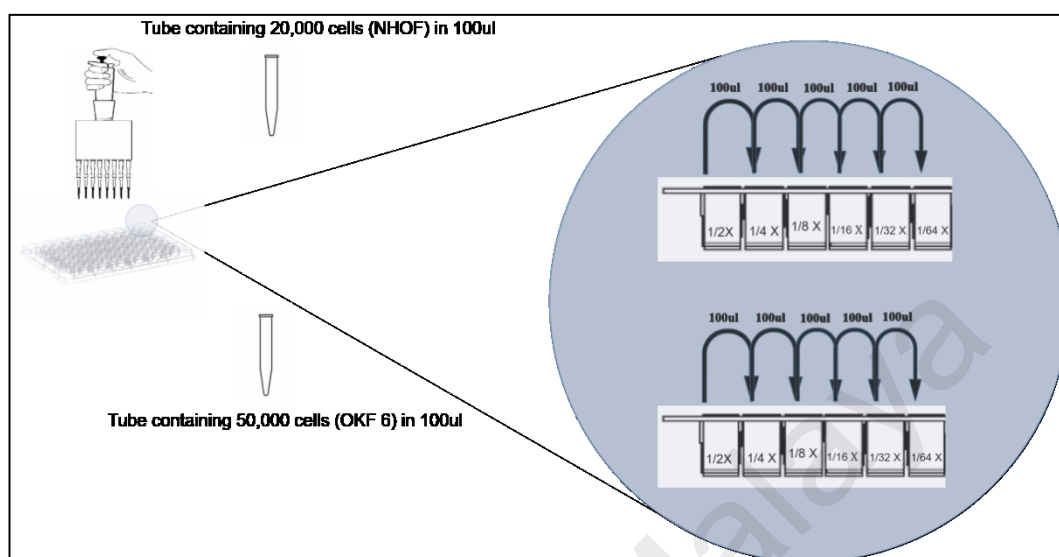
Figure 3.2: Using multichannel pipettes, cell dilution was established directly into 96 well plates and grown up to 5-7 days for OKF 6/TERT 2 and NHOF respectively, prior to MTT assay for every 24 hours to determine optimal seeding density.

3.4 Fabrication of Oral Mucosal Model (OMM) using Human Acellular Dermis

To fabricate stratified oral epithelium, the tissue reconstruct was mechanically supported using an Alvetex 12 well insert with extended wings (ReproCELL Europe LTD, Glasgow, United Kingdom). In this experiment, a total of 3 models were constructed to record histoarchitecture progression starting from day 4 (no air-liquid interface (ALI)), day 7 (after 3 days ALI), and day 10 (after 6 days of ALI) total day culture.

A thin human acellular cadaveric dermis (Alloderm GBR ®, LifeCell Corporation, Branchburg, USA) was aseptically trimmed approximately 12mm diameter in round shape. The specimen then was rehydrated in phosphate buffered saline (PBS) for

30 seconds followed by immersion in culture media for 15 minutes on the day of the experiment.

Based on a protocol established by Tra (2012) of a double seeding protocol (Tra, van Neck, Hovius, van Osch, & Perez-Amodio, 2012), the lamina propria of rehydrated acellular dermis was placed facing upwards in a tube filled with 13 ml solidified 1% agarose gel (Sigma-Aldrich). Next the 1 ml of 1×10^5 fibroblasts suspension was seeded onto the scaffold. The tube containing scaffold and fibroblasts were placed in a centrifuge and the fibroblasts were gently centrifuged into the scaffold, at 500 rpm for 60 min (Figure 3.3), the scaffold with the lamina propria surface containing the fibroblast facing downward (i.e. the basement membrane facing upward) was placed onto the insert base and clamped with the insert body (Figure 3.4). The specimen was kept at an air-liquid interface with cDMEM medium for approximately 5 hours to ensure cell attachment to the scaffold.

After 5 hours of fibroblast attachment to the lamina propria layer, an aliquot of 100ul cell suspension of OKF 6/TERT 2 containing 1×10^6 cells was seeded onto the basement surface of the scaffold. After 2 hours of seeding, serum free media (4ml) (see Appendix A 3) was flooded into the insert replacing cDMEM which was then incubated for 4 days. Culture media was changed every 48 hours. The specimen culture was continued in 10ml air-liquid interface media supplemented with 0.025mM glucose, 1.2mM CaCl$_2$, and 10^{-8} M retinoic acid (Sigma Aldrich Company, Ayrshire, UK) (see Appendix A 4(at the air liquid interface for another 3 days to induce stratification (Figure 3.5)
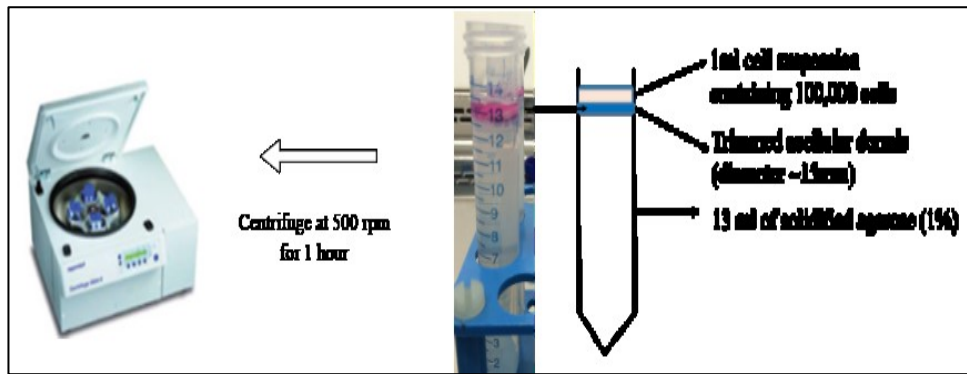
Figure 3.3: Schematic diagram showing the layout of the agarose gel to support the scaffold during centrifugation of fibroblasts into the lamina propria of the acellular dermis.
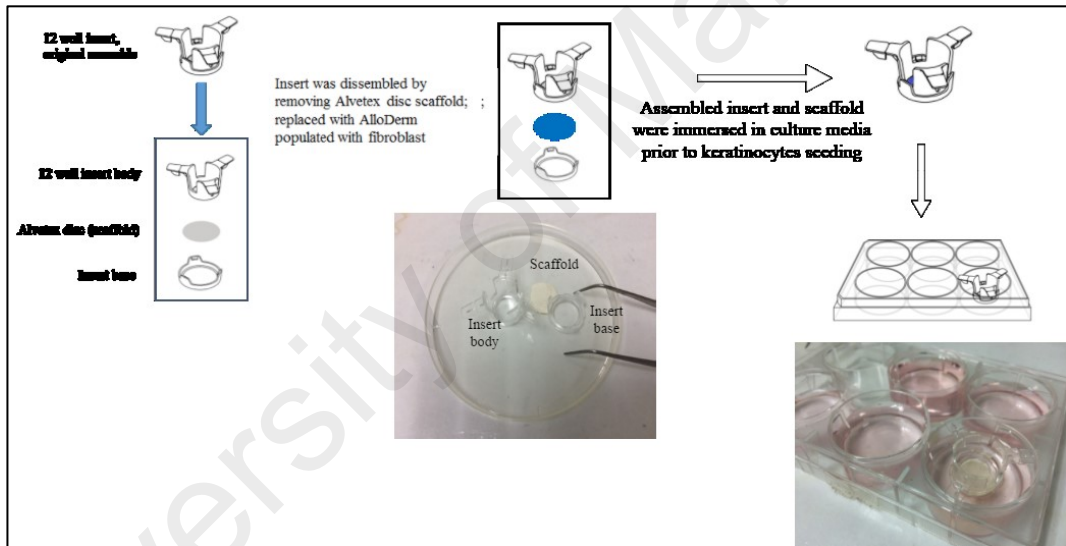
Figure 3.4: Schematic diagram showing the insert was disassembled. Freshly populated lamina propria substitute was clamped into the insert base to prevent the scaffold from floating in the media.
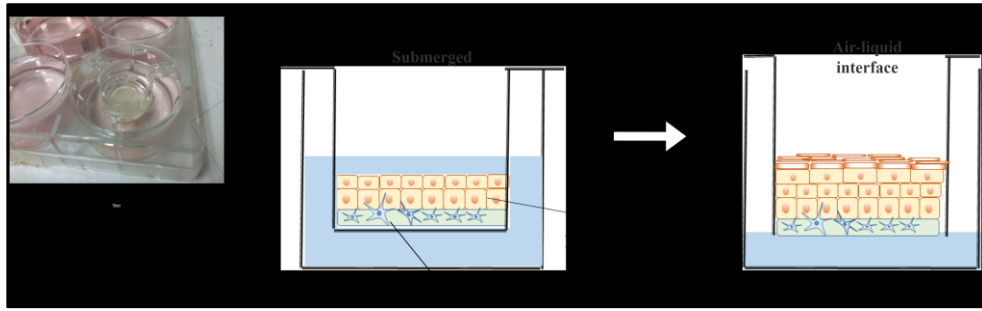
Figure 3.5: Schematic diagram illustrating the layout and culture design of the 3D oral mucosa model during submergence and ALI supported by the culture insert

3.5   Histological Preparation of OMM

At the end of culture, OMM samples were gently washed with phosphate buffered saline (PBS) and fixed in a solution of 4% paraformaldehyde (20x sample volume) for 12-24 hours at 4˚C without removing the clamp**.**On the following day, an alcohol dehydration (30%,50%,70%,80%,90% and 95%) process was carried out manually to handle the fragile tissue reconstruct, followed by immersion with three changes of Xylene. Xylene was then replaced by molten paraffin wax (60˚C) mixed and incubated in an oven for 30 mins. Wax samples were transferred to plastic embedding moulds and oriented into a vertical position and allowed to cool on a cold plate for at least 1-2 hours before sectioning. Once the wax was hardened, the embedded block was removed from the plastic mould and readied for sectioning. The block was positioned on a LEICA RM 2355 microtome (Leica Biosystem, Wetzlar, Germany) and then cut in 5-6um sections. Sections were transferred to a water bath (40˚C) to flatten them out and then were transferred to silane coated glass slides (Muto Pure Chemical Co Ltd,Tokyo,Japan) for immunohistochemistry and Superfrost™ (Fisherbrand, Thermo Scientific™) glass slides for haematoxylin & eosin staining. Prior to staining, it was important to allow the wax section to completely dry. Slides were placed in an oven at 37˚C overnight.

3.5.1 Hematoxylin & Eosin Staining

Prior to histology staining, wax sections were incubated at 60˚C for at least 15 minutes. Wax sections were then deparaffinized in xylene followed by a rehydration step through a graded series of alcohols (100%, 95%, 70%) to water before staining with haematoxylin for 20 minutes. Wax sections were dehydrated through a series of increasing alcohol (80%, 95%, 100%) before eosin staining. Sections were mounted and covered with a glass cover slip.

3.5.2 Immunohistochemistry (IHC)

For immunohistochemistry analysis, wax sections were incubated at 60˚C for 15 mins, immersed in xylene, and incubated again for another 10 minutes. This step was to ensure the wax section adhered securely onto glass slides. Sections were then deparaffinized and rehydrated through grades of alcohol to water. For the antigen retrieval procedure, 0.05% trypsin (Thermo Fisher Scientific, Waltham, Massachusetts, USA) containing 1% calcium chloride was gently dropped onto wax sections and incubated at 37˚C for 20 minutes. When using the Vectastain Universal ELITA ABC kit (Vector Lab Inc., Burlingame, CA, USA), non-specific proteins were blocked with 5% normal horse serum (Vectastain®, Vector Lab Inc., Burlingame, CA, USA) for 30 mins at room temperature. Slides were washed with washing buffer (TBS, 0.1% Tween 20) and endogenous peroxidase was blocked with 10 mins' incubation with DAKO® peroxidase blocking reagent at room temperature. Subsequently, the sections were then incubated overnight at 4°C with mouse antihuman monoclonal primary antibodies (Santa Cruz Biotechnology, Texas, USA) at a concentration of 1:50 for both pancytokeratin AE1/AE3 and vimentin. Following that, the sections were treated with biotinylated antimouse secondary antibodies (Vectastain®, Vector Lab Inc., Burlingame, CA) for 1 hour and then in ABC solution for 30 min. at room temperature. The reactions were visualized by treatment in 0.05% diaminobenzidine (DAB) and 0.005% H_2O_2 in 0.05M Tris buffer, pH 7.6 for 10

min. The sections were finally counterstained with haematoxylin for LM examination. The negative control was processed similarly except without the primary antibody incubation.

3.6   Cell Viability Assay after Bisphosphonate Treatment

Prior to treatment of the tissue reconstruct with the drug, a viability assay was conducted using MTT colorimetric assays (Roche Diagnostics, Indianapolis, IN, USA) with concentrations of ZOL at 1, 3, 10, 30, 100, 300, 1000uM for 24, 48 and 72 hours. Both of the cell lines (OKF 6/TERT 2 and NHOF) were seeded in 96 well plates at 1,000 cells/well (passage 2-4) and at 2,000 cells/well, respectively. After 48 hours of seeding, cells were incubated with drug diluted accordingly from stock (see Appendix A 5) and media was changed every 24 hours. This assay measures the conversion of the yellow tetrazolium salt MTT to purple formazan crystals by dehydrogenases in the mitochondria of viable cells. Optical density was measured at 570 nm with a reference wavelength of 690 nm using a multi-plate reader (Thermo Fisher Scientific, Waltham, MA, USA). All experiments were performed in triplicate and repeated on two separate occasions and the percentage of viability was normalized with non-treated cells. A dose-response curve was represented using a semi-logarithmic plot. On a semi-logarithmic plot, the amount of drug is plotted (on the X axis) as the log of drug concentration and response is plotted (on the Y axis) and represented as a normalized value using a linear scale. IC_{50} was determined using non-linear regression from Prism software. The statistical differences amongst the groups of incubation hours and dosages were determined using an F test (curve comparison) (see Appendix B 5)

3.7 SA-β-Gal Assay on OKF-6 Cell Lines and NHOF (Monolayer)

SA-β-Gal staining (BioVision, USA) was performed according to the manufacturer's protocol. Cells were seeded in 24 well plates based on optimized plating density and treated with zoledronic acid and positive control (5-Aza-2′-deoxycytidine) for 48 hours. Prior to experiment, treatment with 5-Aza-2′-deoxycytidine as a positive control was validated using both immunofluorescent detection of senescence protein p15/p16 and staining of SA-β-Gal in OKF 6/TERT 2 cells (see Appendix B 3). As a negative control, cells were treated with distilled water and culture media. After 48 hours' treatment, cells were stained with β-gal dye for overnight and upon observation under light microscope (LM), cells were counterstained with eosin. For quantification, 100 cells that included both β-Gal-positives and -negatives were counted in a random manner over five areas and the percentages of β-Gal-positive cells was determined using Image J software. Statistical analysis t test was used.

3.8 Drug Treatment of Oral Mucosal Models

Five oral mucosa model samples were prepared based on the optimized procedure in previous chapters. Based on the result from the monolayer cell culture model, selected concentrations of zoledronic acid (ZA) were tested in 3D-OMM. Each treatment consists of duplicate samples and one sample was assigned for a non-treated model (labelled as C1), and the remaining sample was assigned for histology analysis before ZOL treatment (labelled as C2) and 5 aza-CDR treated models as C3.

Prior to drug treatment, these samples were submerged in Alvetex® Scaffold 12 well inserts for 4 days in growth culture media. On day 4, all samples were cultured at air liquid interface for 3 days. After a total of 7 days of culture, the 3D OMM was treated with media containing 3µM 5 aza CDR and 12 µM ZOL in both of the basolateral and

apical side of the model for 48 hours before fixation. Non-treated tissue served as a negative control and a positive control was treated with 5-Aza-2′-deoxycytidine (5 aza CDR). After treatment, the tissue reconstruct was subjected to routine paraffin tissue processing and conditioned culture media from each treatment was collected, centrifuged at 1500 rpm for 10 minutes to discard any cell residuals. Centrifuged samples were aliquoted and kept at -80˚C for ELISA experiments.

3.9   Histological Examination of Epithelium upon Drug Treatment

The slides were all photographed and examined using a digital slide scanner Panoramic™ DESK II (3D HISTECH, Budapest, Hungary) at different magnifications. Using the Panoramic™ viewer software, a third person evaluated the thickness of the epithelial layer at 40x magnification. Linear distance perpendicular to the AlloDerm was measured between the basal surface of basal cells and the keratinized layer. Measurements were taken at 10 random points per section and the mean of 10 values was assigned to the thickness of the sample. (see Appendix B 6).

4.0   Enzyme-Linked Immunosorbent Assay (ELISA)

Senescence-related cytokines MMP-3 and IL-8 from conditioned culture media were measured using Quantikine® ELISA kit (R&D Systems, Minneapolis, USA). All reagents, controls, and samples were prepared based on the manufacturer's instructions. Optical density was measured using a multi-plate reader (Thermo Fisher Scientific, Waltham, MA, USA) at 450nm and correction at 570nm. Results are expressed as pg or ng/ml per tissue deduced from a standard curve (Appendix B 7).

CHAPTER 4:RESULTS

4.1 Characterization of Cell Lines and 3D OMM

As 3D culture is rather expensive and tedious procedure, we did our optimization experiment using monolayer cells. Primary cell lines of oral fibroblasts isolated from gingival tissues were characterized by growth curve analysis within passages and multiple passages. Histological characterization of the 3-dimensional oral mucosa model was performed through routine H&E staining and immunohistochemistry of the oral mucosa keratinization marker pancytokeratin AE1/AE3 and the mesenchymal protein vimentin.

4.1.1 Growth Characteristics of Oral Mucosal Cells

Given approximately 7 days of culture to reach 70% confluency in the flask, doubling time was compared throughout all passages, P1 (passage 1) cells yield the shortest and therefore may provide best source of cells for 3D culture (Figure 4.1). However, it is challenging to maintain cells in P1 as cell isolation is rather tedious. Therefore, to minimize the usage from P1 cells, we utilized them mainly for construction of 3D culture and P2-P4 cells for other experiments.

When cells seeding density was optimized mainly for growing in culture insert, we discovered that NHOF able to proliferate even at highest cell concentration(Figure 4.2) and, we observed that growth rate of OKF 6/TERT 2 cells was rather inconsistent even as number of cells increased (Figure 4.3). We chose 4800 cells/cm^2 for NHOF and 15,625 cells/cm^2 for OKF 6/TERT 2 cells as standardized seeding density for all experiments based on means of the slope of a best-fit line (see Appendix B 2).

After we optimized seeding density, we observed that growth of OKF 6/TERT 2 cells started to decline after 5 days of culture and NHOFs continue to proliferate after 8

days of culture (Figure 4.4). Therefore, we limit our 3D culture duration specifically, during submerge phase to be less than 5 days.
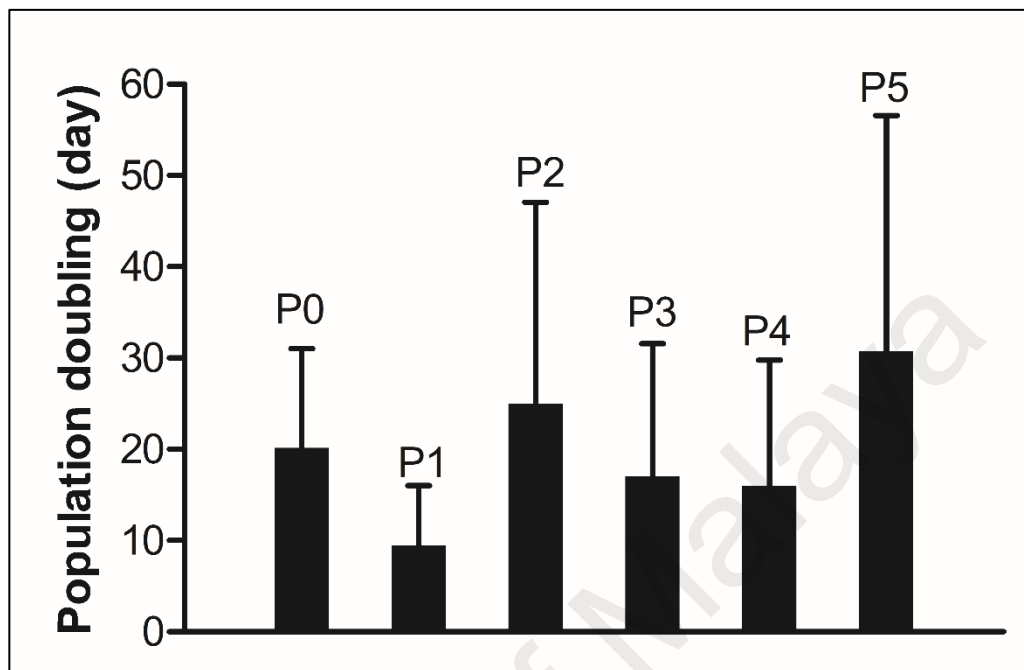
Figure 4.1: Graph comparing population doubling time, plotted on Y axis, vs passage number plotted on X axis for isolated normal human oral fibroblast from two donors. Cell were plated at 1x 10^5 cells until reached 70% confluency before harvested and counted in duplicates. Population doubling time calculated and was determined for all passages (inset) DT: P1=16±9.26; P2 = 47.1±31.18; P3=31.615±20.54; P4=19.4±20.5; P5=56.6±36.53 hours.
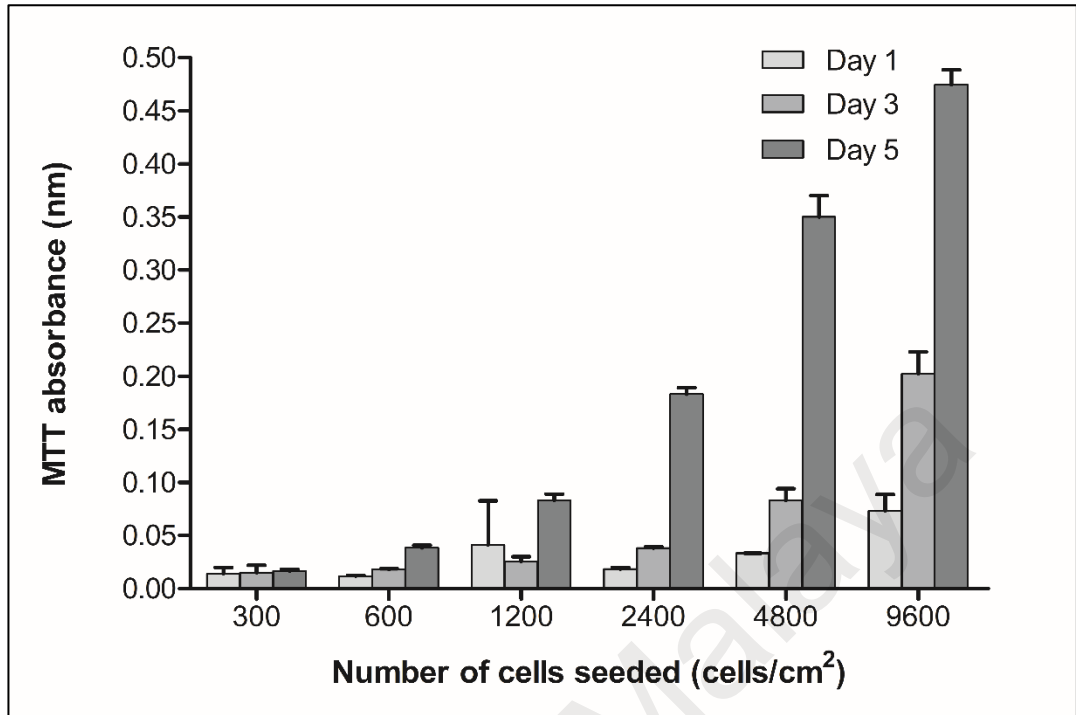
Figure 4.2:Influence of cell seeding density on the growth of NHOF. Cell viability based on MTT absorbance were measured in triplicate every 48 hours to determine optimum seeding density to culture NHOF up to 5 days of culture.
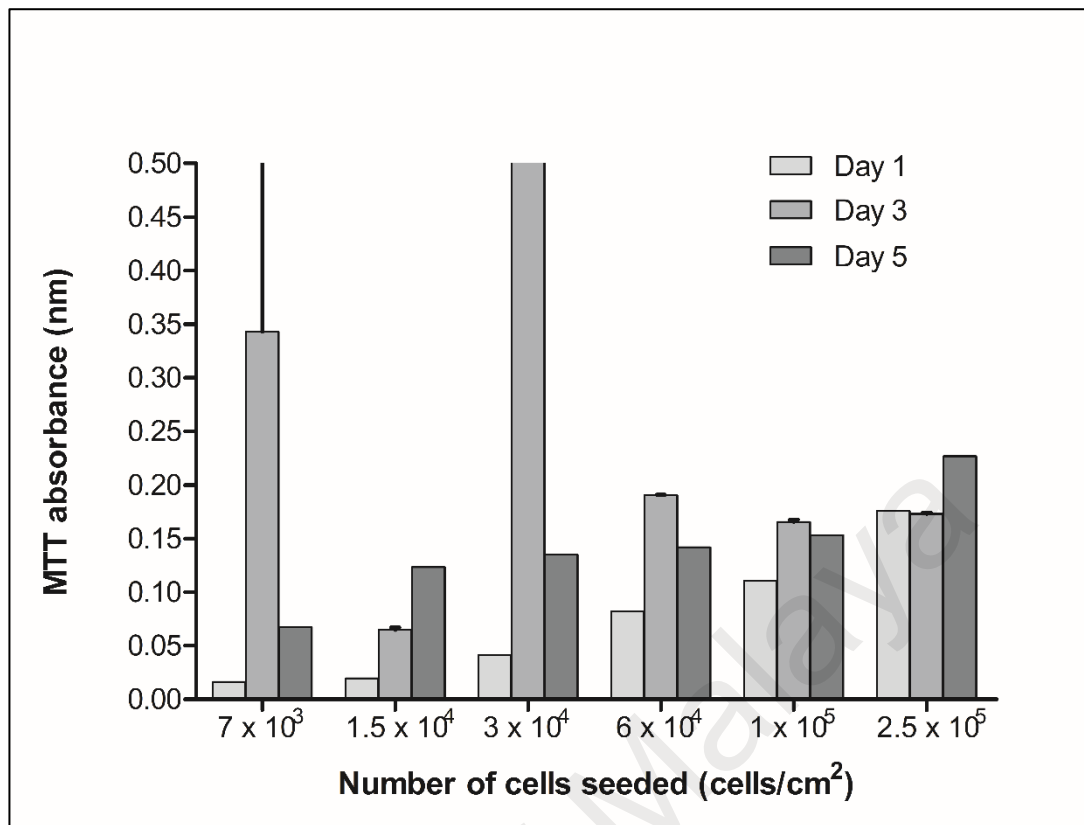
Figure 4.3: Influence of cell seeding density on the growth of OKF 6/TERT-2 cells. Cell viability based on MTT absorbance were measured in triplicate every 48 hours to determine optimum seeding density to culture OKF 6/TERT 2 up to 5 days of culture.
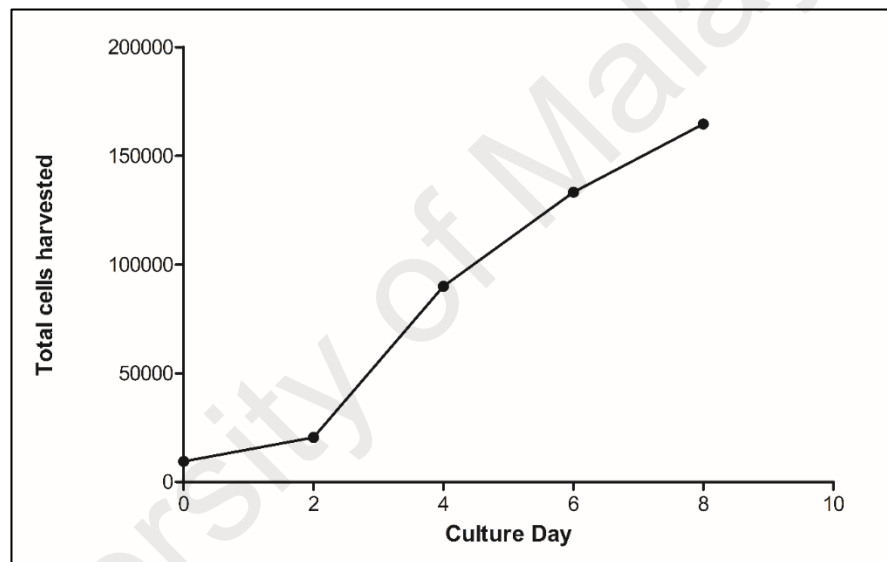
Figure 4.4: Growth kinetics of normal immortalized oral keratinocytes (OKF 6/TERT 2) (top) and primary culture of normal human oral fibroblast (bottom) Based on optimized seeding density, 4800 cells/cm^2 and 15,000 cells/cm^2 for NHOF and OKF 6/TERT-2 respectively, cells were expanded up to 8 days and counted every 48 hours (n=1)

4.1.2   Histology and Characterization of 3D OMM

After oral mucosal cells, both from primary and immortalized cell lines sources were optimized, cells were grown and then harvested to construct 3D cultures. Figure 4.5 shows a representative section of this model stained with haematoxylin and eosin observed under the light microscope. Several layers (1-3) of continuous oral keratinocytes were observed over AlloDerm™ after the culture was submerged for 4 days. The one to two layers of continuous epithelial cells showed little sign of differentiation. The underlying AlloDerm™ consisted of interlacing dense collagen bundles with an intact basement membrane showing no signs of cell infiltration. The tissue reconstruct was cultured for 4 days submerged and 3 days at an air-liquid interface (day 7 equivalent), showing continuous, 3-6 stratified layers of epithelium. During this culture, histoarchitecture mimicking gingival tissues was evident compared to before raising the reconstruct to an air-liquid interface. Hence, the model consists of a stratum basale, having one layer of columnar to round cells, a relatively flattened stratum spinosum and stratum granulosum, and a non-keratinized stratum corneum. After 10 days of culture, cells appeared thinner and less nucleated, however layers of epithelial cells begin to reduce. A strong stain of pancytokeratin AE1/AE3 indicated this model expressed many cytokeratins including cytokeratins 10, 14, 15, and 16, and also the low molecular weight cytokeratin 19. Clone AE3 detects the high molecular weight cytokeratins 1, 2, 3, 4, 5, and 6, and the low molecular weight cytokeratins 7 and 8. Figure 4.6 also showed expression of mesenchymal protein vimentin by the fibroblasts distributed in the lamina propria of tissue engineered oral mucosa.
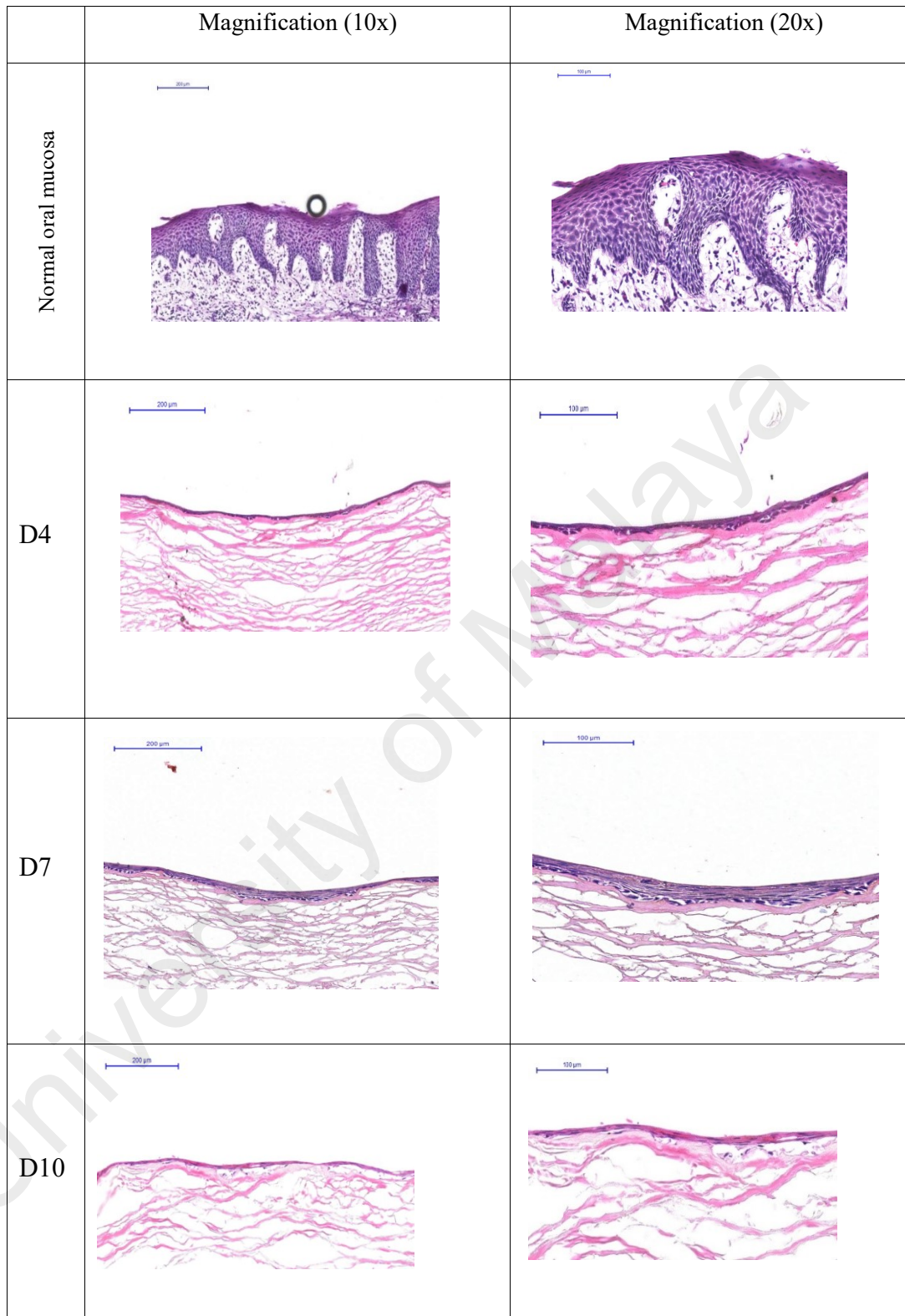
Figure 4.5: Histological analysis of 3-D OMM on total days of culture D4, D7 and D10 corresponded to air-liquid interface at 0d, 3d and 6d respectively. OMM demonstrating increasing suprabasal layer after 3d ALI and started to reduce after 6d ALI with appearance of flatter cells and absence of intact basement membrane and basal cell layer (n=4)(Original magnification 10X and 20X), scale bar 200um and 100um)
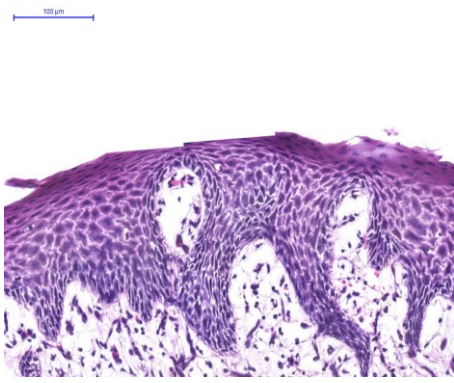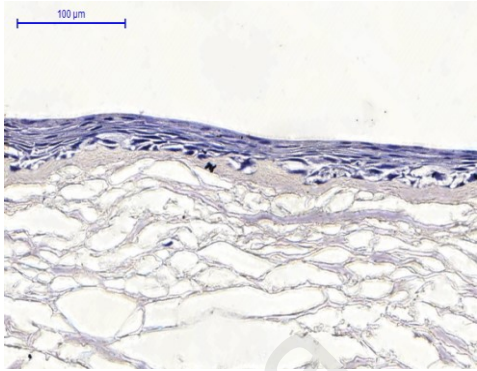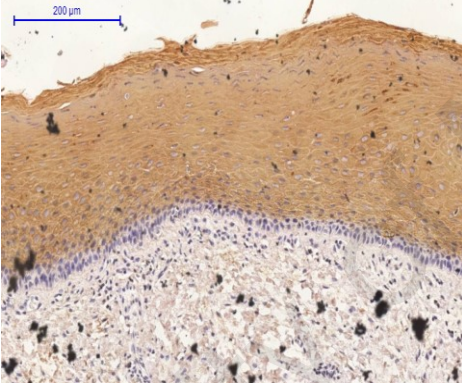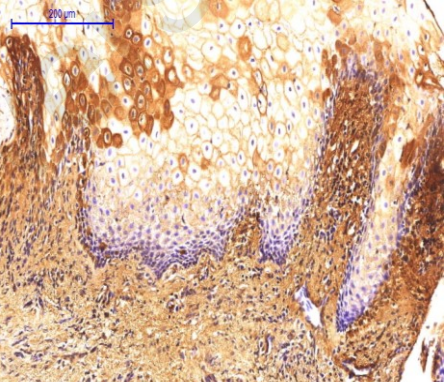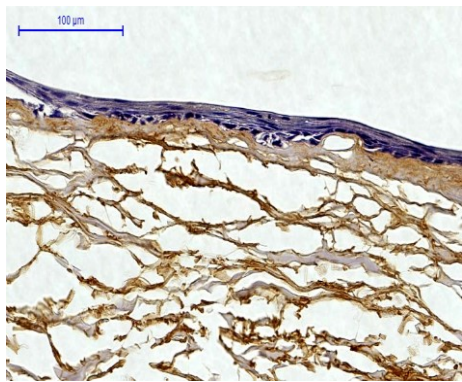
Antibody	Normal oral mucosa	Tissue Engineered Oral Mucosa OMM(OMM)
Negative control		
Pancytokeratin AE1/AE3		
Vimentin		

Figure 4.6: Immunohistochemical analysis of OMM. Immunostaining of pancytokeratin AE1/AE3 and vimentin in normal oral mucosa and oral mucosa model. Pancytokeratin AE1/AE3 stained densely in suprabasal layer and less dense in basal cell layer. Vimentin stained locally in lamina propria substitute (n=3) (Original magnification 20X), scale bar, 100um)

4.2   Effect of ZOL on Monolayer Cells and 3D OMM

After the established protocol for development of the 3D OMM using the immortalized cell lines of OKF 6/TERT 2 and NHOF, the 3D model was tested for tissue toxicity upon drug treatment with zoledronic acid. Prior to drug treatment on the tissue reconstruct, a few optimization experiments were conducted. First, the concentration of the drug was accurately determined using MTT viability and SA-β-Gal assays on the monolayer culture. This step is crucial to avoid severe toxicity to fragile epithelium tissues within the reconstruct model which would result in detached epithelium before further assessment.

Based on MTT viability assay for OKF 6/TERT 2 cell lines, the IC50 for 24, 48 and 72 incubation hours were determined to be 9.975±1.275,12.37±1.706, 0.9955±1.282 μM, respectively (Figure 4.7b). In contrast, NHOF cells required a higher dosage to inhibit cell growth. Based on the dose response curve (Figure 4.7a), IC50 values for 24, 48 and 72 hours were 349.98±1.119, 49.26±1.362,15.77±1.148 μM, respectively. Interestingly, the IC50 values for NHOF cells are rather toxic to OKF6 cells. Therefore, concentration used in oral mucosa model was utilized from IC50 of oral keratinocytes because we hypothesized that topical administration of ZOL will be directly in contact with oral keratinocytes rather than oral fibroblast which embedded in the layer of connective tissues. Based on interpolated values, from nonlinear regression, cell viability at concentration 12 μM was compared between cells at different incubation hours. (Figure 4.8). As the result, treatment of 12 μM ZOL for 48 hours was regarded as appropriate to be utilized in 3D culture and corresponded to a 50% and 29% decrease for OKF 6/TERT 2 and NHOF monolayer cells, respectively.

ZOL-treated OKF 6/TERT 2 contained 8.2 ±3.8% SA-ß-Gal-positive cells, significantly increased compared to untreated (P=0.0398; n =9)whereas 5 aza CdR-treated OKF 6/TERT 2 contained 34.5 ± 2.1% (ZOL *vs* 5-Aza-CdR: P < 0.0001; n=9)(Figure 4.9) . No changes were observed in NHOF cells (data not shown). Therefore, to further characterize ZOL-induced senescence in 3-dimensional culture, 12 μM was regarded as an appropriate concentration.
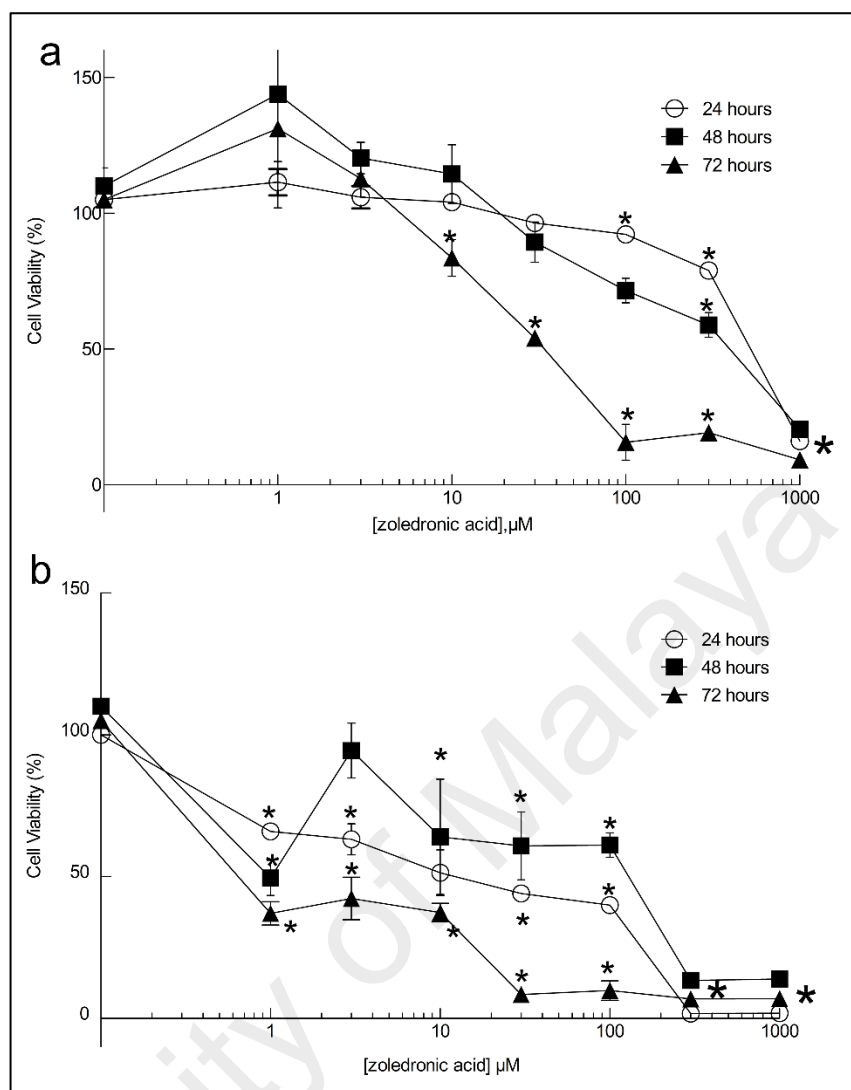
Incubation time (hours)	IC_{50} Normal human oral fibroblast (μM)	IC_{50} Immortalized oral keratinocytes (μM)
24	349.8 ± 1.119	9.975 ± 1.275
48	49.26 ± 1.362	12.37 ± 1.706
72	15.77 ± 1.148	0.9955 ± 1.282

Figure 4.7: Effect of ZOL on a) normal human oral fibroblast cells (NHOF) and b) OKF 6 cells viability at different incubation time of 24 (open circle), 48 (filled square) , and 72 hours (filled triangle) to determine the respective 50% inhibitory concentration (IC50). Data are expressed as percentage (mean ± s.d of seven replicates) of control values, which refer to untreated cells. Error bars represent standard deviation (s.d). Where error bars would be hidden by the symbol, they are shown at the edge of the symbol. The statistical differences amongst group of dosages were determined using ANOVA test. The asterisks (*P ≤ 0.05) represent statistically significant differences compared to untreated cells (n=3)
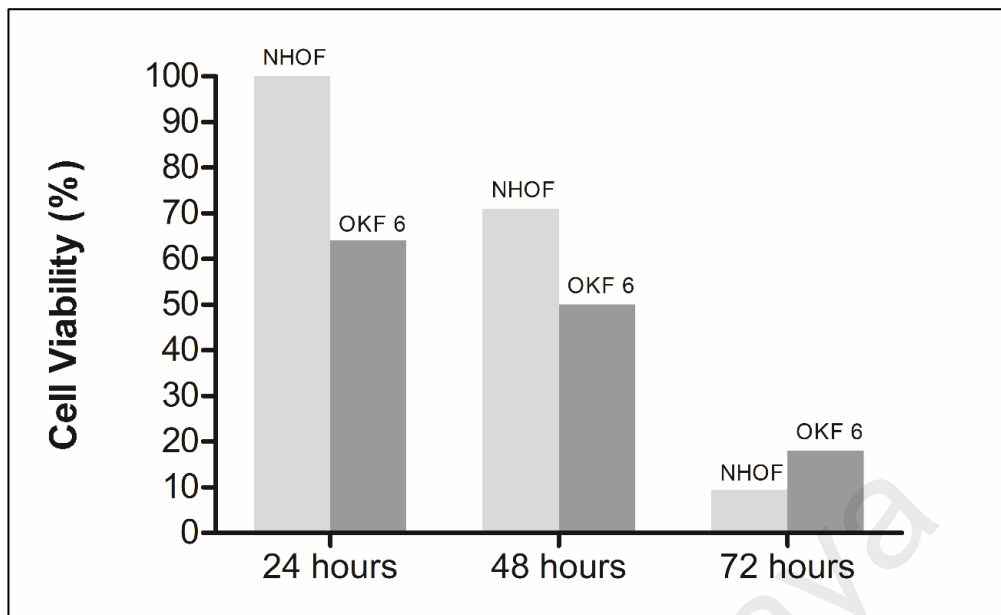
Figure 4.8: Bar chart represent comparison of cell viability of both oral mucosa cells when treated with 12uM of zoledronic acid at different incubation hours. Based on interpolated values, at 24 hours, viability of NHOF was not affected, but reduced OKF 6/TERT 2's viability to 64%. At 48 hours, viability in NHOF cells reduced to 71% and OKF 6/TERT 2 cells reduced to half. At 72 hours, viability of both cells reduced to less than 20%.
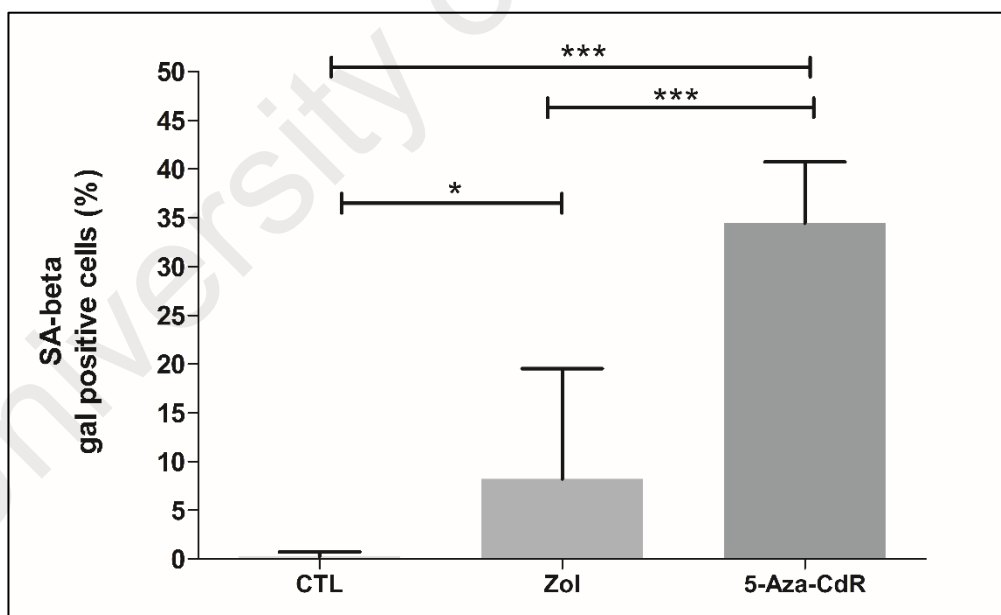
Figure 4.9: Bar chart represent percentage of cells with positive stain of ß-galactosidase activity after treated with the chosen dosage (12uM) for 48 hours. Degree of cell senescence was quantified as the percentage of SA-β-Gal positive cells after treatment with zoledronic acid and 5 aza CdR. Asterisk (*) indicates $P \leq 0.05$ and (***) indicates $P \leq 0.001$. Error bars represent standard deviation (s.d) (n=9).

Following the optimization procedure, the 3D OMM was prepared and the drug treatment was conducted accordingly. Soft tissue toxicity was assessed histologically, followed by measurement of epithelial thickness. Based on histological analysis, epithelial thickness was significantly reduced (Figure 4.11) and the basement membrane protein was degraded with the presence of epithelial invasion into the lamina propria (Figure 4.10)

After observing the unfavourable apparent of oral mucosa model histoarchitecture, we investigated whether there was senescence inflammation stimulation involved. Senescence-associated secretory molecule expression from ZOL-treated oral mucosal models highlighted significantly increased MMP-3 *(P = 0.0006)* and IL-8 *(P = 0.0004)* compared with untreated models (Figure 4.12). In the ZOL-treated oral mucosal model, expression of MMP-3 increased up to 0.5-fold compared to the untreated model. For the 5-aza CdR-treated oral mucosal model, expression of MMP-3 increased up to 1.8 -fold compared to the untreated model (inset, Figure 4.12a). (5 aza CdR *vs* untreated: *P <0.05;* n=2) (untreated model: 4.34 ± 4.004 ng/ml ; ZOL-treated oral mucosal model:7.09 ± 4.25; 5-aza CdR treated oral mucosal model 12.9 ± 4.09 ng/ml) are expressed as the mean with standard deviation from duplicate samples. Expression of IL-8 increased up to 0.5-fold in ZOL-treated oral mucosal models, compared to untreated (inset, Figure 4.12b). For the 5-aza CdR-treated oral mucosal model, expression of IL-8 increased up to 0.6-fold compared to the untreated model(inset, Figure 5.13b) (5 aza CdR *vs* untreated: *P <0.05;* n=2) (untreated model: 2236.4 ± 109 pg/ml; ZOL-treated oral mucosal model: 3414.6 ± 40 pg/ml; 5-aza CdR-treated oral mucosal model: 3569.7 ± 84 pg/ml).
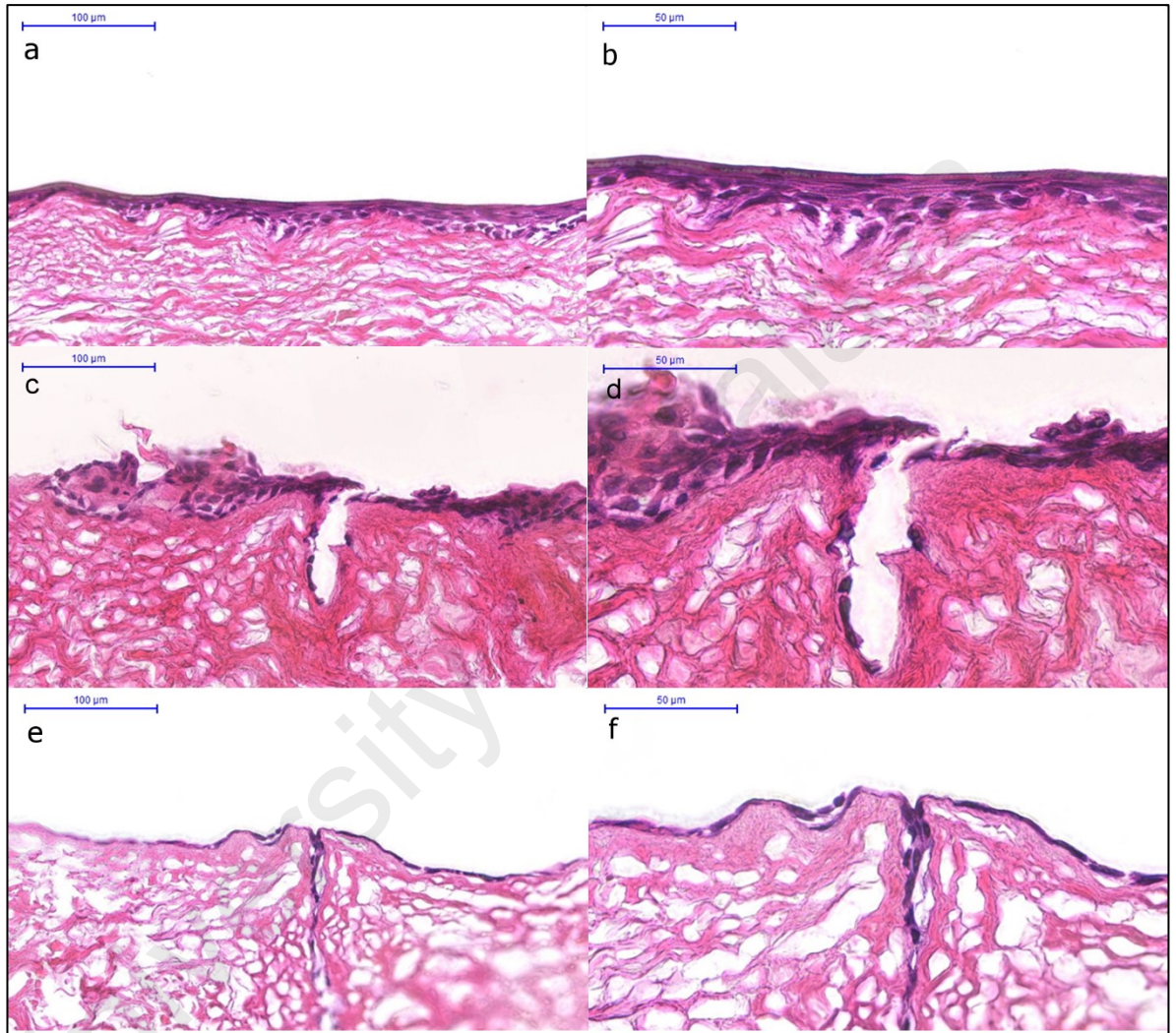
Figure 4.10: Histological appearance of 3D OMM after being treated in zoledronic acid and 5-aza-CdR and figure above shows tissue histology changes in 20x (a,c,e) and 40x magnification (b,d,f). After treatment with zoledronic acid, invasion of epithelial cells toward the lamina propria was observed accompanied by degradation of basement membrane barrier at magnification c) 20x and d) 40x. Similar histology was observed in treatment with 5-aza CDR (e,f)) in comparison with untreated model (a,b) (Original magnification, 20X; scale bar=100 µm and original magnification, 40X; scale bar=50 µm) (n=5)
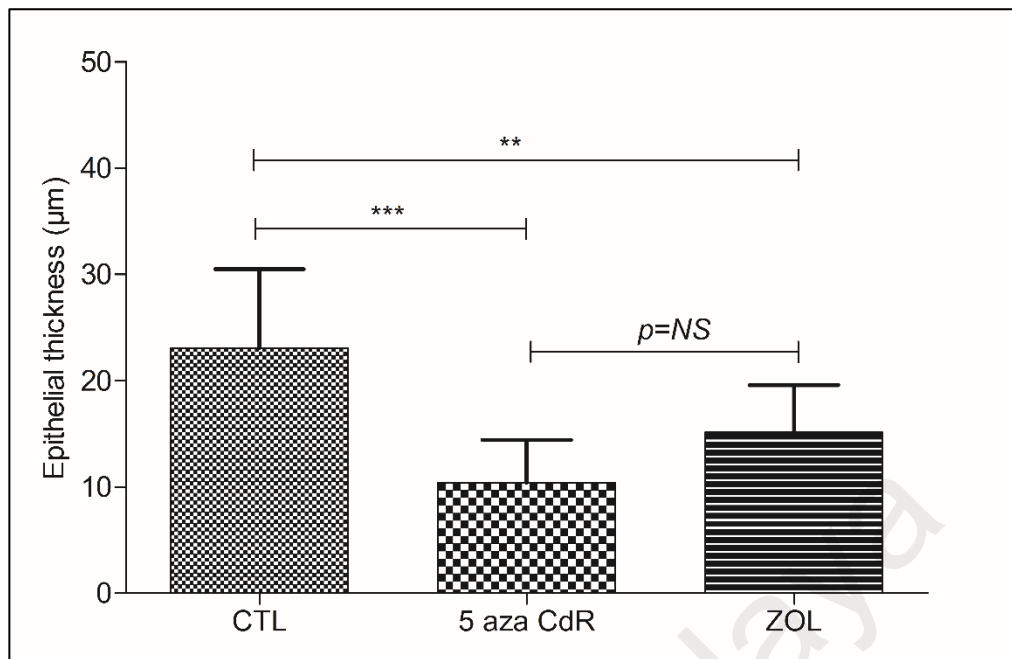
Figure 4.11: Graph reported on epithelial thickness of untreated , ZOL and 5 aza CdR -treated model. Asterisk (*) indicates P value ≤ 0.05 and (***) indicates P ≤0.001. Error bars represent standard deviation (s.d) N.S. not significant different between ZOL treated model and positive control. Error bars represent standard deviation (s.d) (n=13)
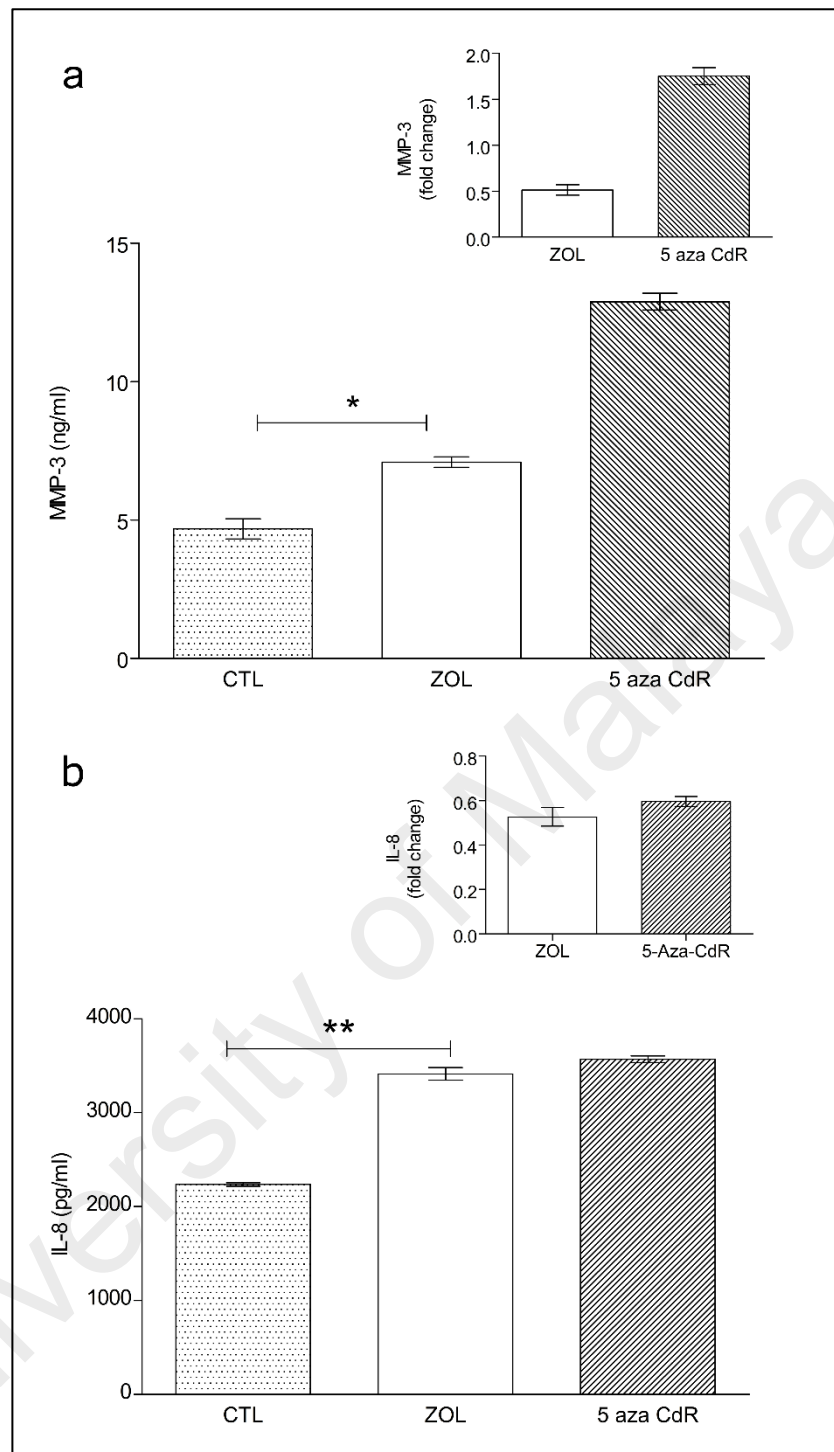
Figure 4.12: MMP-3(a) and IL-8 (b) released after exposure of the 3-D oral mucosa model to zoledronic acid and 5 aza CdR for 48 hours. Graph in inset indicates fold change values in relative to untreated. Asterisk (*) indicates *P* value ≤ 0.05 and (**) indicates *P* ≤0.001 vs untreated model. For MMP-3 analysis, untreated model: 4.34 ± 4.004 ng/ml ; ZOL-treated oral mucosal model:7.09 ± 4.25; 5-aza CdR treated oral mucosal model 12.9 ± 4.09 ng/ml) Error bars represent standard deviation (s.d). In analysis of IL-8 expression, untreated model: 2236.4 ± 109 pg/ml; ZOL-treated oral mucosal model: 3414.6 ±40 pg/ml; 5-aza CdR-treated oral mucosal model: 3569.7 ± 84 pg/ml) (n=3).

CHAPTER 5: DISCUSSION

To date the necessity for intravenous treatment with nitrogen-containing bisphosphonates for patients with skeletal-related disease has increased due to the drug effectiveness in inhibiting bone resorption. However, the drug has a higher tendency to cause painful exposure of maxillofacial and mandibular bone that impairs patient quality of life, especially in cancer patients. This condition is known as bisphosphonate related osteonecrosis of the jaw (BRONJ). Currently, BRONJ shows a poor response in standard treatments, such as drug holiday, antimicrobial drugs, and resection of necrotized tissue procedures (Shirota et al., 2009). Since the lesion only involves bone in the maxillofacial and mandibular region, most researchers have agreed that soft tissues around this bone region are an important onset factor for these lesions. Recent findings have supported that N-BP triggers keratinocyte senescence, which leads to unhealing mucosa observed in BRONJ. However, to date there are no studies that have addressed senescence in response to drug toxicity affecting a full thickness, tissue engineered oral mucosa constructed from immortalized keratinocytes. The drug toxicity effect towards soft tissue has only been developed in primary cultures of normal oral keratinocytes that eventually enter a state of permanent growth arrest, known as replicative senescence, therefore the model remains biased. Development of a three-dimensional oral mucosa model mimicking native histoarchitecture, but generated from immortalized cell lines will facilitate the development of novel drug therapies for BRONJ and may improve responses to currently available therapies prior to *in vivo* studies.

The goal of recreating organ function *ex vivo* has been broadly studied, especially in skin and oral mucosa. In pursuit of this goal, a wide range of techniques have been developed in terms of cellular inputs and scaffolds. Regardless of the variety of cellular inputs and scaffolds involved, the culture format of organotypic culture remains

mechanically supported. This culture format has been consistent throughout the years and has been proven to allow cultures exposure to air to mediate stratification; mimicking the barrier function of the oral mucosa and skin. Due to the high intensity of *in vivo* architecture mimicry in comparison with the monolayer system, the 3D oral mucosa model has been in demand to help scientists elucidate a variety of cellular mechanisms that drive tissue development, disease development, biomaterial compatibility and pharmaceutical screening for drug discovery. Throughout the years, the type of cellular input has been playing a significant role in the world of three-dimensional reconstructs, especially in *in vitro* studies. In common practice, primary normal oral keratinocytes have been used as the main cellular input to generate 3-dimensional oral mucosa as a reliable platform to switch from proliferation mode to terminal differentiation in culture.

However, one of the main constraints in culturing the primary oral keratinocytes is their limited *in vitro* life span. They normally subculture only up to a fourth time (Rouabhia et al., 2012) due to senescence-based growth arrest (Dongari-Bagtzoglou & Kashleva, 2006a) and irreversible commitment of keratinocytes from proliferation to differentiation (Vande Vannet & Hanssens, 2007). This feature may restrain the researchers in their ability to grow enough cells for the number of OMM in the experiment and hinder progress of the exhaustive assays needed to generate repeatable data. In addition to the limited life span *in vitro*, the primary cell lines suffer from donor variation, thus introducing inconsistency in 3D architecture (Dongari-Bagtzoglou & Kashleva, 2006b) and variable constitutive and inducible expression of proteins highly dependent on the donor (Cox et al., 1992; Devalia et al., 1999; Dongari-Bagtzoglou & Kashleva, 2003b; Dongari-Bagtzoglou et al., 2004; Dongari-Bagtzoglou et al., 1999; Feucht et al., 2003). The inconsistency of successful culture rate and protein expression introduced by a population of oral keratinocytes derived from normal tissues will hinder construction of reproducible and homogenous organotypic oral mucosa for *in vitro* experimental study.

Reduced healing of oral mucosa has been elucidated from *in vitro* studies that highlighted N-BP triggering senescence as a keratinocyte-specific toxicity. However, both types of studies used tissue engineered oral mucosa constructed from primary cell culture. Although oral keratinocytes isolated from tissues are favored due to the reliable platform for performing functional studies such as intracellular calcium levels, migration of proteins, cell-cell interactions, and signaling pathways, the procurement, propagation and long-term functionality are major challenges faced in primary mammalian cell culture systems, especially those isolated from adult tissues. This is due to the finding that primary cells isolated from adult tissues result in terminal differentiation or senescence. However, in regards to current studies, reliable models that can address the senescence mechanism should not be models that are prone to senescence; hence immortalized cells are favored over primary cells.

Normal immortalized oral keratinocyte (OKF 6/TERT 2) cell lines have been a main cellular input in generating 3-dimensional oral mucosa models on fibroblast embedded collagen for the study of oral *candidiasis* infection (Dongari-Bagtzoglou & Kashleva, 2006c) and to demonstrate a transformation model of oral–esophageal cancer cells by using a limited set of genetic alterations frequently observed in the corresponding human cancer (Goessel et al., 2005). Optimization of these culture techniques has been challenging and this is the first experiment reported on a 3-dimensional model of OKF-6 cells seeded onto fibroblasts populated on acellular dermis. The scaffold used in this study is commercially known as AlloDerm ™ and was chosen for its easy handling, noncontractile nature and firmness (Presland & Jurevic, 2002) and has been reported in various *in vivo* studies of tissue transplantation (Izumi, Song, & Feinberg, 2004; Izumi, Terashi, Marcelo, & Feinberg, 2000). Apart from that, this scaffold is able to withstand mechanical stress, as the oral mucosa is continuously exposed to a significant degree of mechanical stress, especially during severe histological assessment. Most of all, the

presence of a basement membrane preserved in the scaffold acts as a functional separator between epithelium and connective tissue. In fact, basement membrane protein is a critical component in organotypic models since it has been used as a criteria to be assessed in the study of invasion of oral carcinoma cell lines in 3-dimensional models (Kulasekara et al., 2009). In addition, researchers have agreed that stratification of oral epithelium is facilitated by fibroblasts that play a role in producing endogenous growth factors and collagen fibers (Costea, Loro, Dimba, Vintermyr, & Johannessen, 2003) despite the presence of extracellular matrix (ECM) fibers in acellular dermis. However, it is rather challenging to diffuse fibroblasts into acellular dermis due to the dense architecture of the scaffold itself (Rodrigues et al., 2010). Hence in the current study fibroblasts were diffused into the scaffold by a centrifugation force adapted from a previous protocol (Tra et al., 2012).

In this study, we developed a 3D oral mucosa model generated from immortalized normal human oral mucosa keratinocytes (OKF 6/TERT 2 cell line) seeded onto an acellular dermis re-populated with oral fibroblasts. Through a combination of histology staining and immunohistochemistry, we managed to confirm creation of stratified oral mucosa that recapitulates native oral mucosa consisting of a representative epithelium, a basement membrane and lamina propria. OKF 6/TERT 2 cells has been isolated from normal mucosa at the floor of the mouth (Goessel et al., 2005) and immortalized by two-stages, loss of p16INK4A function and TERT ectopic expression (Dickson et al., 2000). Despite being immortalized, OKF 6/TERT 2 cell lines have been described to undergo a non-keratinizing form of suprabasal differentiation when seeded onto fibroblast-embedded collagen (Dickson et al., 2000; Dongari-Bagtzoglou & Kashleva, 2006b) which was confirmed by immunohistochemical analysis of the differentiation specific protein K13 (Dickson et al., 2000),K4 and K19 (Dongari-Bagtzoglou & Kashleva, 2006b) in separate studies. In the current study, our model shows positive detection of

pancytokeratin AE1/AE3; a mixture of low and high molecular cytokeratins were detected with the two antibody clones, AE1 and AE3. As the name implies, AE1 detects molecular weight cytokeratins 10,14,15, 16 and 19. Meanwhile clone AE3 detects low molecular weight cytokeratins 1, 2, 3, 4, 5, 6, 7 and 8. Cytokeratin 19 has been claimed to be an informative subtype-specific marker because only basal cells of non-keratinizing epithelial cells express CK19 *in vivo* and in culture. This cytokeratin expression pattern of our model is similar with the non-keratinizing protein marker of OKF 6/TERT 2 cells grown in a multilayer structure and is consistent with stratified, non-keratinizing epithelia (expressing keratins 4 and 19) as shown by the laboratory that developed these cell lines (Dickson et al., 2000).

Our current model consists of at least three layers of epithelium: basal, intermediate, and superficial. A basal layer consists of a single layer of cuboidal epithelial cells overlying a basement membrane. An intermediate layer is composed of larger, stacked, polyhedral-shaped cells appearing larger than basal layer cells. The superficial layer on the other hand, is composed of even larger stacked polyhedral cells with outer cells flattening into squames. This layer indicates shedding or loss as they mature and die during turnover. However, in previous studies, OKF 6/TERT 2 generated oral mucosa models did not exhibit a superficial layer (McLeod, Moutasim, Brennan, Thomas, & Jenei, 2014), probably due to the absence of retinoic acid in culture media which has been claimed to induce more accurate recapitulation of *in vivo* histology (Dickson et al., 2000). In our current model, flattening cells have started to form even before being exposed to air. During air-liquid interface for 3 days, the superficial layer increases from 3 to 6 layers and begins to show shedding. However, an unexpected finding revealed that after 7 days of ALI, basal and intermediate cell layers started to disappear, and we were only able to observe flattening cells at the uppermost layer. Therefore, we assumed that the model was unable to be sustained after 7 days of ALI duration. However, this is not the case in the

previous study in which we were able to culture for longer, 12-15 days of ALI on fibroblasts embedded in collagen (Dongari-Bagtzoglou & Kashleva, 2006c). Based on these findings, there are two possible explanations that might be related to each other 1) the cell differentiation rate is higher than cell proliferation 2) basal cells lose adherence to the basement membrane protein, therefore causing cells to stop generating a new layer of cells.

The importance of homeostatic balance between proliferation and differentiation in oral mucosa has been reflected in providing a shield against bacteria, viruses, and other damaging agents toward the human body. To recapitulate this function in *in vitro* three-dimensional models, there are two main culture techniques involved which are 1) a scaffold for basal cells to adhere to and proliferate from 2) air-liquid interface method to induce stratification and differentiation. Based on the current model, cells started to mature aggressively in comparison with the proliferation rate of basal cells. Previous findings have related the proliferation rate to the strength of adherence of the basal cell to the basement membrane through linking proteins of the hemidesmosomes. However, it should not be a problem when acellular dermis is used as a support system. In comparison with fibroblast-populated collagen, acellular dermis preserves the basement membrane (BM) components that contain collagen type IV, laminins and collagen type VII. The BM provides strong anchorage to support oral keratinocyte migration upward and results in multi-layered oral epithelium. With the presence of BM components readily available, cells do not have to deposit these BM components themselves to generate new epithelial layers (Tra et al., 2012). It is essential to note that previous studies seeded primary normal oral keratinocytes on precoated AlloDerm™ with collagen type IV to increase adherence of basal cells to the basement membrane (Izumi et al., 2004; Izumi et al., 2000). Therefore, when seeding cells onto AlloDerm™, it is crucial to consider pre-coating the scaffold with collagen. Without proper anchorage of basal cells to the scaffold,

homeostatic balance of proliferation and differentiation in the oral mucosa model remains allusive.

One of the limitations of the studies discussed from the literature is the tendency of such tissue reconstructs to acquire tumorigenic phenotype with either benign or malignant growth properties, which can be detected when transplanted into immunocompromised mice (Tomakidi et al., 2003). However, OKF 6/TERT 2 tissue reconstructs have been transplanted as surface skin grafts onto athymic mice and present no evidence of invasion of the underlying connective tissue for 42 days (Dickson et al., 2000). Apart from that, it is worth noting the incapacity of the current model to proliferate to a longer duration as this capacity represents the function of oral mucosa *in vivo.* This current study provided a challenge during immunohistochemistry in that it required a heat antigen retrieval technique. In comparison with biopsy, tissue culture is more challenging since it has fewer cells to adhere to glass slides during histology staining. As a result, the tissue section tends to fall off upon exposure to heat even when coated glass slides are used. Therefore, it is worth considering a frozen, fixed technique which in comparison with FFPE doesn't include deparaffinization that might cause loss of more cells.

Previous challenges in the construction of 3D oral mucosa models were the ability of cells to stratify upon exposure to the air-liquid interface, which result in inconsistency stratification when using primary oral keratinocytes as the main cellular input. Exhaustive culture of primary normal oral keratinocytes has hindered the experimental progress that would otherwise use molecular manipulation, such as genetic transformation and protein knockout to express a certain trait. With the ability of immortalized cell lines to stratify in 3-dimensional culture, scientists should be able to mold the oral mucosa model into the next level of 3-dimensional *in vitro* studies which will allow scientists to expand the research horizon into a more controlled study environment which is lacking in animal

studies. In fact, there is a study that has started to modify cells into expressing a fluorescence marker as a scoring index for inflammation as a toxicity assessment in tissues. Therefore, it is concluded that immortalized cell lines are an improved, reproducible 3-dimensional model to study the senescence effect of N-BP towards soft tissues without compromising histoarchitecture of native tissues.

Scientists have agreed that impairment of soft tissue healing observed in BRONJ lesions might be facilitated by a senescence mechanism occurring in keratinocytes (R. H. Kim et al., 2011b; H. Ohnuki et al., 2012). Interestingly, several studies revealed that a senescence mechanism is not restricted to a growth arrest phenotype, but may also be associated with a heightened inflammatory response that involves multiple networks of cells and might play a deleterious role in tissue architecture if the inflammation reaches a certain magnitude. Currently, there is no study addressing the effect of a senescence inflammatory response on tissue architecture of 3D oral mucosa. In the present study, we reported that ZOL treatment affected histoarchitecture of 3D OMM by reducing epithelial thickness and unexpectedly degraded the basement membrane. Further testing then confirmed heightened senescence- related inflammatory cytokine expression of MMP-3, potentially responsible for degrading the tissue microenvironment, including the basement membrane.

In this study, we assessed the histoarchitecture of a 3D OMM upon exposure to an optimum concentration of zoledronic acid to resemble the soft tissue toxicity in BRONJ by H&E staining. Our histoarchitecture analysis revealed significant reduction in epithelial thickness and an unexpected finding of invasion of the epithelium towards the lamina propria accompanied by degradation of the basement membrane and extracellular matrix proteins. We further measured secreted senescence associated phenotype (SASP) in the media and identified significant increases in MMP-3 that might be responsible for

degradation of basement membrane protein. This is consistent with a finding from a previous study (R. H. Kim et al., 2011b; H. Ohnuki et al., 2012) that shows increasing MMP-3 mRNA extracted from reconstructed epithelium. However, in this study we managed to demonstrate the presence of degradation of basement membrane protein that has been proven intact compared with collagen-based oral mucosa models (Chai et al., 2012). Subsequently, one of the factors associated with impairment of wound healing is proteolytic enzyme imbalance that favors tissue degradation over repair (Dovi et al., 2004). Based on this result, we propose that impairment of soft tissue healing observed in BRONJ is caused by adverse inflammation from senescence induced by bisphosphonate. On the other hand, invasion of epithelium towards the lamina propria is consistent (Figure 4.10) with the effect of SASP that triggers EMT (epithelial-mesenchymal transition) in a previous study (Coppe et al., 2008). There is still lack of evidence to undermine how senescence can directly cause cell invasion without pointing at the role of SASP molecules. However further assays need to be performed in this study to confirm transition has occurred upon drug treatment. Apart from that, the increase in IL-8 produced from our 3D OMM is assumed to occur from senescent cells which can serve as potent attractors and activators of innate immune cells, destroying tissue environments by the oxidizing molecules they release (Orjalo, Bhaumik, Gengler, Scott, & Campisi, 2009).

Besides the undetermined pathophysiology of BRONJ in soft tissues, one of the challenges in this field is to mimic the dosage of bisphosphonate that is needed to induce BRONJ in the 3-D OMM (Hisashi Ohnuki et al., 2012). In this study, non-healing features of soft tissue were recapitulated *in vitro* by dose dependent assay on viability using MTT assay of monolayer models of NHOK, NHOF and OKF-6 cell lines prior to tissue reconstruct and consequently, using IC50, senescence activity was then measured using senescence inflammatory cytokine IL-8 and MMP-3 measurements. The ZOL inhibitory

concentration at 12µM is consistent with other previous studies that include normal human oral keratinocytes and fibroblasts (R. H. Kim et al., 2011b; Hisashi Ohnuki et al., 2012; Saito et al., 2014; Scheper et al., 2009). However, in our viability assay performed separately on fibroblasts and OKF 6/TERT 2, fibroblasts acquired more resistance towards drug treatment compared to OKF 6/TERT 2 by showing higher IC50 values.

This study also highlighted the finding of a senescence-specific mechanism that occurred in bisphosphonate treated cells. To test a wide range of doses (1 – 10uM) in 3D OMM that consists of a co-culture of two different types of cells is challenging. Previous studies have confirmed that ZOL induces senescence related markers such as DNA damage response (DDR) (H. Ohnuki et al., 2012) and senescence in oral keratinocytes, but not oral fibroblasts (R. H. Kim et al., 2011b). On the other hand, some studies suggest apoptosis as a potential toxicity mechanism in oral keratinocytes (Pabst et al., 2012; Scheper et al., 2009) and fibroblasts (Scheper et al., 2009), but this is not consistent with animal studies (Aguirre et al., 2012; Allam et al., 2011), as well as *in vitro* studies (R. H. Kim et al., 2011b; H. Ohnuki et al., 2012). Interestingly, the previous studies concluded senescence is the toxicity mechanism in normal human oral keratinocytes (NHOK), which are somatic cells that naturally possess no telomerase to maintain telomeres at a sufficient length (Harley et al., 1990; Masutomi et al., 2003), thus cells are subjected to DNA damage response which relates to senescence. Hence, NHOK as a study model will lead to false positive results of senescence.

Alternatively, in current study, normal immortalized OKF 6/TERT 2 was chosen as the study model to address senescence toxicity by bisphosphonates. We sought to assess whether OKF 6/TERT 2 cells despite being immortalized, has the potential to activate senescence mechanism by treatment with 5-aza-2'-deoxycytidine, a cytidine analogue. Generally, this chemical has been reported to effectively lead to demethylation of

DNA(Creusot, Acs, & Christman, 1982; Michalowsky & Jones, 1987) and may restore transcription from promoters that were inactivated by hypermethylation. This has lead to the finding in 1998, in which squamous cell carcinoma lines can re-express p16INK4A by restoring a functional RB pathway in response to treatment with a demethylating agent (Timmermann, Hinds, & Munger, 1998). On the other hand, treatment of 5-aza-2'-deoxycytidine was also reported to exhibit DNA damage response as assessed by formation of DNA double strand breaks, which are also hallmark of senescence (Palii, Van Emburgh, Sankpal, Brown, & Robertson, 2008). Interestingly, we found that OKF 6/TERT 2 cells expressed p15/p16 protein after treatment with demethylating agent, as assessed by immunofluorescence, hence supported the notion that OKF 6/TERT 2 can be induced to undergo senescence. This finding however, is contrary to the spontaneous loss of p16INK4A expression after ectopic expression of hTERT was performed and later was detected to acquire homozygous deletion in all three exons of CDKN2A/INK4A locus. However a closer examination revealed that previous study (Dickson et al., 2000) utilized specific antibody to detect p16INK4A and detection of p15 protein was not conducted even (Figure 5.1) p15 protein was also reported to be upregulated in TGF-β mediated cell cycle arrest and, shared similar function as p16, by inhibition of cdk4 and cdk6 kinases(Park & Vogelstein, 2003). We also entertained the possibility that detection of p15/p16 in OKF 6/TERT 2 cells after treatment with 5-aza-2'-deoxycytidine by immunofluorescence might due to expression of p15 protein that tagged along with the antibody used as the marker. However, further downstream assays should be conducted to confirm the activation of p15 protein in OKF 6/TERT 2 cell lines. This study confirmed senescence activity for OKF 6/TERT 2 cells at 12uM for 48 hours is significant (Figure 4.9) based on SA-β gal assay, however for oral fibroblasts, senescence was negative even at P5 which is consistent with a study by Kim et al.(2011) that concluded bisphosphonate induced apoptosis in fibroblasts, and senescence on

keratinocytes. (R. H. Kim et al., 2011b). Although it is currently the standard for detecting senescent cells, it should be cautioned, however several conditions such as high cell confluence or treatment with hydrogen peroxide can stimulate SA-β-gal activity leading to false positives (N. C. Yang & Hu, 2005). Of note, none of the currently available markers are sufficient on their own for conclusively identifying senescent cells in vivo or in vitro (van Deursen, 2014) and a study has suggested combination with proliferative marker to add more confidence in the test (Lawless et al., 2010)

The current viewpoint assays in the field to assess soft tissue toxicity using a 3-dimensional model of oral mucosa were based on histological assessment of impairment of re-epithelialization after the "wound" was created (R. H. Kim et al., 2011b). This includes validation of proliferative protein markers PCNA and Ki-67 (proliferative labelling index), epithelial thickness and migration proteins. Recapitulating a wound in 3D reconstructs is technically challenging and requires longer duration of culture up to 11-14 days for wound closure to occur (R. H. Kim et al., 2011b; Saito et al., 2014). Based on the current viability assay, OKF 6/TERT 2 cells showed decreased viability after 5 days of culture (Figure 4.4), therefore it will be challenging to proceed with wound closure experiments.

We also found technical difficulties in detecting protein via immunohistochemistry that depends on heat-induced epitope retrieval (HIER). Most of the time, wax sections would detach before incubation with primary antibodies. It is rather challenging to perform immunohistochemistry on tissue culture compared to fresh biopsy, probably due to smaller numbers of cells present.

Senescent cells are far from passive: they are metabolically and transcriptionally active and secrete molecules continuously for prolonged periods (Lasry & Ben-Neriah, 2015). Whereas many organisms harbor mechanisms for eliminating senescent cells from tissues

by immune clearance, some senescent cells may persist in tissue for years. Prolonged presence of senescent cells in a tissue may promote considerable damage, mainly due to the persistence of associated inflammatory responses. Nevertheless, there is possibility that impairment of mucosa healing treated with bisphosphonate not only due to inhibition of proliferation as cells entered senescence phase, but also the consequence of senescence through inflammatory network that provide greater inhibitory effect on tissue function and histoarchitecture. This is consistent with a majority of BRONJ patients that have been immunocompromised due to chemotherapy treatment. Therefore, they might not be able to clear senescent cells as optimally as possible compared to healthy people. This study is crucial to better understand the senescence effect, especially given the paracrine network that can be induced through secreted cytokines. Given that inflammatory agents primarily mediate both the maintenance of senescence and its paracrine effects, the most likely means of controlling adverse senescence due to bisphosphonate treatment would be anti-inflammatory drugs. Ideally, such drugs would preferentially target senescence-associated inflammatory responses, such as the secreted senescence associated phenotype or the senescence inflammatory response (Lasry & Ben-Neriah, 2015).
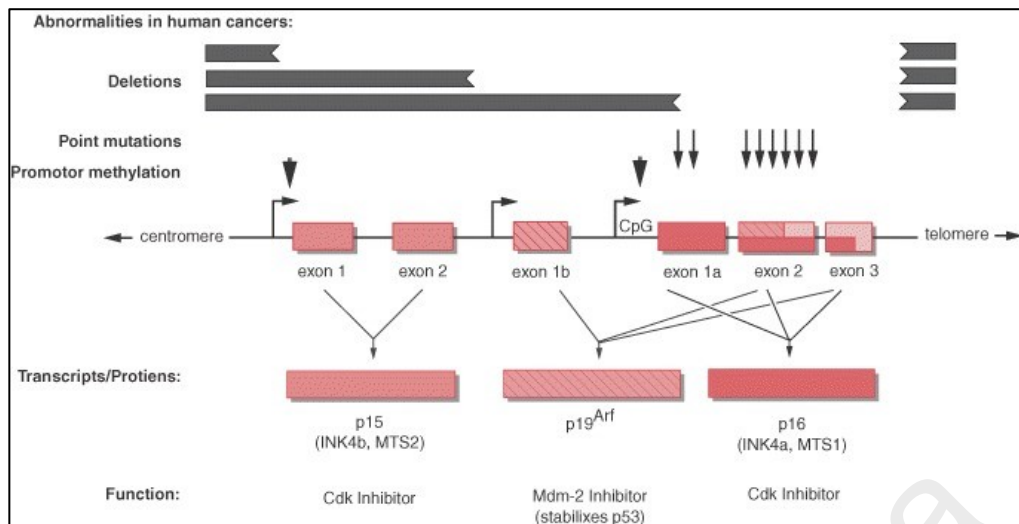
Figure 5.1: Genomic structure, mutations, and transcripts of the *INK4b* (p15) and *INK4a* (p16/p19ARF) locus. The origin of the p15, p16, and p19ARF transcripts is shown schematically, along with a representative depiction of genomic deletions, point mutations (arrows), and promoter methylation (arrowheads) noted in human cancers. The exons of the *INK4b* and *INK4a* loci are shown as rectangles. The transcripts/proteins and presumed functions of the transcripts/proteins are indicated. The speckled rectangles indicate the open reading frame in transcripts encoding p15; the hatched rectangles indicate the open reading frame present in transcripts encoding p19ARF; and the solid rectangles indicate the open reading frame present in transcripts encoding p16. The size of the locus, exons, and transcripts are not shown to scale. (Modified and reproduced with permission from Haber DA. Splicing into senescence: the curious case of p16 and p19ARF. Cell 91:555–558, 1997

(Park & Vogelstein, 2003)

CHAPTER 6:CONCLUSION

As conclusion, this project has demonstrated the establishment of improvised histoarchitecture of oral mucosal model that applied normal immortalized oral keratinocytes co-cultured with oral fibroblast on acellular dermis. The presence of complete structure of basement membrane protein that mimic native tissues, has facilitate the response of senescence associated secretory protein (SASP) on degradation of basement membrane protein. It is essentially to note that senescence is far from passive, and action of these secretory protein towards tissue architecture need to be further investigated.

REFERENCES

Abu-Id, M. H., Warnke, P. H., Gottschalk, J., Springer, I., Wiltfang, J., Acil, Y., . . . Kreusch, T. (2008). "Bis-phossy jaws" - high and low risk factors for bisphosphonate-induced osteonecrosis of the jaw. *J Craniomaxillofac Surg, 36*(2), 95-103. doi: 10.1016/j.jcms.2007.06.008

Acosta, J. C., Banito, A., Wuestefeld, T., Georgilis, A., Janich, P., Morton, J. P., . . . Gil, J. (2013). A complex secretory program orchestrated by the inflammasome controls paracrine senescence. *Nat Cell Biol, 15*(8), 978-990. doi: 10.1038/ncb2784

Adams, P. D. (2009). Healing and hurting: molecular mechanisms, functions, and pathologies of cellular senescence. *Mol Cell, 36*(1), 2-14. doi: 10.1016/j.molcel.2009.09.021

Aguirre, J. I., Akhter, M. P., Kimmel, D. B., Pingel, J. E., Williams, A., Jorgensen, M., . . . Wronski, T. J. (2012). Oncologic doses of zoledronic acid induce osteonecrosis of the jaw-like lesions in rice rats (Oryzomys palustris) with periodontitis. *J Bone Miner Res, 27*(10), 2130-2143. doi: 10.1002/jbmr.1669

Allam, E., Allen, M., Chu, T. M., Ghoneima, A., & Jack Windsor, L. (2011). In vivo effects of zoledronic acid on oral mucosal epithelial cells. *Oral Dis, 17*(3), 291-297. doi: 10.1111/j.1601-0825.2010.01739.x

Althubiti, M., Lezina, L., Carrera, S., Jukes-Jones, R., Giblett, S. M., Antonov, A., . . . Macip, S. (2014). Characterization of novel markers of senescence and their prognostic potential in cancer. *Cell Death Dis, 5*, e1528. doi: 10.1038/cddis.2014.489

Andrian, E., Mostefaoui, Y., Rouabhia, M., & Grenier, D. (2007). Regulation of matrix metalloproteinases and tissue inhibitors of matrix metalloproteinases by Porphyromonas gingivalis in an engineered human oral mucosa model. *J Cell Physiol, 211*(1), 56-62. doi: 10.1002/jcp.20894

Ashcroft, G. S., Mills, S. J., & Ashworth, J. J. (2002). Ageing and wound healing. *Biogerontology, 3*(6), 337-345.

Bae, S., Sun, S., Aghaloo, T., Oh, J. E., McKenna, C. E., Kang, M. K., . . . Kim, R. H. (2014). Development of oral osteomucosal tissue constructs in vitro and localization of fluorescently-labeled bisphosphonates to hard and soft tissue. *Int J Mol Med, 34*(2), 559-563. doi: 10.3892/ijmm.2014.1802

Balin, A. K., Goodman, D. B., Rasmussen, H., & Cristofalo, V. J. (1977). The effect of oxygen and vitamin E on the lifespan of human diploid cells in vitro. *J Cell Biol, 74*(1), 58-67.

Bandyopadhyay, D., Timchenko, N., Suwa, T., Hornsby, P. J., Campisi, J., & Medrano, E. E. (2001). The human melanocyte: a model system to study the complexity of cellular aging and transformation in non-fibroblastic cells. *Exp Gerontol, 36*(8), 1265-1275.

Bao, K., Akguel, B., & Bostanci, N. (2014). Establishment and characterization of immortalized gingival epithelial and fibroblastic cell lines for the development of organotypic cultures. *Cells Tissues Organs, 199*(4), 228-237. doi: 10.1159/000363694

Barrick, B., Campbell, E. J., & Owen, C. A. (1999). Leukocyte proteinases in wound healing: roles in physiologic and pathologic processes. *Wound Repair Regen, 7*(6), 410-422.

Barrientos, S., Stojadinovic, O., Golinko, M. S., Brem, H., & Tomic-Canic, M. (2008). Growth factors and cytokines in wound healing. *Wound Repair Regen, 16*(5), 585-601. doi: 10.1111/j.1524-475X.2008.00410.x

Bart Vande Vannet , J.-L. H. a. H. W. (2007). The use of three-dimensional oral mucosa cell cultures to assess the toxicity of soldered and welded wires. *The European Journal of Orthodontics*, 60-66. doi: doi:10.1093/ejo/cjl063

Bassett, C. A., Donath, A., Macagno, F., Preisig, R., Fleisch, H., & Francis, M. D. (1969). Diphosphonates in the treatment of myositis ossificans. *Lancet, 2*(7625), 845.

Belibasakis, G. N., Bostanci, N., Hashim, A., Johansson, A., Aduse-Opoku, J., Curtis, M. A., & Hughes, F. J. (2007). Regulation of RANKL and OPG gene expression in human gingival fibroblasts and periodontal ligament cells by Porphyromonas gingivalis: a putative role of the Arg-gingipains. *Microb Pathog, 43*(1), 46-53. doi: 10.1016/j.micpath.2007.03.001

Bell, B. M., & Bell, R. E. (2008). Oral bisphosphonates and dental implants: a retrospective study. *J Oral Maxillofac Surg, 66*(5), 1022-1024. doi: 10.1016/j.joms.2007.12.040

Bergmeister, P., Gasser,K.,Lang,A. (2012). Drug-induced osteonecrosis of the jaw. *magazine of european medical oncology, 5*, 57-62.

Berndt, A., Hyckel, P., Konneker, A., & Kosmehl, H. (1998). [3-dimensional in vitro invasion model for oral squamous epithelial carcinomas. Evaluation of tumor and stromal cell properties as well as extracellular matrix]. *Mund Kiefer Gesichtschir, 2*(5), 256-260. doi: 10.1016/S0266-4356(98)90471-5

Bhargava, S., Chapple, C. R., Bullock, A. J., Layton, C., & MacNeil, S. (2004). Tissue-engineered buccal mucosa for substitution urethroplasty. *BJU Int, 93*(6), 807-811. doi: 10.1111/j.1464-410X.2003.04723.x

Biasotto, M., Chiandussi, S., Dore, F., Rinaldi, A., Rizzardi, C., Cavalli, F., & Di Lenarda, R. (2006). Clinical aspects and management of bisphosphonates-associated osteonecrosis of the jaws. *Acta Odontol Scand, 64*(6), 348-354. doi: 10.1080/00016350600844360

Bisdas, S., Chambron Pinho, N., Smolarz, A., Sader, R., Vogl, T. J., & Mack, M. G. (2008). Biphosphonate-induced osteonecrosis of the jaws: CT and MRI spectrum of findings in 32 patients. *Clin Radiol, 63*(1), 71-77. doi: 10.1016/j.crad.2007.04.023

Bisphosphonates (marketed as Actonel, Actonel+Ca, Aredia, Boniva, Didronel, Fosamax, Fosamax+D,Reclast, Skelid, and Zometa). . (2009).

Black, D. M., Delmas, P. D., Eastell, R., Reid, I. R., Boonen, S., Cauley, J. A., . . . Trial, H. P. F. (2007). Once-yearly zoledronic acid for treatment of postmenopausal osteoporosis. *N Engl J Med, 356*(18), 1809-1822. doi: 10.1056/NEJMoa067312

Blackburn, E. H. (1994). Telomeres: no end in sight. *Cell, 77*(5), 621-623.

Blackburn, E. H. (2000). Telomere states and cell fates. *Nature, 408*(6808), 53-56. doi: 10.1038/35040500

Blomquist, E., Westermark, B., & Ponten, J. (1980). Ageing of human glial cells in culture: increase in the fraction of non-dividers as demonstrated by a minicloning technique. *Mech Ageing Dev, 12*(2), 173-182.

Bodnar, A. G., Ouellette, M., Frolkis, M., Holt, S. E., Chiu, C. P., Morin, G. B., . . . Wright, W. E. (1998). Extension of life-span by introduction of telomerase into normal human cells. *Science, 279*(5349), 349-352.

Body, J. J. (2006). Bisphosphonates for malignancy-related bone disease: current status, future developments. *Support Care Cancer, 14*(5), 408-418. doi: 10.1007/s00520-005-0913-5

Bone, H. G., Hosking, D., Devogelaer, J. P., Tucci, J. R., Emkey, R. D., Tonino, R. P., . . . Alendronate Phase, I. I. I. O. T. S. G. (2004). Ten years' experience with alendronate for osteoporosis in postmenopausal women. *N Engl J Med, 350*(12), 1189-1199. doi: 10.1056/NEJMoa030897

Borromeo, G. L., Tsao, C. E., Darby, I. B., & Ebeling, P. R. (2011). A review of the clinical implications of bisphosphonates in dentistry. *Aust Dent J, 56*(1), 2-9. doi: 10.1111/j.1834-7819.2010.01283.x

Boukamp, P., Petrussevska, R. T., Breitkreutz, D., Hornung, J., Markham, A., & Fusenig, N. E. (1988). Normal keratinization in a spontaneously immortalized aneuploid human keratinocyte cell line. *J Cell Biol, 106*(3), 761-771.

Boukamp, P., Popp, S., Altmeyer, S., Hulsen, A., Fasching, C., Cremer, T., & Fusenig, N. E. (1997). Sustained nontumorigenic phenotype correlates with a largely stable chromosome content during long-term culture of the human keratinocyte line HaCaT. *Genes Chromosomes Cancer, 19*(4), 201-214.

Braig, M., Lee, S., Loddenkemper, C., Rudolph, C., Peters, A. H., Schlegelberger, B., . . . Schmitt, C. A. (2005). Oncogene-induced senescence as an initial barrier in lymphoma development. *Nature, 436*(7051), 660-665. doi: 10.1038/nature03841

Brenner, A. J., Stampfer, M. R., & Aldaz, C. M. (1998). Increased p16 expression with first senescence arrest in human mammary epithelial cells and extended growth capacity with p16 inactivation. *Oncogene, 17*(2), 199-205. doi: 10.1038/sj.onc.1201919

Buckley, K. A., & Fraser, W. D. (2002). Receptor activator for nuclear factor kappaB ligand and osteoprotegerin: regulators of bone physiology and immune responses/potential therapeutic agents and biochemical markers. *Ann Clin Biochem, 39*(Pt 6), 551-556.

Campisi, J. (2005). Senescent cells, tumor suppression, and organismal aging: good citizens, bad neighbors. *Cell, 120*(4), 513-522. doi: 10.1016/j.cell.2005.02.003

Campisi, J., & d'Adda di Fagagna, F. (2007). Cellular senescence: when bad things happen to good cells. *Nat Rev Mol Cell Biol, 8*(9), 729-740. doi: 10.1038/nrm2233

Chai, W. L., Brook, I. M., Emanuelsson, L., Palmquist, A., van Noort, R., & Moharamzadeh, K. (2011). Ultrastructural analysis of implant-soft tissue interface on a three dimensional tissue-engineered oral mucosal model. *J Biomed Mater Res A*. doi: 10.1002/jbm.a.33245

Chai, W. L., Brook, I. M., Palmquist, A., van Noort, R., & Moharamzadeh, K. (2012). The biological seal of the implant-soft tissue interface evaluated in a tissue-engineered oral mucosal model. *J R Soc Interface, 9*(77), 3528-3538. doi: 10.1098/rsif.2012.0507

Chai, W. L., Moharamzadeh, K., Brook, I. M., Emanuelsson, L., Palmquist, A., & van Noort, R. (2010). Development of a novel model for the investigation of implant-soft tissue interface. *J Periodontol, 81*(8), 1187-1195. doi: 10.1902/jop.2010.090648

Charalambous, C., Virrey, J., Kardosh, A., Jabbour, M. N., Qazi-Abdullah, L., Pen, L., . . . Hofman, F. M. (2007). Glioma-associated endothelial cells show evidence of replicative senescence. *Exp Cell Res, 313*(6), 1192-1202. doi: 10.1016/j.yexcr.2006.12.027

Che, Z. M., Jung, T. H., Choi, J. H., Yoon do, J., Jeong, H. J., Lee, E. J., & Kim, J. (2006). Collagen-based co-culture for invasive study on cancer cells-fibroblasts interaction. *Biochem Biophys Res Commun, 346*(1), 268-275. doi: 10.1016/j.bbrc.2006.05.111

Chen, H., Zheng, X., & Zheng, Y. (2014). Age-associated loss of lamin-B leads to systemic inflammation and gut hyperplasia. *Cell, 159*(4), 829-843. doi: 10.1016/j.cell.2014.10.028

Chen, Q. M. (2000). Replicative senescence and oxidant-induced premature senescence. Beyond the control of cell cycle checkpoints. *Ann N Y Acad Sci, 908*, 111-125.

Chen, Q. M., Bartholomew, J. C., Campisi, J., Acosta, M., Reagan, J. D., & Ames, B. N. (1998). Molecular analysis of H2O2-induced senescent-like growth arrest in normal human fibroblasts: p53 and Rb control G1 arrest but not cell replication. *Biochem J, 332 (Pt 1)*, 43-50.

Chen, Z., Trotman, L. C., Shaffer, D., Lin, H. K., Dotan, Z. A., Niki, M., . . . Pandolfi, P. P. (2005). Crucial role of p53-dependent cellular senescence in suppression of Pten-deficient tumorigenesis. *Nature, 436*(7051), 725-730. doi: 10.1038/nature03918

Chicas, A., Wang, X., Zhang, C., McCurrach, M., Zhao, Z., Mert, O., . . . Lowe, S. W. (2010). Dissecting the unique role of the retinoblastoma tumor suppressor during cellular senescence. *Cancer Cell, 17*(4), 376-387. doi: 10.1016/j.ccr.2010.01.023

Childs, B. G., Durik, M., Baker, D. J., & van Deursen, J. M. (2015). Cellular senescence in aging and age-related disease: from mechanisms to therapy. *Nat Med, 21*(12), 1424-1435. doi: 10.1038/nm.4000

Collado, M., Gil, J., Efeyan, A., Guerra, C., Schuhmacher, A. J., Barradas, M., . . . Serrano, M. (2005). Tumour biology: senescence in premalignant tumours. *Nature, 436*(7051), 642. doi: 10.1038/436642a

Colley, H. E., Macneil, S., Jones, A.V.,Thornhill, M.H.,Murdoch, C. (2009). *The development of in vitro models of squamous cell carcinoma of the oral mucosa – From mild dysplasia to an*

expanding carcinoma. Paper presented at the Poster Session I/Oral Oncology Supplement 3.

Coppe, J. P., Desprez, P. Y., Krtolica, A., & Campisi, J. (2010). The senescence-associated secretory phenotype: the dark side of tumor suppression. *Annu Rev Pathol, 5*, 99-118. doi: 10.1146/annurev-pathol-121808-102144

Coppe, J. P., Patil, C. K., Rodier, F., Sun, Y., Munoz, D. P., Goldstein, J., . . . Campisi, J. (2008). Senescence-associated secretory phenotypes reveal cell-nonautonomous functions of oncogenic RAS and the p53 tumor suppressor. *PLoS Biol, 6*(12), 2853-2868. doi: 10.1371/journal.pbio.0060301

Costea, D. E., Loro, L. L., Dimba, E. A., Vintermyr, O. K., & Johannessen, A. C. (2003). Crucial effects of fibroblasts and keratinocyte growth factor on morphogenesis of reconstituted human oral epithelium. *J Invest Dermatol, 121*(6), 1479-1486. doi: 10.1111/j.1523-1747.2003.12616.x

Courtois-Cox, S., Genther Williams, S. M., Reczek, E. E., Johnson, B. W., McGillicuddy, L. T., Johannessen, C. M., . . . Cichowski, K. (2006). A negative feedback signaling network underlies oncogene-induced senescence. *Cancer Cell, 10*(6), 459-472. doi: 10.1016/j.ccr.2006.10.003

Cox, G., Gauldie, J., & Jordana, M. (1992). Bronchial epithelial cell-derived cytokines (G-CSF and GM-CSF) promote the survival of peripheral blood neutrophils in vitro. *Am J Respir Cell Mol Biol, 7*(5), 507-513. doi: 10.1165/ajrcmb/7.5.507

Cozin, M., Pinker, B. M., Solemani, K., Zuniga, J. M., Dadaian, S. C., Cremers, S., . . . Raghavan, S. (2011). Novel therapy to reverse the cellular effects of bisphosphonates on primary human oral fibroblasts. *J Oral Maxillofac Surg, 69*(10), 2564-2578. doi: 10.1016/j.joms.2011.03.005

Cremers, S. C., Pillai, G., & Papapoulos, S. E. (2005). Pharmacokinetics/pharmacodynamics of bisphosphonates: use for optimisation of intermittent therapy for osteoporosis. *Clin Pharmacokinet, 44*(6), 551-570.

Creusot, F., Acs, G., & Christman, J. K. (1982). Inhibition of DNA methyltransferase and induction of Friend erythroleukemia cell differentiation by 5-azacytidine and 5-aza-2'-deoxycytidine. *J Biol Chem, 257*(4), 2041-2048.

d'Adda di Fagagna, F., Reaper, P. M., Clay-Farrace, L., Fiegler, H., Carr, P., Von Zglinicki, T., . . . Jackson, S. P. (2003). A DNA damage checkpoint response in telomere-initiated senescence. *Nature, 426*(6963), 194-198. doi: 10.1038/nature02118

De Cecco, M., Criscione, S. W., Peckham, E. J., Hillenmeyer, S., Hamm, E. A., Manivannan, J., . . . Sedivy, J. M. (2013). Genomes of replicatively senescent cells undergo global epigenetic changes leading to gene silencing and activation of transposable elements. *Aging Cell, 12*(2), 247-256. doi: 10.1111/acel.12047

de Groen, P. C., Lubbe, D. F., Hirsch, L. J., Daifotis, A., Stephenson, W., Freedholm, D., . . . Wang, K. K. (1996). Esophagitis associated with the use of alendronate. *N Engl J Med, 335*(14), 1016-1021. doi: 10.1056/NEJM199610033351403

Demaria, M., Ohtani, N., Youssef, S. A., Rodier, F., Toussaint, W., Mitchell, J. R., . . . Campisi, J. (2014). An essential role for senescent cells in optimal wound healing through secretion of PDGF-AA. *Dev Cell, 31*(6), 722-733. doi: 10.1016/j.devcel.2014.11.012

Denoyelle, C., Abou-Rjaily, G., Bezrookove, V., Verhaegen, M., Johnson, T. M., Fullen, D. R., . . . Soengas, M. S. (2006). Anti-oncogenic role of the endoplasmic reticulum differentially activated by mutations in the MAPK pathway. *Nat Cell Biol, 8*(10), 1053-1063. doi: 10.1038/ncb1471

Devalia, J. L., Bayram, H., Abdelaziz, M. M., Sapsford, R. J., & Davies, R. J. (1999). Differences between cytokine release from bronchial epithelial cells of asthmatic patients and non-asthmatic subjects: effect of exposure to diesel exhaust particles. *Int Arch Allergy Immunol, 118*(2-4), 437-439. doi: 10.1159/000024157

Dhomen, N., Reis-Filho, J. S., da Rocha Dias, S., Hayward, R., Savage, K., Delmas, V., . . . Marais, R. (2009). Oncogenic Braf induces melanocyte senescence and melanoma in mice. *Cancer Cell, 15*(4), 294-303. doi: 10.1016/j.ccr.2009.02.022

Diab, D. L., & Watts, N. B. (2013). Bisphosphonate drug holiday: who, when and how long. *Ther Adv Musculoskelet Dis, 5*(3), 107-111. doi: 10.1177/1759720X13477714

Dickson, M. A., Hahn, W. C., Ino, Y., Ronfard, V., Wu, J. Y., Weinberg, R. A., . . . Rheinwald, J. G. (2000). Human keratinocytes that express hTERT and also bypass a p16(INK4a)-enforced mechanism that limits life span become immortal yet retain normal growth and differentiation characteristics. *Mol Cell Biol, 20*(4), 1436-1447.

Dimri, G. P., Lee, X., Basile, G., Acosta, M., Scott, G., Roskelley, C., . . . et al. (1995). A biomarker that identifies senescent human cells in culture and in aging skin in vivo. *Proc Natl Acad Sci U S A, 92*(20), 9363-9367.

Dongari-Bagtzoglou, A., & Kashleva, H. (2003a). Candida albicans triggers interleukin-8 secretion by oral epithelial cells. *Microb Pathog, 34*(4), 169-177. doi: 10.1016/S0882-4010(03)00004-4

Dongari-Bagtzoglou, A., & Kashleva, H. (2003b). Candida albicans triggers interleukin-8 secretion by oral epithelial cells. *Microb Pathog, 34*(4), 169-177.

Dongari-Bagtzoglou, A., & Kashleva, H. (2003c). Granulocyte-macrophage colony-stimulating factor responses of oral epithelial cells to Candida albicans. *Oral Microbiol Immunol, 18*(3), 165-170. doi: 10.1034/j.1399-302X.2003.00061.x

Dongari-Bagtzoglou, A., & Kashleva, H. (2006a). Development of a highly reproducible three-dimensional organotypic model of the oral mucosa. *Nat Protoc, 1*(4), 2012-2018. doi: Doi 10.1038/Nprot.2006.323

Dongari-Bagtzoglou, A., & Kashleva, H. (2006b). Development of a highly reproducible three-dimensional organotypic model of the oral mucosa. *Nat Protoc, 1*(4), 2012-2018. doi: 10.1038/nprot.2006.323

Dongari-Bagtzoglou, A., & Kashleva, H. (2006c). Development of a novel three-dimensional in vitro model of oral Candida infection. *Microb Pathog, 40*(6), 271-278. doi: doi:10.1016/j.micpath.2006.02.004

Dongari-Bagtzoglou, A., Kashleva, H., & Villar, C. C. (2004). Bioactive interleukin-1alpha is cytolytically released from Candida albicans-infected oral epithelial cells. *Med Mycol, 42*(6), 531-541.

Dongari-Bagtzoglou, A., Wen, K., & Lamster, I. B. (1999). Candida albicans triggers interleukin-6 and interleukin-8 responses by oral fibroblasts in vitro. *Oral Microbiol Immunol, 14*(6), 364-370.

Dovi, J. V., Szpaderska, A. M., & DiPietro, L. A. (2004). Neutrophil function in the healing wound: adding insult to injury? *Thromb Haemost, 92*(2), 275-280. doi: 10.1160/TH03-11-0720

Drake, M. T., Clarke, B. L., & Khosla, S. (2008). Bisphosphonates: mechanism of action and role in clinical practice. *Mayo Clin Proc, 83*(9), 1032-1045. doi: 10.4065/83.9.1032

Dumont, P., Burton, M., Chen, Q. M., Gonos, E. S., Frippiat, C., Mazarati, J. B., . . . Toussaint, O. (2000). Induction of replicative senescence biomarkers by sublethal oxidative stresses in normal human fibroblast. *Free Radic Biol Med, 28*(3), 361-373.

Dunford, J. E., Thompson, K., Coxon, F. P., Luckman, S. P., Hahn, F. M., Poulter, C. D., . . . Rogers, M. J. (2001). Structure-activity relationships for inhibition of farnesyl diphosphate synthase in vitro and inhibition of bone resorption in vivo by nitrogen-containing bisphosphonates. *J Pharmacol Exp Ther, 296*(2), 235-242.

Duong, H. S., Le, A. D., Zhang, Q., & Messadi, D. V. (2005). A novel 3-dimensional culture system as an in vitro model for studying oral cancer cell invasion. *Int J Exp Pathol, 86*(6), 365-374. doi: 10.1111/j.0959-9673.2005.00441.x

Durie, B. G. (2007). Use of bisphosphonates in multiple myeloma: IMWG response to Mayo Clinic consensus statement. *Mayo Clin Proc, 82*(4), 516-517; author reply 517-518. doi: 10.4065/82.4.516

Effros, R. B., & Walford, R. L. (1984). T cell cultures and the Hayflick limit. *Hum Immunol, 9*(1), 49-65.

Ewald, J. A., Desotelle, J. A., Wilding, G., & Jarrard, D. F. (2010). Therapy-induced senescence in cancer. *J Natl Cancer Inst, 102*(20), 1536-1546. doi: 10.1093/jnci/djq364

Faragher, R. G., & Kill, I. R. (2009). The in vitro kinetics of senescence of Fischer 344 rat embryo fibroblasts. *Biogerontology, 10*(3), 285-289. doi: 10.1007/s10522-008-9198-7

Feng, X., & McDonald, J. M. (2011). Disorders of bone remodeling. *Annu Rev Pathol, 6*, 121-145. doi: 10.1146/annurev-pathol-011110-130203

Ferbeyre, G., de Stanchina, E., Lin, A. W., Querido, E., McCurrach, M. E., Hannon, G. J., & Lowe, S. W. (2002). Oncogenic ras and p53 cooperate to induce cellular senescence. *Mol Cell Biol, 22*(10), 3497-3508.

Feucht, E. C., DeSanti, C. L., & Weinberg, A. (2003). Selective induction of human beta-defensin mRNAs by Actinobacillus actinomycetemcomitans in primary and immortalized oral epithelial cells. *Oral Microbiol Immunol, 18*(6), 359-363. doi: 10.1046/j.0902-0055.2002.00097.x

Fleisch, H., & Bisaz, S. (1962). Isolation from urine of pyrophosphate, a calcification inhibitor. *Am J Physiol, 203*, 671-675.

Francis, M. D., Gray, J. A., & Griebstein, W. J. (1968). The formation and influence of surface phases on calcium phosphate solids. *Adv Oral Biol, 3*, 83-120.

Francis, M. D., & Valent, D. J. (2007). Historical perspectives on the clinical development of bisphosphonates in the treatment of bone diseases. *J Musculoskelet Neuronal Interact, 7*(1), 2-8.

Freedberg, I. M., Tomic-Canic, M., Komine, M., & Blumenberg, M. (2001). Keratins and the keratinocyte activation cycle. *J Invest Dermatol, 116*(5), 633-640. doi: 10.1046/j.0022-202x.2001.doc.x

Freund, A., Orjalo, A. V., Desprez, P. Y., & Campisi, J. (2010). Inflammatory networks during cellular senescence: causes and consequences. *Trends Mol Med, 16*(5), 238-246. doi: 10.1016/j.molmed.2010.03.003

Fugazzotto, P. A., Lightfoot, W. S., Jaffin, R., & Kumar, A. (2007). Implant placement with or without simultaneous tooth extraction in patients taking oral bisphosphonates: postoperative healing, early follow-up, and the incidence of complications in two private practices. *J Periodontol, 78*(9), 1664-1669. doi: 10.1902/jop.2007.060514

Gallucci, R. M., Sloan, D. K., Heck, J. M., Murray, A. R., & O'Dell, S. J. (2004). Interleukin 6 indirectly induces keratinocyte migration. *J Invest Dermatol, 122*(3), 764-772. doi: 10.1111/j.0022-202X.2004.22323.x

Georgakopoulou, E. A., Tsimaratou, K., Evangelou, K., Fernandez Marcos, P. J., Zoumpourlis, V., Trougakos, I. P., . . . Gorgoulis, V. G. (2013). Specific lipofuscin staining as a novel biomarker to detect replicative and stress-induced senescence. A method applicable in cryo-preserved and archival tissues. *Aging (Albany NY), 5*(1), 37-50. doi: 10.18632/aging.100527

Gill, S. E., & Parks, W. C. (2008). Metalloproteinases and their inhibitors: regulators of wound healing. *Int J Biochem Cell Biol, 40*(6-7), 1334-1347. doi: 10.1016/j.biocel.2007.10.024

Gniadecki, R. (1998). Regulation of keratinocyte proliferation. *Gen Pharmacol, 30*(5), 619-622.

Goessel, G., Quante, M., Hahn, W. C., Harada, H., Heeg, S., Suliman, Y., . . . Opitz, O. G. (2005). Creating oral squamous cancer cells: a cellular model of oral-esophageal carcinogenesis. *Proc Natl Acad Sci U S A, 102*(43), 15599-15604. doi: 10.1073/pnas.0409730102

Goffinet, M., Thoulouzan, M., Pradines, A., Lajoie-Mazenc, I., Weinbaum, C., Faye, J. C., & Seronie-Vivien, S. (2006). Zoledronic acid treatment impairs protein geranyl-geranylation for biological effects in prostatic cells. *BMC Cancer, 6*, 60. doi: 10.1186/1471-2407-6-60

Goldstein, J. L., & Brown, M. S. (1990). Regulation of the mevalonate pathway. *Nature, 343*(6257), 425-430. doi: 10.1038/343425a0

Gorgoulis, V. G., & Halazonetis, T. D. (2010). Oncogene-induced senescence: the bright and dark side of the response. *Curr Opin Cell Biol, 22*(6), 816-827. doi: 10.1016/j.ceb.2010.07.013

Gosain, A., & DiPietro, L. A. (2004). Aging and wound healing. *World J Surg, 28*(3), 321-326. doi: 10.1007/s00268-003-7397-6

Grant, B. T., Amenedo, C., Freeman, K., & Kraut, R. A. (2008). Outcomes of placing dental implants in patients taking oral bisphosphonates: a review of 115 cases. *J Oral Maxillofac Surg, 66*(2), 223-230. doi: 10.1016/j.joms.2007.09.019

Gruber, H. E., Ivey, J. L., Baylink, D. J., Matthews, M., Nelp, W. B., Sisom, K., & Chesnut, C. H., 3rd. (1984). Long-term calcitonin therapy in postmenopausal osteoporosis. *Metabolism, 33*(4), 295-303.

Guo, S., & Dipietro, L. A. (2010). Factors affecting wound healing. *J Dent Res, 89*(3), 219-229. doi: 10.1177/0022034509359125

Gurtner, G. C., Werner, S., Barrandon, Y., & Longaker, M. T. (2008). Wound repair and regeneration. *Nature, 453*(7193), 314-321. doi: 10.1038/nature07039

Hagi-Pavli, E., Williams, D. M., Rowland, J. L., Thornhill, M., & Cruchley, A. T. (2014). Characterizing the immunological effects of oral healthcare ingredients using an in vitro reconstructed human epithelial model. *Food Chem Toxicol, 74*, 139-148. doi: 10.1016/j.fct.2014.09.007

Hansen, T., Kunkel, M., Weber, A., & James Kirkpatrick, C. (2006). Osteonecrosis of the jaws in patients treated with bisphosphonates - histomorphologic analysis in comparison with infected osteoradionecrosis. *Journal of Oral Pathology & Medicine, 35*(3), 155-160. doi: 10.1111/j.1600-0714.2006.00391.x

Harley, C. B., Futcher, A. B., & Greider, C. W. (1990). Telomeres shorten during ageing of human fibroblasts. *Nature, 345*(6274), 458-460. doi: 10.1038/345458a0

Hayflick, L., & Moorhead, P. S. (1961). The serial cultivation of human diploid cell strains. *Exp Cell Res, 25*, 585-621.

Heng, C., Badner, V. M., Vakkas, T. G., Johnson, R., & Yeo, Y. (2012). Bisphosphonate-related osteonecrosis of the jaw in patients with osteoporosis. *Am Fam Physician, 85*(12), 1134-1141.

Heng, M. C. (2011). Wound healing in adult skin: aiming for perfect regeneration. *Int J Dermatol, 50*(9), 1058-1066. doi: 10.1111/j.1365-4632.2011.04940.x

Herskind, C., & Rodemann, H. P. (2000). Spontaneous and radiation-induced differentiationof fibroblasts. *Exp Gerontol, 35*(6-7), 747-755.

Hubackova, S., Krejcikova, K., Bartek, J., & Hodny, Z. (2012). IL1- and TGFbeta-Nox4 signaling, oxidative stress and DNA damage response are shared features of replicative, oncogene-induced, and drug-induced paracrine 'bystander senescence'. *Aging (Albany NY), 4*(12), 932-951. doi: 10.18632/aging.100520

Hug, N., & Lingner, J. (2006). Telomere length homeostasis. *Chromosoma, 115*(6), 413-425. doi: 10.1007/s00412-006-0067-3

Hughes, D. E., MacDonald, B. R., Russell, R. G., & Gowen, M. (1989). Inhibition of osteoclast-like cell formation by bisphosphonates in long-term cultures of human bone marrow. *J Clin Invest, 83*(6), 1930-1935. doi: 10.1172/JCI114100

Hughes, D. E., Wright, K. R., Uy, H. L., Sasaki, A., Yoneda, T., Roodman, G. D., . . . Boyce, B. F. (1995). Bisphosphonates promote apoptosis in murine osteoclasts in vitro and in vivo. *J Bone Miner Res, 10*(10), 1478-1487. doi: 10.1002/jbmr.5650101008

Ibrahim, A., Scher, N., Williams, G., Sridhara, R., Li, N., Chen, G., . . . Pazdur, R. (2003). Approval summary for zoledronic acid for treatment of multiple myeloma and cancer bone metastases. *Clin Cancer Res, 9*(7), 2394-2399.

Ivanov, A., Pawlikowski, J., Manoharan, I., van Tuyn, J., Nelson, D. M., Rai, T. S., . . . Adams, P. D. (2013). Lysosome-mediated processing of chromatin in senescence. *J Cell Biol, 202*(1), 129-143. doi: 10.1083/jcb.201212110

Izumi, K., Song, J., & Feinberg, S. E. (2004). Development of a tissue-engineered human oral mucosa: from the bench to the bed side. *Cells Tissues Organs, 176*(1-3), 134-152. doi: 10.1159/000075034

Izumi, K., Terashi, H., Marcelo, C. L., & Feinberg, S. E. (2000). Development and characterization of a tissue-engineered human oral mucosa equivalent produced in a serum-free culture system. *J Dent Res, 79*(3), 798-805.

Jacobs, J. J., & de Lange, T. (2004). Significant role for p16INK4a in p53-independent telomere-directed senescence. *Curr Biol, 14*(24), 2302-2308. doi: 10.1016/j.cub.2004.12.025

Jang, D. H., Bhawal, U. K., Min, H. K., Kang, H. K., Abiko, Y., & Min, B. M. (2015). A transcriptional roadmap to the senescence and differentiation of human oral keratinocytes. *J Gerontol A Biol Sci Med Sci, 70*(1), 20-32. doi: 10.1093/gerona/glt212

Jeffcoat, M. K. (2006). Safety of oral bisphosphonates: controlled studies on alveolar bone. *Int J Oral Maxillofac Implants, 21*(3), 349-353.

Jha, K. K., Banga, S., Palejwala, V., & Ozer, H. L. (1998). SV40-Mediated immortalization. *Exp Cell Res, 245*(1), 1-7. doi: 10.1006/excr.1998.4272

Jiang, C. K., Tomic-Canic, M., Lucas, D. J., Simon, M., & Blumenberg, M. (1995). TGF beta promotes the basal phenotype of epidermal keratinocytes: transcriptional induction of K#5 and K#14 keratin genes. *Growth Factors, 12*(2), 87-97.

Jilka, R. L. (1998). Cytokines, bone remodeling, and estrogen deficiency: a 1998 update. *Bone, 23*(2), 75-81.

Jilka, R. L. (2003). Biology of the basic multicellular unit and the pathophysiology of osteoporosis. *Med Pediatr Oncol, 41*(3), 182-185. doi: 10.1002/mpo.10334

Jun, J. I., & Lau, L. F. (2010). The matricellular protein CCN1 induces fibroblast senescence and restricts fibrosis in cutaneous wound healing. *Nat Cell Biol, 12*(7), 676-685. doi: 10.1038/ncb2070

Jurk, D., Wang, C., Miwa, S., Maddick, M., Korolchuk, V., Tsolou, A., . . . von Zglinicki, T. (2012). Postmitotic neurons develop a p21-dependent senescence-like phenotype driven by a DNA damage response. *Aging Cell, 11*(6), 996-1004. doi: 10.1111/j.1474-9726.2012.00870.x

Kang, M. K., Guo, W., & Park, N. H. (1998). Replicative senescence of normal human oral keratinocytes is associated with the loss of telomerase activity without shortening of telomeres. *Cell Growth Differ, 9*(1), 85-95.

Kanis, J. A. (1995). Bone and cancer: pathophysiology and treatment of metastases. *Bone, 17*(2 Suppl), 101S-105S.

Kavanagh, K. L., Guo, K., Dunford, J. E., Wu, X., Knapp, S., Ebetino, F. H., . . . Oppermann, U. (2006). The molecular mechanism of nitrogen-containing

bisphosphonates as antiosteoporosis drugs. *Proc Natl Acad Sci U S A, 103*(20), 7829-7834. doi: 10.1073/pnas.0601643103

Kennel, K. A., & Drake, M. T. (2009). Adverse effects of bisphosphonates: implications for osteoporosis management. *Mayo Clin Proc, 84*(7), 632-637; quiz 638. doi: 10.1016/S0025-6196(11)60752-0

Khan, S. A., Kanis, J. A., Vasikaran, S., Kline, W. F., Matuszewski, B. K., McCloskey, E. V., . . . Porras, A. G. (1997). Elimination and biochemical responses to intravenous alendronate in postmenopausal osteoporosis. *J Bone Miner Res, 12*(10), 1700-1707. doi: 10.1359/jbmr.1997.12.10.1700

Khosla, S., Burr, D., Cauley, J., Dempster, D. W., Ebeling, P. R., Felsenberg, D., . . . Mineral, R. (2007). Bisphosphonate-associated osteonecrosis of the jaw: report of a task force of the American Society for Bone and Mineral Research. *J Bone Miner Res, 22*(10), 1479-1491. doi: 10.1359/jbmr.0707onj

Khovidhunkit, S. O., Yingsaman, N., Chairachvit, K., Surarit, R., Fuangtharnthip, P., & Petsom, A. (2011). In vitro study of the effects of plaunotol on oral cell proliferation and wound healing. *J Asian Nat Prod Res, 13*(2), 149-159. doi: 10.1080/10286020.2010.546790

Kim, R. H., Lee, R. S., Williams, D., Bae, S., Woo, J., Lieberman, M., . . . Park, N. H. (2011a). Bisphosphonates Induce Senescence in Normal Human Oral Keratinocytes. *J Dent Res, 90*(6), 810-816. doi: Doi 10.1177/0022034511402995

Kim, R. H., Lee, R. S., Williams, D., Bae, S., Woo, J., Lieberman, M., . . . Park, N. H. (2011b). Bisphosphonates induce senescence in normal human oral keratinocytes. *J Dent Res, 90*(6), 810-816. doi: 10.1177/0022034511402995

Kim, W. Y., & Sharpless, N. E. (2006). The regulation of INK4/ARF in cancer and aging. *Cell, 127*(2), 265-275. doi: 10.1016/j.cell.2006.10.003

Kipling, D., & Cooke, H. J. (1990). Hypervariable ultra-long telomeres in mice. *Nature, 347*(6291), 400-402. doi: 10.1038/347400a0

Kirchhoff, C., Araki, Y., Huhtaniemi, I., Matusik, R. J., Osterhoff, C., Poutanen, M., . . . Orgebin-Crist, M. C. (2004). Immortalization by large T-antigen of the adult epididymal duct epithelium. *Mol Cell Endocrinol, 216*(1-2), 83-94. doi: 10.1016/j.mce.2003.10.073

Kiyono, T., Foster, S. A., Koop, J. I., McDougall, J. K., Galloway, D. A., & Klingelhutz, A. J. (1998). Both Rb/p16INK4a inactivation and telomerase activity are required to immortalize human epithelial cells. *Nature, 396*(6706), 84-88. doi: 10.1038/23962

Korting, H. C., Patzak, U., Schaller, M., & Maibach, H. I. (1998). A model of human cutaneous candidosis based on reconstructed human epidermis for the light and electron microscopic study of pathogenesis and treatment. *J Infect, 36*(3), 259-267.

Krizhanovsky, V., Yon, M., Dickins, R. A., Hearn, S., Simon, J., Miething, C., . . . Lowe, S. W. (2008). Senescence of activated stellate cells limits liver fibrosis. *Cell, 134*(4), 657-667. doi: 10.1016/j.cell.2008.06.049

Kuilman, T., Michaloglou, C., Mooi, W. J., & Peeper, D. S. (2010). The essence of senescence. *Genes Dev, 24*(22), 2463-2479. doi: 10.1101/gad.1971610

Kuilman, T., Michaloglou, C., Vredeveld, L. C., Douma, S., van Doorn, R., Desmet, C. J., . . . Peeper, D. S. (2008). Oncogene-induced senescence relayed by an interleukin-dependent inflammatory network. *Cell, 133*(6), 1019-1031. doi: 10.1016/j.cell.2008.03.039

Kulasekara, K. K., Lukandu, O. M., Neppelberg, E., Vintermyr, O. K., Johannessen, A. C., & Costea, D. E. (2009). Cancer progression is associated with increased expression of basement membrane proteins in three-dimensional in vitro models of human oral cancer. *Arch Oral Biol, 54*(10), 924-931. doi: 10.1016/j.archoralbio.2009.07.004

Kulkarni, P. S., Sundqvist, K., Betsholtz, C., Hoglund, P., Wiman, K. G., Zhivotovsky, B., . . . Grafstrom, R. C. (1995). Characterization of human buccal epithelial cells transfected with the simian virus 40 T-antigen gene. *Carcinogenesis, 16*(10), 2515-2521.

Kumar, S., Millis, A. J., & Baglioni, C. (1992). Expression of interleukin 1-inducible genes and production of interleukin 1 by aging human fibroblasts. *Proc Natl Acad Sci U S A, 89*(10), 4683-4687.

Kwek, E. B., Koh, J. S., & Howe, T. S. (2008). More on atypical fractures of the femoral diaphysis. *N Engl J Med, 359*(3), 316-317; author reply 317-318. doi: 10.1056/NEJMc080861

Laberge, R. M., Awad, P., Campisi, J., & Desprez, P. Y. (2012). Epithelial-mesenchymal transition induced by senescent fibroblasts. *Cancer Microenviron, 5*(1), 39-44. doi: 10.1007/s12307-011-0069-4

Lacey, D. L., Timms, E., Tan, H. L., Kelley, M. J., Dunstan, C. R., Burgess, T., . . . Boyle, W. J. (1998). Osteoprotegerin ligand is a cytokine that regulates osteoclast differentiation and activation. *Cell, 93*(2), 165-176.

Landesberg, R., Cozin, M., Cremers, S., Woo, V., Kousteni, S., Sinha, S., . . . Raghavan, S. (2008). Inhibition of oral mucosal cell wound healing by bisphosphonates. *J Oral Maxillofac Surg, 66*(5), 839-847. doi: 10.1016/j.joms.2008.01.026

Landesberg, R., Woo, V., Cremers, S., Cozin, M., Marolt, D., Vunjak-Novakovic, G., . . . Raghavan, S. (2011). Potential pathophysiological mechanisms in osteonecrosis of the jaw. *Ann N Y Acad Sci, 1218*, 62-79. doi: 10.1111/j.1749-6632.2010.05835.x

Lasry, A., & Ben-Neriah, Y. (2015). Senescence-associated inflammatory responses: aging and cancer perspectives. *Trends Immunol, 36*(4), 217-228. doi: 10.1016/j.it.2015.02.009

Lawless, C., Wang, C., Jurk, D., Merz, A., Zglinicki, T., & Passos, J. F. (2010). Quantitative assessment of markers for cell senescence. *Exp Gerontol, 45*(10), 772-778. doi: 10.1016/j.exger.2010.01.018

Lee, B., Vouthounis, C., Stojadinovic, O., Brem, H., Im, M., & Tomic-Canic, M. (2005). From an enhanceosome to a repressosome: molecular antagonism between glucocorticoids and EGF leads to inhibition of wound healing. *J Mol Biol, 345*(5), 1083-1097. doi: 10.1016/j.jmb.2004.11.027

Lenart, B. A., Lorich, D. G., & Lane, J. M. (2008). Atypical fractures of the femoral diaphysis in postmenopausal women taking alendronate. *N Engl J Med, 358*(12), 1304-1306. doi: 10.1056/NEJMc0707493

Levine, A. J., & Oren, M. (2009). The first 30 years of p53: growing ever more complex. *Nat Rev Cancer, 9*(10), 749-758. doi: 10.1038/nrc2723

Lewiecki, E. M. (2009). Current and emerging pharmacologic therapies for the management of postmenopausal osteoporosis. *J Womens Health (Larchmt), 18*(10), 1615-1626. doi: 10.1089/jwh.2008.1086

Lin, A. W., Barradas, M., Stone, J. C., van Aelst, L., Serrano, M., & Lowe, S. W. (1998). Premature senescence involving p53 and p16 is activated in response to constitutive MEK/MAPK mitogenic signaling. *Genes Dev, 12*(19), 3008-3019.

Liu, D., & Hornsby, P. J. (2007). Senescent human fibroblasts increase the early growth of xenograft tumors via matrix metalloproteinase secretion. *Cancer Res, 67*(7), 3117-3126. doi: 10.1158/0008-5472.CAN-06-3452

Liu, J., Bian, Z., Kuijpers-Jagtman, A. M., & Von den Hoff, J. W. (2010). Skin and oral mucosa equivalents: construction and performance. *Orthodontics & Craniofacial Research, 13*(1), 11-20.

Liu, J. P., Cassar, L., Pinto, A., & Li, H. (2006). Mechanisms of cell immortalization mediated by EB viral activation of telomerase in nasopharyngeal carcinoma. *Cell Res, 16*(10), 809-817. doi: 10.1038/sj.cr.7310098

Lloyd, A. C., Obermuller, F., Staddon, S., Barth, C. F., McMahon, M., & Land, H. (1997). Cooperating oncogenes converge to regulate cyclin/cdk complexes. *Genes Dev, 11*(5), 663-677.

Loo, D. T., Fuquay, J. I., Rawson, C. L., & Barnes, D. W. (1987). Extended culture of mouse embryo cells without senescence: inhibition by serum. *Science, 236*(4798), 200-202.

Luckman, S. P., Hughes, D. E., Coxon, F. P., Graham, R., Russell, G., & Rogers, M. J. (1998). Nitrogen-containing bisphosphonates inhibit the mevalonate pathway and prevent post-translational prenylation of GTP-binding proteins, including Ras. *J Bone Miner Res, 13*(4), 581-589. doi: 10.1359/jbmr.1998.13.4.581

Mackenzie, I. C. (2004). Growth of malignant oral epithelial stem cells after seeding into organotypical cultures of normal mucosa. *Journal of Oral Pathology & Medicine, 33*(2), 71-78. doi: DOI 10.1111/j.1600-0714.2004.00157.x

Marikovsky, M., Vogt, P., Eriksson, E., Rubin, J. S., Taylor, W. G., Joachim, S., & Klagsbrun, M. (1996). Wound fluid-derived heparin-binding EGF-like growth factor (HB-EGF) is synergistic with insulin-like growth factor-I for Balb/MK keratinocyte proliferation. *J Invest Dermatol, 106*(4), 616-621.

Marx, R. E. (2003). Pamidronate (Aredia) and zoledronate (Zometa) induced avascular necrosis of the jaws: a growing epidemic. *J Oral Maxillofac Surg, 61*(9), 1115-1117.

Marx, R. E., Cillo, J. E., Jr., & Ulloa, J. J. (2007). Oral bisphosphonate-induced osteonecrosis: risk factors, prediction of risk using serum CTX testing, prevention, and treatment. *J Oral Maxillofac Surg, 65*(12), 2397-2410. doi: 10.1016/j.joms.2007.08.003

Marx, R. E., Sawatari, Y., Fortin, M., & Broumand, V. (2005). Bisphosphonate-induced exposed bone (osteonecrosis/osteopetrosis) of the jaws: risk factors, recognition, prevention, and treatment. *J Oral Maxillofac Surg, 63*(11), 1567-1575. doi: 10.1016/j.joms.2005.07.010

Masutomi, K., Yu, E. Y., Khurts, S., Ben-Porath, I., Currier, J. L., Metz, G. B., . . . Hahn, W. C. (2003). Telomerase maintains telomere structure in normal human cells. *Cell, 114*(2), 241-253.

McAllister, J. M., & Hornsby, P. J. (1987). Improved clonal and nonclonal growth of human, rat and bovine adrenocortical cells in culture. *In Vitro Cell Dev Biol, 23*(10), 677-685.

McLeod, N. M., Moutasim, K. A., Brennan, P. A., Thomas, G., & Jenei, V. (2014). In vitro effect of bisphosphonates on oral keratinocytes and fibroblasts. *J Oral Maxillofac Surg, 72*(3), 503-509. doi: 10.1016/j.joms.2013.08.007

Menaa, C., Reddy, S. V., Kurihara, N., Maeda, H., Anderson, D., Cundy, T., . . . Roodman, G. D. (2000). Enhanced RANK ligand expression and responsivity of bone marrow cells in Paget's disease of bone. *J Clin Invest, 105*(12), 1833-1838. doi: 10.1172/JCI9133

Mendez, M. V., Stanley, A., Park, H. Y., Shon, K., Phillips, T., & Menzoian, J. O. (1998). Fibroblasts cultured from venous ulcers display cellular characteristics of senescence. *J Vasc Surg, 28*(5), 876-883.

Meraw, S. J., & Reeve, C. M. (1999). Qualitative analysis of peripheral peri-implant bone and influence of alendronate sodium on early bone regeneration. *J Periodontol, 70*(10), 1228-1233. doi: 10.1902/jop.1999.70.10.1228

Meraw, S. J., Reeve, C. M., & Wollan, P. C. (1999). Use of alendronate in peri-implant defect regeneration. *J Periodontol, 70*(2), 151-158. doi: 10.1902/jop.1999.70.2.151

Michaloglou, C., Vredeveld, L. C., Soengas, M. S., Denoyelle, C., Kuilman, T., van der Horst, C. M., . . . Peeper, D. S. (2005). BRAFE600-associated senescence-like cell cycle arrest of human naevi. *Nature, 436*(7051), 720-724. doi: 10.1038/nature03890

Michalowsky, L. A., & Jones, P. A. (1987). Differential nuclear protein binding to 5-azacytosine-containing DNA as a potential mechanism for 5-aza-2'-deoxycytidine resistance. *Mol Cell Biol, 7*(9), 3076-3083.

Miller, P. D. (2009). Denosumab: anti-RANKL antibody. *Curr Osteoporos Rep, 7*(1), 18-22.

Minamino, T., Orimo, M., Shimizu, I., Kunieda, T., Yokoyama, M., Ito, T., . . . Komuro, I. (2009). A crucial role for adipose tissue p53 in the regulation of insulin resistance. *Nat Med, 15*(9), 1082-1087. doi: 10.1038/nm.2014

Miranti, C. K., & Brugge, J. S. (2002). Sensing the environment: a historical perspective on integrin signal transduction. *Nat Cell Biol, 4*(4), E83-90. doi: 10.1038/ncb0402-e83

Moharamzadeh, K., Brook, I. M., Scutt, A. M., Thornhill, M. H., & Van Noort, R. (2008). Mucotoxicity of dental composite resins on a tissue-engineered human oral mucosal model. *J Dent, 36*(5), 331-336. doi: 10.1016/j.jdent.2008.01.019

Moharamzadeh, K., Brook, I. M., Van Noort, R., Scutt, A. M., Smith, K. G., & Thornhill, M. H. (2008). Development, optimization and characterization of a full-thickness tissue engineered human oral mucosal model for biological assessment of dental biomaterials. *J Mater Sci Mater Med, 19*(4), 1793-1801. doi: 10.1007/s10856-007-3321-1

Mundy, G. R. (1987). Bone resorption and turnover in health and disease. *Bone, 8 Suppl 1*, S9-16.

Munoz-Espin, D., Canamero, M., Maraver, A., Gomez-Lopez, G., Contreras, J., Murillo-Cuesta, S., . . . Serrano, M. (2013). Programmed cell senescence during mammalian embryonic development. *Cell, 155*(5), 1104-1118. doi: 10.1016/j.cell.2013.10.019

Nardella, C., Clohessy, J. G., Alimonti, A., & Pandolfi, P. P. (2011). Pro-senescence therapy for cancer treatment. *Nat Rev Cancer, 11*(7), 503-511. doi: 10.1038/nrc3057

Nguyen, B. P., Ryan, M. C., Gil, S. G., & Carter, W. G. (2000). Deposition of laminin 5 in epidermal wounds regulates integrin signaling and adhesion. *Curr Opin Cell Biol, 12*(5), 554-562.

Nicke, B., Bastien, J., Khanna, S. J., Warne, P. H., Cowling, V., Cook, S. J., . . . Hancock, D. C. (2005). Involvement of MINK, a Ste20 family kinase, in Ras oncogene-induced growth arrest in human ovarian surface epithelial cells. *Mol Cell, 20*(5), 673-685. doi: 10.1016/j.molcel.2005.10.038

Nielsen, H. M., & Rassing, M. R. (2000). TR146 cells grown on filters as a model of human buccal epithelium: IV. Permeability of water, mannitol, testosterone and beta-adrenoceptor antagonists. Comparison to human, monkey and porcine buccal mucosa. *Int J Pharm, 194*(2), 155-167. doi: 10.1016/s0378-5173(99)00368-3

Nikolopoulos, S. N., Blaikie, P., Yoshioka, T., Guo, W., Puri, C., Tacchetti, C., & Giancotti, F. G. (2005). Targeted deletion of the integrin beta4 signaling domain suppresses laminin-5-dependent nuclear entry of mitogen-activated protein kinases and NF-kappaB, causing defects in epidermal growth and migration. *Mol Cell Biol, 25*(14), 6090-6102. doi: 10.1128/MCB.25.14.6090-6102.2005

Nogawa, M., Yuasa, T., Kimura, S., Kuroda, J., Segawa, H., Sato, K., . . . Maekawa, T. (2005). Zoledronic acid mediates Ras-independent growth inhibition of prostate cancer cells. *Oncol Res, 15*(1), 1-9.

Oh, J., Lee, Y. D., & Wagers, A. J. (2014). Stem cell aging: mechanisms, regulators and therapeutic opportunities. *Nat Med, 20*(8), 870-880. doi: 10.1038/nm.3651

Ohnuki, H., Izumi, K., Terada, M., Saito, T., Kato, H., Suzuki, A., . . . Maeda, T. (2012). Zoledronic acid induces S-phase arrest via a DNA damage response in normal human oral keratinocytes. *Arch Oral Biol, 57*(7), 906-917. doi: http://dx.doi.org/10.1016/j.archoralbio.2011.11.015

Ohnuki, H., Izumi, K., Terada, M., Saito, T., Kato, H., Suzuki, A., . . . Maeda, T. (2012). Zoledronic acid induces S-phase arrest via a DNA damage response in normal human oral keratinocytes. *Arch Oral Biol, 57*(7), 906-917. doi: 10.1016/j.archoralbio.2011.11.015

Okuyama, R., LeFort, K., & Dotto, G. P. (2004). A dynamic model of keratinocyte stem cell renewal and differentiation: role of the p21WAF1/Cip1 and Notch1 signaling pathways. *J Investig Dermatol Symp Proc, 9*(3), 248-252. doi: 10.1111/j.1087-0024.2004.09308.x

Olsen, C. L., Gardie, B., Yaswen, P., & Stampfer, M. R. (2002). Raf-1-induced growth arrest in human mammary epithelial cells is p16-independent and is overcome in immortal cells during conversion. *Oncogene, 21*(41), 6328-6339. doi: 10.1038/sj.onc.1205780

Orjalo, A. V., Bhaumik, D., Gengler, B. K., Scott, G. K., & Campisi, J. (2009). Cell surface-bound IL-1alpha is an upstream regulator of the senescence-associated IL-6/IL-8 cytokine network. *Proc Natl Acad Sci U S A, 106*(40), 17031-17036. doi: 10.1073/pnas.0905299106

Pabst, A. M., Ziebart, T., Koch, F. P., Taylor, K. Y., Al-Nawas, B., & Walter, C. (2012). The influence of bisphosphonates on viability, migration, and apoptosis of human oral keratinocytes--in vitro study. *Clin Oral Investig, 16*(1), 87-93. doi: 10.1007/s00784-010-0507-6

Pacifici, R. (1998). Cytokines, estrogen, and postmenopausal osteoporosis--the second decade. *Endocrinology, 139*(6), 2659-2661. doi: 10.1210/endo.139.6.6087

Palii, S. S., Van Emburgh, B. O., Sankpal, U. T., Brown, K. D., & Robertson, K. D. (2008). DNA methylation inhibitor 5-Aza-2'-deoxycytidine induces reversible genome-wide DNA damage that is distinctly influenced by DNA methyltransferases 1 and 3B. *Mol Cell Biol, 28*(2), 752-771. doi: 10.1128/MCB.01799-07

Palm, W., & de Lange, T. (2008). How shelterin protects mammalian telomeres. *Annu Rev Genet, 42*, 301-334. doi: 10.1146/annurev.genet.41.110306.130350

Park, B. H., & Vogelstein, B. (2003). *The INK4A Locus and the p16INK4A and p19 ARF Genes* (D. W. Kufu, Pollock,R.E,Weichselbaum RR Ed. 6 ed.). Holland-Frei Cancer Medicine 6th Edition: Hamilton (ON):BC Decker.

Parrinello, S., Coppe, J. P., Krtolica, A., & Campisi, J. (2005). Stromal-epithelial interactions in aging and cancer: senescent fibroblasts alter epithelial cell differentiation. *J Cell Sci, 118*(Pt 3), 485-496. doi: 10.1242/jcs.01635

Pastar, I., Stojadinovic, O., Yin, N. C., Ramirez, H., Nusbaum, A. G., Sawaya, A., . . . Tomic-Canic, M. (2014). Epithelialization in Wound Healing: A Comprehensive Review. *Adv Wound Care (New Rochelle), 3*(7), 445-464. doi: 10.1089/wound.2013.0473

Phan, T. C., Xu, J., & Zheng, M. H. (2004). Interaction between osteoblast and osteoclast: impact in bone disease. *Histol Histopathol, 19*(4), 1325-1344.

Pilcher, B. K., Wang, M., Qin, X. J., Parks, W. C., Senior, R. M., & Welgus, H. G. (1999). Role of matrix metalloproteinases and their inhibition in cutaneous wound healing and allergic contact hypersensitivity. *Ann N Y Acad Sci, 878*, 12-24.

Presland, R. B., & Jurevic, R. J. (2002). Making sense of the epithelial barrier: what molecular biology and genetics tell us about the functions of oral mucosal and epidermal tissues. *J Dent Educ, 66*(4), 564-574.

Pribluda, A., Elyada, E., Wiener, Z., Hamza, H., Goldstein, R. E., Biton, M., . . . Ben-Neriah, Y. (2013). A senescence-inflammatory switch from cancer-inhibitory to cancer-promoting mechanism. *Cancer Cell, 24*(2), 242-256. doi: 10.1016/j.ccr.2013.06.005

Prowse, K. R., & Greider, C. W. (1995). Developmental and tissue-specific regulation of mouse telomerase and telomere length. *Proc Natl Acad Sci U S A, 92*(11), 4818-4822.

Qiao, B., Gopalan, V., Chen, Z., Smith, R. A., Tao, Q., & Lam, A. K. (2012). Epithelial-mesenchymal transition and mesenchymal-epithelial transition are essential for the acquisition of stem cell properties in hTERT-immortalised oral epithelial cells. *Biol Cell, 104*(8), 476-489. doi: 10.1111/boc.201100077

Rainaldi, G., Pinto, B., Piras, A., Vatteroni, L., Simi, S., & Citti, L. (1991). Reduction of proliferative heterogeneity of CHEF18 Chinese hamster cell line during the progression toward tumorigenicity. *In Vitro Cell Dev Biol, 27A*(12), 949-952.

Rajagopalan, S., & Long, E. O. (2012). Cellular senescence induced by CD158d reprograms natural killer cells to promote vascular remodeling. *Proc Natl Acad Sci U S A, 109*(50), 20596-20601. doi: 10.1073/pnas.1208248109

Ramirez, R. D., Morales, C. P., Herbert, B. S., Rohde, J. M., Passons, C., Shay, J. W., & Wright, W. E. (2001). Putative telomere-independent mechanisms of replicative

aging reflect inadequate growth conditions. *Genes Dev, 15*(4), 398-403. doi: 10.1101/gad.859201

Rautava, J., Pollanen, M., Laine, M. A., Willberg, J., Lukkarinen, H., & Soukka, T. (2012). Effects of tacrolimus on an organotypic raft-culture model mimicking oral mucosa. *Clin Exp Dermatol, 37*(8), 897-903. doi: 10.1111/j.1365-2230.2012.04372.x

Reid, I. R. (2009). Osteonecrosis of the jaw: who gets it, and why? *Bone, 44*(1), 4-10. doi: 10.1016/j.bone.2008.09.012

Reid, I. R., Bolland, M. J., & Grey, A. B. (2007). Is bisphosphonate-associated osteonecrosis of the jaw caused by soft tissue toxicity? *Bone, 41*(3), 318-320. doi: 10.1016/j.bone.2007.04.196

Rheinwald, J. G., & Green, H. (1975). Serial cultivation of strains of human epidermal keratinocytes: the formation of keratinizing colonies from single cells. *Cell, 6*(3), 331-343. doi: 10.1016/s0092-8674(75)80001-8

Rheinwald, J. G., Hahn, W. C., Ramsey, M. R., Wu, J. Y., Guo, Z., Tsao, H., . . . O'Toole, K. M. (2002). A two-stage, p16(INK4A)- and p53-dependent keratinocyte senescence mechanism that limits replicative potential independent of telomere status. *Mol Cell Biol, 22*(14), 5157-5172.

Robles, S. J., & Adami, G. R. (1998). Agents that cause DNA double strand breaks lead to p16INK4a enrichment and the premature senescence of normal fibroblasts. *Oncogene, 16*(9), 1113-1123. doi: 10.1038/sj.onc.1201862

Rodier, F., Coppe, J. P., Patil, C. K., Hoeijmakers, W. A., Munoz, D. P., Raza, S. R., . . . Campisi, J. (2009). Persistent DNA damage signalling triggers senescence-associated inflammatory cytokine secretion. *Nat Cell Biol, 11*(8), 973-979. doi: 10.1038/ncb1909

Rodrigues, A. Z., Oliveira, P. T., Novaes, A. B., Jr., Maia, L. P., Souza, S. L., & Palioto, D. B. (2010). Evaluation of in vitro human gingival fibroblast seeding on acellular dermal matrix. *Braz Dent J, 21*(3), 179-189.

Roesch-Ely, M., Steinberg, T., Bosch, F. X., Mussig, E., Whitaker, N., Wiest, T., . . . Tomakidi, P. (2006). Organotypic co-cultures allow for immortalized human gingival keratinocytes to reconstitute a gingival epithelial phenotype in vitro. *Differentiation, 74*(9-10), 622-637. doi: 10.1111/j.1432-0436.2006.00099.x

Rogers, M. J., Watts, D. J., & Russell, R. G. (1997). Overview of bisphosphonates. *Cancer, 80*(8 Suppl), 1652-1660.

Rouabhia, M., Semlali, A., Chandra, J., Mukherjee, P., Chmielewski, W., & Ghannoum, M. A. (2012). Disruption of the ECM33 gene in Candida albicans prevents biofilm formation, engineered human oral mucosa tissue damage and gingival cell necrosis/apoptosis. *Mediators Inflamm, 2012*, 398207. doi: 10.1155/2012/398207

Ruggiero, S., Gralow, J., Marx, R. E., Hoff, A. O., Schubert, M. M., Huryn, J. M., . . . Valero, V. (2006). Practical guidelines for the prevention, diagnosis, and

treatment of osteonecrosis of the jaw in patients with cancer. *J Oncol Pract, 2*(1), 7-14. doi: 10.1200/jop.2006.2.1.7

Ruggiero, S. L. (2011). Bisphosphonate-related osteonecrosis of the jaw: an overview. *Ann N Y Acad Sci, 1218*, 38-46. doi: 10.1111/j.1749-6632.2010.05768.x

Ruggiero, S. L., Dodson, T. B., Assael, L. A., Landesberg, R., Marx, R. E., Mehrotra, B., . . . Maxillofacial, S. (2009). American Association of Oral and Maxillofacial Surgeons position paper on bisphosphonate-related osteonecrosis of the jaw - 2009 update. *Aust Endod J, 35*(3), 119-130. doi: 10.1111/j.1747-4477.2009.00213.x

Ruggiero, S. L., Mehrotra, B., Rosenberg, T. J., & Engroff, S. L. (2004). Osteonecrosis of the jaws associated with the use of bisphosphonates: a review of 63 cases. *J Oral Maxillofac Surg, 62*(5), 527-534.

Russell, R. G. (2006). Bisphosphonates: from bench to bedside. *Ann N Y Acad Sci, 1068*, 367-401. doi: 10.1196/annals.1346.041

Russell, R. G. (2011). Bisphosphonates: the first 40 years. *Bone, 49*(1), 2-19. doi: 10.1016/j.bone.2011.04.022

Saito, T., Izumi, K., Shiomi, A., Uenoyama, A., Ohnuki, H., Kato, H., . . . Maeda, T. (2014). Zoledronic acid impairs re-epithelialization through down-regulation of integrin alphavbeta6 and transforming growth factor beta signalling in a three-dimensional in vitro wound healing model. *Int J Oral Maxillofac Surg, 43*(3), 373-380. doi: 10.1016/j.ijom.2013.06.016

Salama, R., Sadaie, M., Hoare, M., & Narita, M. (2014). Cellular senescence and its effector programs. *Genes Dev, 28*(2), 99-114. doi: 10.1101/gad.235184.113

Sander, C., Nielsen, H. M., & Jacobsen, J. (2013). Buccal delivery of metformin: TR146 cell culture model evaluating the use of bioadhesive chitosan discs for drug permeability enhancement. *Int J Pharm, 458*(2), 254-261. doi: 10.1016/j.ijpharm.2013.10.026

Sanna, G., Zampino, M. G., Pelosi, G., Nole, F., & Goldhirsch, A. (2005). Jaw avascular bone necrosis associated with long-term use of biphosphonates. *Ann Oncol, 16*(7), 1207-1208. doi: 10.1093/annonc/mdi206

Santoro, M. M., Gaudino, G., & Marchisio, P. C. (2003). The MSP receptor regulates alpha6beta4 and alpha3beta1 integrins via 14-3-3 proteins in keratinocyte migration. *Dev Cell, 5*(2), 257-271.

Saracino, S., Canuto, R. A., Maggiora, M., Oraldi, M., Scoletta, M., Ciuffreda, L., . . . Muzio, G. (2012). Exposing human epithelial cells to zoledronic acid can mediate osteonecrosis of jaw: an in vitro model. *Journal of Oral Pathology & Medicine, 41*(10), 788-792. doi: 10.1111/j.1600-0714.2012.01173.x

Sarin, J., DeRossi, S. S., & Akintoye, S. O. (2008). Updates on bisphosphonates and potential pathobiology of bisphosphonate-induced jaw osteonecrosis. *Oral Dis, 14*(3), 277-285. doi: 10.1111/j.1601-0825.2007.01381.x

Sarkisian, C. J., Keister, B. A., Stairs, D. B., Boxer, R. B., Moody, S. E., & Chodosh, L. A. (2007). Dose-dependent oncogene-induced senescence in vivo and its evasion during mammary tumorigenesis. *Nat Cell Biol, 9*(5), 493-505. doi: 10.1038/ncb1567

Sarper, G. R. B. Y. S. A. A. G. P. E. M. (2011). A Pilot Study of the Primary Culture of the Oral Mucosa Keratinocytes by the Direct Explant Technique. *Oral Health and Dental Management*

10(2).

Sato, M., & Grasser, W. (1990). Effects of bisphosphonates on isolated rat osteoclasts as examined by reflected light microscopy. *J Bone Miner Res, 5*(1), 31-40. doi: 10.1002/jbmr.5650050107

Savagner, P., Kusewitt, D. F., Carver, E. A., Magnino, F., Choi, C., Gridley, T., & Hudson, L. G. (2005). Developmental transcription factor slug is required for effective re-epithelialization by adult keratinocytes. *J Cell Physiol, 202*(3), 858-866. doi: 10.1002/jcp.20188

Schaller, M., Mailhammer, R., & Korting, H. C. (2002). Cytokine expression induced by Candida albicans in a model of cutaneous candidosis based on reconstituted human epidermis. *J Med Microbiol, 51*(8), 672-676.

Scheper, M. A., Badros, A., Chaisuparat, R., Cullen, K. J., & Meiller, T. F. (2009). Effect of zoledronic acid on oral fibroblasts and epithelial cells: a potential mechanism of bisphosphonate-associated osteonecrosis. *Br J Haematol, 144*(5), 667-676. doi: 10.1111/j.1365-2141.2008.07504.x

Sedivy, J. M., Banumathy, G., & Adams, P. D. (2008). Aging by epigenetics--a consequence of chromatin damage? *Exp Cell Res, 314*(9), 1909-1917. doi: 10.1016/j.yexcr.2008.02.023

Semlali, A., Leung, K. P., Curt, S., & Rouabhia, M. (2011). Antimicrobial decapeptide KSL-W attenuates Candida albicans virulence by modulating its effects on Toll-like receptor, human beta-defensin, and cytokine expression by engineered human oral mucosa. *Peptides, 32*(5), 859-867. doi: 10.1016/j.peptides.2011.01.020

Serrano, M., Lin, A. W., McCurrach, M. E., Beach, D., & Lowe, S. W. (1997). Oncogenic ras provokes premature cell senescence associated with accumulation of p53 and p16INK4a. *Cell, 88*(5), 593-602.

Shelton, D. N., Chang, E., Whittier, P. S., Choi, D., & Funk, W. D. (1999). Microarray analysis of replicative senescence. *Curr Biol, 9*(17), 939-945.

Sherr, C. J., & DePinho, R. A. (2000). Cellular senescence: mitotic clock or culture shock? *Cell, 102*(4), 407-410.

Sherr, C. J., & McCormick, F. (2002). The RB and p53 pathways in cancer. *Cancer Cell, 2*(2), 103-112.

Shirota, T., Nakamura, A., Matsui, Y., Hatori, M., Nakamura, M., & Shintani, S. (2009). Bisphosphonate-related osteonecrosis of the jaw around dental implants in the maxilla: report of a case. *Clin Oral Implants Res, 20*(12), 1402-1408. doi: 10.1111/j.1600-0501.2009.01801.x

Siddiqui, J. A., & Partridge, N. C. (2016). Physiological Bone Remodeling: Systemic Regulation and Growth Factor Involvement. *Physiology (Bethesda), 31*(3), 233-245. doi: 10.1152/physiol.00061.2014

Silverman, S. L., & Landesberg, R. (2009). Osteonecrosis of the jaw and the role of bisphosphonates: a critical review. *Am J Med, 122*(2 Suppl), S33-45. doi: 10.1016/j.amjmed.2008.12.005

Smogorzewska, A., & de Lange, T. (2002). Different telomere damage signaling pathways in human and mouse cells. *EMBO J, 21*(16), 4338-4348.

Sogabe, Y., Abe, M., Yokoyama, Y., & Ishikawa, O. (2006). Basic fibroblast growth factor stimulates human keratinocyte motility by Rac activation. *Wound Repair Regen, 14*(4), 457-462. doi: 10.1111/j.1743-6109.2006.00143.x

Squier, C. A., & Kremer, M. J. (2001). Biology of oral mucosa and esophagus. *J Natl Cancer Inst Monogr*(29), 7-15.

Stampfer, M. R., & Yaswen, P. (2003). Human epithelial cell immortalization as a step in carcinogenesis. *Cancer Lett, 194*(2), 199-208.

Stanley, A., & Osler, T. (2001). Senescence and the healing rates of venous ulcers. *J Vasc Surg, 33*(6), 1206-1211.

Starck, W. J., & Epker, B. N. (1995). Failure of osseointegrated dental implants after diphosphonate therapy for osteoporosis: a case report. *Int J Oral Maxillofac Implants, 10*(1), 74-78.

Stefanick, M. L. (2005). Estrogens and progestins: background and history, trends in use, and guidelines and regimens approved by the US Food and Drug Administration. *Am J Med, 118 Suppl 12B*, 64-73. doi: 10.1016/j.amjmed.2005.09.059

Stein, G. H., Drullinger, L. F., Soulard, A., & Dulic, V. (1999). Differential roles for cyclin-dependent kinase inhibitors p21 and p16 in the mechanisms of senescence and differentiation in human fibroblasts. *Mol Cell Biol, 19*(3), 2109-2117.

Storer, M., Mas, A., Robert-Moreno, A., Pecoraro, M., Ortells, M. C., Di Giacomo, V., . . . Keyes, W. M. (2013). Senescence is a developmental mechanism that contributes to embryonic growth and patterning. *Cell, 155*(5), 1119-1130. doi: 10.1016/j.cell.2013.10.041

Studebaker, A. W., Storci, G., Werbeck, J. L., Sansone, P., Sasser, A. K., Tavolari, S., . . . Hall, B. M. (2008). Fibroblasts isolated from common sites of breast cancer metastasis enhance cancer cell growth rates and invasiveness in an interleukin-6-dependent manner. *Cancer Res, 68*(21), 9087-9095. doi: 10.1158/0008-5472.CAN-08-0400

Sun, T., Jackson, S., Haycock, J. W., & MacNeil, S. (2006). Culture of skin cells in 3D rather than 2D improves their ability to survive exposure to cytotoxic agents. *J Biotechnol, 122*(3), 372-381. doi: 10.1016/j.jbiotec.2005.12.021

Suyama, K., Noguchi, Y., Tanaka, T., Yoshida, T., Shibata, T., Saito, Y., & Tatsuno, I. (2007). Isoprenoid-independent pathway is involved in apoptosis induced by risedronate, a bisphosphonate, in which Bim plays a critical role in breast cancer cell line MCF-7. *Oncol Rep, 18*(5), 1291-1298.

Tang, A., & Gilchrest, B. A. (1996). Regulation of keratinocyte growth factor gene expression in human skin fibroblasts. *J Dermatol Sci, 11*(1), 41-50.

Teronen, O., Heikkila, P., Konttinen, Y. T., Laitinen, M., Salo, T., Hanemaaijer, R., . . . Sorsa, T. (1999). MMP inhibition and downregulation by bisphosphonates. *Ann N Y Acad Sci, 878*, 453-465.

Thornton, S. C., Mueller, S. N., & Levine, E. M. (1983). Human endothelial cells: use of heparin in cloning and long-term serial cultivation. *Science, 222*(4624), 623-625.

Timmermann, S., Hinds, P. W., & Munger, K. (1998). Re-expression of endogenous p16ink4a in oral squamous cell carcinoma lines by 5-aza-2'-deoxycytidine treatment induces a senescence-like state. *Oncogene, 17*(26), 3445-3453. doi: 10.1038/sj.onc.1202244

Tomakidi, P., Stark, H. J., Herold-Mende, C., Bosch, F. X., Steinbauer, H., Fusenig, N. E., & Breitkreutz, D. (2003). Discriminating expression of differentiation markers evolves in transplants of benign and malignant human skin keratinocytes through stromal interactions. *J Pathol, 200*(3), 298-307. doi: 10.1002/path.1366

Tominaga, K. (2015). The emerging role of senescent cells in tissue homeostasis and pathophysiology. *Pathobiol Aging Age Relat Dis, 5*, 27743. doi: 10.3402/pba.v5.27743

Tra, W. M., Tuk, B., van Neck, J. W., Hovius, S. E., & Perez-Amodio, S. (2013). Tissue-engineered mucosa is a suitable model to quantify the acute biological effects of ionizing radiation. *Int J Oral Maxillofac Surg, 42*(8), 939-948. doi: 10.1016/j.ijom.2013.01.025

Tra, W. M., van Neck, J. W., Hovius, S. E., van Osch, G. J., & Perez-Amodio, S. (2012). Characterization of a three-dimensional mucosal equivalent: similarities and differences with native oral mucosa. *Cells Tissues Organs, 195*(3), 185-196. doi: 10.1159/000324918

Vahtsevanos, K., Kyrgidis, A., Verrou, E., Katodritou, E., Triaridis, S., Andreadis, C. G., . . . Antoniades, K. (2009). Longitudinal cohort study of risk factors in cancer patients of bisphosphonate-related osteonecrosis of the jaw. *J Clin Oncol, 27*(32), 5356-5362. doi: 10.1200/JCO.2009.21.9584

van Deursen, J. M. (2014). The role of senescent cells in ageing. *Nature, 509*(7501), 439-446. doi: 10.1038/nature13193

Vande Vannet, B. M., & Hanssens, J. L. (2007). Cytotoxicity of two bonding adhesives assessed by three-dimensional cell culture. *Angle Orthod, 77*(4), 716-722. doi: 10.2319/052706-212.1

Verdun, R. E., & Karlseder, J. (2007). Replication and protection of telomeres. *Nature, 447*(7147), 924-931. doi: 10.1038/nature05976

Vescovi, P., Merigo, E., Meleti, M., Manfredi, M., Fornaini, C., & Nammour, S. (2012). Surgical Approach and Laser Applications in BRONJ Osteoporotic and Cancer Patients. *J Osteoporos, 2012*, 585434. doi: 10.1155/2012/585434

Vitte, C., Fleisch, H., & Guenther, H. L. (1996). Bisphosphonates induce osteoblasts to secrete an inhibitor of osteoclast-mediated resorption. *Endocrinology, 137*(6), 2324-2333. doi: 10.1210/endo.137.6.8641182

von Zglinicki, T., Saretzki, G., Docke, W., & Lotze, C. (1995). Mild hyperoxia shortens telomeres and inhibits proliferation of fibroblasts: a model for senescence? *Exp Cell Res, 220*(1), 186-193. doi: 10.1006/excr.1995.1305

Wang, L., Yang, L., Debidda, M., Witte, D., & Zheng, Y. (2007). Cdc42 GTPase-activating protein deficiency promotes genomic instability and premature aging-like phenotypes. *Proc Natl Acad Sci U S A, 104*(4), 1248-1253. doi: 10.1073/pnas.0609149104

Wang, S., Moerman, E. J., Jones, R. A., Thweatt, R., & Goldstein, S. (1996). Characterization of IGFBP-3, PAI-1 and SPARC mRNA expression in senescent fibroblasts. *Mech Ageing Dev, 92*(2-3), 121-132.

Wellinger, R. J. (2010). When the caps fall off: responses to telomere uncapping in yeast. *FEBS Lett, 584*(17), 3734-3740. doi: 10.1016/j.febslet.2010.06.031

Werner, S., Smola, H., Liao, X., Longaker, M. T., Krieg, T., Hofschneider, P. H., & Williams, L. T. (1994). The function of KGF in morphogenesis of epithelium and reepithelialization of wounds. *Science, 266*(5186), 819-822.

Whitaker, M., Guo, J., Kehoe, T., & Benson, G. (2012). Bisphosphonates for osteoporosis--where do we go from here? *N Engl J Med, 366*(22), 2048-2051. doi: 10.1056/NEJMp1202619

Woo, S. B., Hellstein, J. W., & Kalmar, J. R. (2006). Narrative [corrected] review: bisphosphonates and osteonecrosis of the jaws. *Ann Intern Med, 144*(10), 753-761.

Wright, W. E., Piatyszek, M. A., Rainey, W. E., Byrd, W., & Shay, J. W. (1996). Telomerase activity in human germline and embryonic tissues and cells. *Dev Genet, 18*(2), 173-179. doi: 10.1002/(SICI)1520-6408(1996)18:2<173::AID-DVG10>3.0.CO;2-3

Xue, W., Zender, L., Miething, C., Dickins, R. A., Hernando, E., Krizhanovsky, V., . . . Lowe, S. W. (2007). Senescence and tumour clearance is triggered by p53 restoration in murine liver carcinomas. *Nature, 445*(7128), 656-660. doi: 10.1038/nature05529

Yadev, N. P., Murdoch, C., Saville, S. P., & Thornhill, M. H. (2011). Evaluation of tissue engineered models of the oral mucosa to investigate oral candidiasis. *Microb Pathog, 50*(6), 278-285. doi: 10.1016/j.micpath.2010.11.009

Yang, G., Rosen, D. G., Mercado-Uribe, I., Colacino, J. A., Mills, G. B., Bast, R. C., Jr., . . . Liu, J. (2007). Knockdown of p53 combined with expression of the catalytic subunit of telomerase is sufficient to immortalize primary human ovarian surface epithelial cells. *Carcinogenesis, 28*(1), 174-182. doi: 10.1093/carcin/bgl115

Yang, N. C., & Hu, M. L. (2005). The limitations and validities of senescence associated-beta-galactosidase activity as an aging marker for human foreskin fibroblast Hs68 cells. *Exp Gerontol, 40*(10), 813-819. doi: 10.1016/j.exger.2005.07.011

Yasuda, H., Shima, N., Nakagawa, N., Yamaguchi, K., Kinosaki, M., Mochizuki, S., . . . Suda, T. (1998). Osteoclast differentiation factor is a ligand for osteoprotegerin/osteoclastogenesis-inhibitory factor and is identical to TRANCE/RANKL. *Proc Natl Acad Sci U S A, 95*(7), 3597-3602.

Yoshinari, M., Oda, Y., Inoue, T., Matsuzaka, K., & Shimono, M. (2002). Bone response to calcium phosphate-coated and bisphosphonate-immobilized titanium implants. *Biomaterials, 23*(14), 2879-2885.

Young, A. R., & Narita, M. (2009). SASP reflects senescence. *EMBO Rep, 10*(3), 228-230. doi: 10.1038/embor.2009.22

Yuh, D. Y., Chang, T. H., Huang, R. Y., Chien, W. C., Lin, F. G., & Fu, E. (2014). The national-scale cohort study on bisphosphonate-related osteonecrosis of the jaw in Taiwan. *J Dent, 42*(10), 1343-1352. doi: 10.1016/j.jdent.2014.05.001

Zambruno, G., Marchisio, P. C., Marconi, A., Vaschieri, C., Melchiori, A., Giannetti, A., & De Luca, M. (1995). Transforming growth factor-beta 1 modulates beta 1 and beta 5 integrin receptors and induces the de novo expression of the alpha v beta 6 heterodimer in normal human keratinocytes: implications for wound healing. *J Cell Biol, 129*(3), 853-865.

Zhong, W. B., Liang, Y. C., Wang, C. Y., Chang, T. C., & Lee, W. S. (2005). Lovastatin suppresses invasiveness of anaplastic thyroid cancer cells by inhibiting Rho geranylgeranylation and RhoA/ROCK signaling. *Endocr Relat Cancer, 12*(3), 615-629. doi: 10.1677/erc.1.01012

Ziebart, T., Koch, F., Klein, M. O., Guth, J., Adler, J., Pabst, A., . . . Walter, C. (2011). Geranylgeraniol - a new potential therapeutic approach to bisphosphonate associated osteonecrosis of the jaw. *Oral Oncol, 47*(3), 195-201. doi: 10.1016/j.oraloncology.2010.12.003

LIST OF PUBLICATIONS AND PAPERS PRESENTED

1. Poster Presentation title An *in vitro* Organotypic Oral Mucosal Equivalent Constructed by Co-Culturing of Immortalized Oral Keratinocytes OKF-6 and Human Oral Fibroblast on Acellular Dermis: Presented in 15th Annual Scientific Meeting & 17th Annual General Meeting Malaysian Section IADR (15 February 2016)

APPENDICES

APPENDIX A – PREPARATION OF REAGENT/CULTURE MEDIA

Appendix A 1: Preparation of Complete Dulbecco's Modified Eagle Medium (cDMEM)

For every 500ml of high glucose (4.5g/l) Dulbecco modified Eagle medium (DMEM) (Gibco, Thermo Fischer Scientific Company, Waltham, USA), it was supplemented with:

- 10% v/v of fetal bovine serum (FBS) (Gibco, Thermo Fischer Scientific Company, Waltham, USA)

- 5ml of Glutamax 2mM (Gibco, Thermo Fischer Scientific Company, Waltham, USA)

- 1ml of 100 units/ml penicillin and 100 ug/ml streptomycin (Gibco, Thermo Fischer Scientific Company, Waltham, USA)

Appendix A 2: Preparation of Keratinocytes-Serum Free Medium

For every 500ml of high glucose (4.5g/l) Dulbecco modified Eagle medium (DMEM) (Gibco, Thermo Fischer Scientific Company, Waltham, USA), it was supplemented with:

- 30µg/ml of bovine pituitary extract, (BPE) (Gibco, Thermo Fischer Scientific Company, Waltham, USA)

- 0.8ml of 100 units/ml penicillin and 100 ug/ml streptomycin (Gibco, Thermo Fischer Scientific Company, Waltham, USA)

- 0.1ng/ml of epidermal growth factor (EGF) (Gibco, Thermo Fischer Scientific Company, Waltham, USA)

- 0.4mM of calcium chloride (Sigma Aldrich Company, Ayrshire, UK)

Appendix A 3: Preparation of Growth Media (Submerge-3D culture)

For every 100ml of keratinocytes serum free media (K-SFM) it was supplemented with:

- 30μg/ml of bovine pituitary extract, (BPE) (Gibco, Thermo Fischer Scientific Company, Waltham, USA)

- 1 ml of 100 units/ml penicillin and 100 ug/ml streptomycin (Gibco, Thermo Fischer Scientific Company, Waltham, USA)

- 1ng/ml of epidermal growth factor (EGF) (Gibco, Thermo Fischer Scientific Company, Waltham, USA)

- 0.4mM of calcium chloride (Sigma Aldrich Company, Ayrshire, UK)

Appendix A 4: Preparation of Growth Media (Air-Liquid Interface-3D culture)

For every 100ml of keratinocytes serum free media (K-SFM) it was supplemented with:

- 4ng/ml of epidermal growth factor (EGF) (Gibco, Thermo Fischer Scientific Company, Waltham, USA)

- 0.025mM Glucose (Sigma Aldrich Company, Ayrshire, UK)

- 30 µg/ml of bovine pituitary extract, (BPE) (Gibco, Thermo Fischer Scientific Company, Waltham, USA)

- 3mM of calcium chloride (Sigma Aldrich Company, Ayrshire, UK)

- 5% v/v of fetal bovine serum (FBS) ((Gibco, Thermo Fischer Scientific Company, Waltham, USA)

- 10^{-8}M all transretinoic acid (Sigma Aldrich Company, Ayrshire, UK)

Appendix A 5: Preparation of Zoledronic Acid and 5 aza CDR Stock

Zoledronic Acid (1000x)

10 mg of ZOL mixed in 207µl of NaOH (0.1N) then make it up to 3.45ml of distilled water. Sterile filter and aliquot to 1ml/tube.Keep at -20˚C

5 aza CDR (1000x)

5mg of 5 aza CDR mixed with 438µl DMSO then make it up to 7.3ml of distilled water. Sterile filter and aliquot to 20µl/tube.Keep at -20˚C

APPENDIX B-PROTOCOL AND PILOT STUDY

Appendix B 1: Cell Freezing and Thawing

Freezing cells was performed in freezing media containing 90% FBS and 10% DMSO (Sigma-Aldrich Company, Ayrshire, UK) at a density of 1 x 10^6 cells/ml. Frozen cells were kept in Mr Frosty ™ (Nalgene, Thermo Fisher Scientific) at -80°C overnight before transferring to a liquid nitrogen tank for long-term storage. Upon thawing, frozen cells between passages 2 to 4 (for primary normal human oral fibroblasts) were thawed, resuspended in 5-10ml culture media gently and centrifuged for 1000 rpm for 5 minutes. The cell pellet was resuspended in culture media to a desired total number of cells and plated into a T-75 flask. Culture media was changed after 24-48 hours depending on the percentage of cells that had attached onto the flasks

Appendix B 2: Analysis of Seeding Density Optimization for OKF 6/TERT 2 and NHOF cells

Raw data: OKF 6/TERT 2

	Day 1	Day 2	Day 3	Day 4	Day 5	Equation	Growth rate (absorbance/day)
7813 cells/cm^2	0.0155	0.0226	0.0479	0.1242	0.0675	y = 0.0206x - 0.0061	0.0206
15,625 cells/cm^2	0.0182	0.0359	0.0623	0.1217	0.1237	y = 0.0297x -0.0167	0.0297
31,250 cells/cm^2	0.0413	0.0656	0.0774	0.1695	0.1353	y = 0.0292x + 0.0103	0.0292
62,500 cells/cm^2	0.0776	0.127	0.1902	0.2458	0.1417	y = 0.0247x + 0.0824	0.0247
125,000 cells/cm^2	0.1011	0.1745	0.1638	0.2476	0.1531	y = 0.0177x + 0.1149	0.0177
250,000 cells/cm^2	0.171	0.2332	0.1734	0.1869	0.2268	y = 0.0065x + 0.1787	0.0065

Raw data: NHOF cells

	Day 1	Day 3	Day 5	Day 7	Equation	Growth rate (absorbance/day)
300 cells/cm^2	0.0105	0.0115	0.0152	0.0629	y = 0.0161x - 0.0152	0.0161
600 cells/cm^2	0.0115	0.0175	0.0365	0.1707	y = 0.0497x - 0.0651	0.0497
1200 cells/cm^2	0.0174	0.0205	0.0797	0.2989	y = 0.0904x - 0.1218	0.0904
2400 cells/cm^2	0.0186	0.0385	0.1794	0.4503	y = 0.1436x - 0.1873	0.1436
4800 cells/cm^2	0.0332	0.0898	0.3298	0.5008	y = 0.1643x - 0.1723	0.1643
9600 cells/cm^2	0.06	0.2072	0.4631	0.4803	y = 0.1517x - 0.0765	0.1517

Appendix B 3: Validation of 5 aza CDR Treatment on OKF 6/TERT 2 cells by Co-Staining S-A-β Galactosidase and Immunofluorescence Detection of p15/p16

Based on confirmation of senescence activity due treatment 5 aza CDR in published study(Timmermann et al., 1998), in this project we validated this treatment on OKF 6/TERT 2 cells before further used as positive control. To confirm presence of senescence, S-A-β gal assay was co-stain with detection of p15/p16 (H43, mouse monoclonal IgG_1 200ug/ml; Clone V9, Santa Cruz Biotechnology, Inc with <0.1% sodium azide and 0.1% gelatin) by immunofluorescence. Cells were plated on glass coverslips (22mm x 22mm) in 6 well plates at 1,000 cells/well for 24 hours before treated with 3µM 5 aza CDR for 48 hours. After treatment, cells were washed, fixed and stained for S-A-β gal activity. Cells were washed with PBS twice after blue color is developed. Cells were permeabilized with 0.5% Triton X-100 for 5 minutes before proceed with blocking, incubation with primary antibody at 1:100 overnight at 4˚C. Coverslips were washed five times with PBS and incubated for 1 hour at room temperature with 1:75

dilution of FITC-conjugated bovine anti-mouse IgG (Santa Cruz Biotechnology, Inc) diluted in the same buffer used for the first antibody. To visualize the nucleus, Fluoroshield™ with DAPI (Sigma Aldrich Company, Ayrshire, UK) was mounted to the coverslip. Images were acquired with a Leica DMI3000 B inverted micorscope with fluorescence (Leica Microsystem,Germany) using 20x magnification (Figure 7.1) .
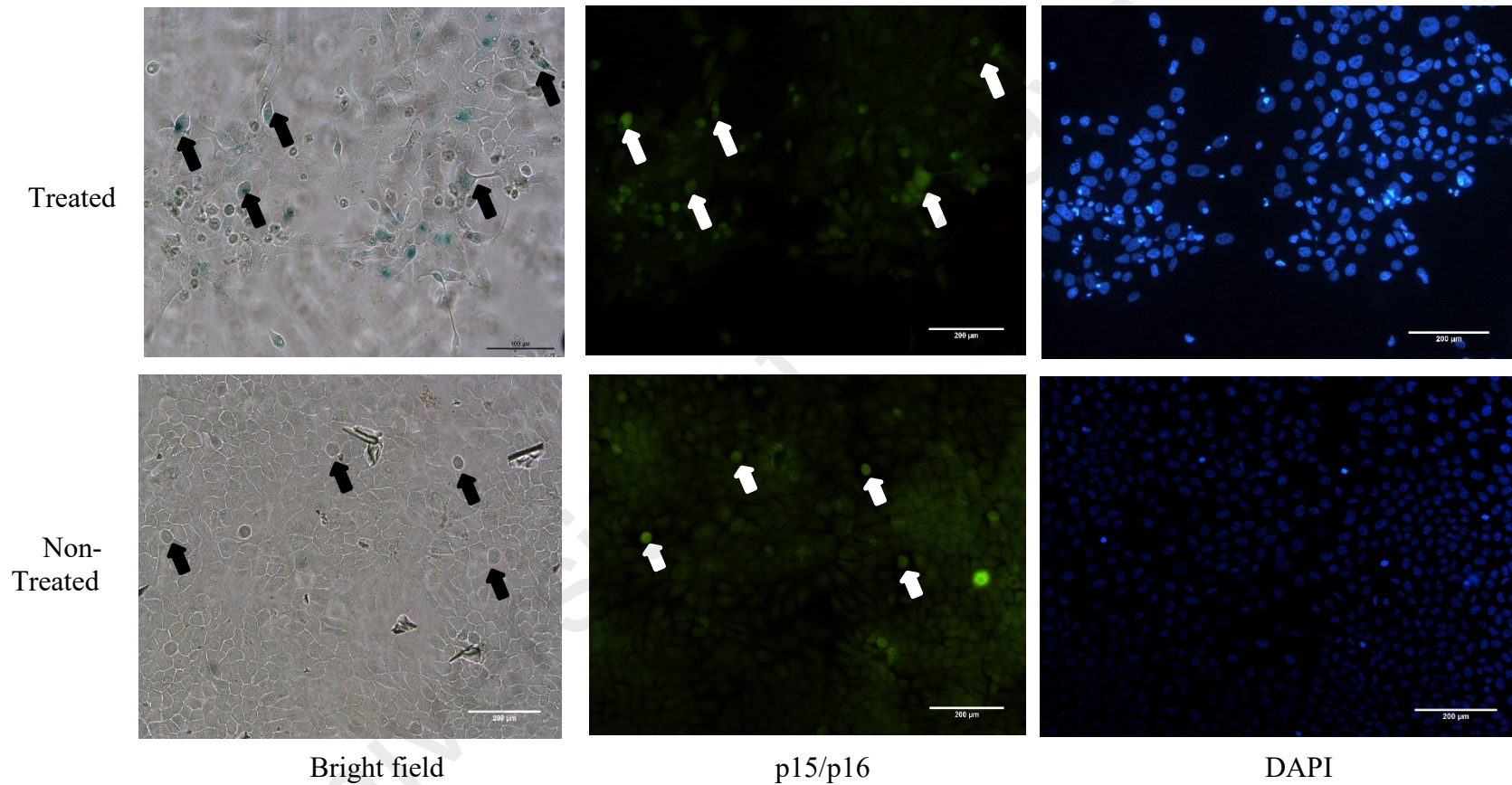
Figure 6.1: SA-β gal staining, DAPI staining and immunostaining of cultured cell. Strong p15/p16 expression was correlated with S-A-β gal and higher DAPI staining. on treated cells. This shows OKF 6/TERT 2 can undergo senescence with re-expression of p15/p16 protein, hence can be used as positive control.

Appendix B 4: Protocol MTT Viability Assay

To optimize seeding density, a modified protocol of MTT viability assay was performed Culture media was aspirated out and diluted MTT reagent (5 mg/ml) was added into the well. After 4 hours of incubation, culture fluid was removed and DMSO (MTT solvent) was added in an amount equal to the original culture volume (200ul). MTT formazan crystals were dissolved with gentle stirring before absorbance reading within 1 hour.

Appendix B 5: Determination of IC50 using F-test Curve Analysis on Dose Response Curve

Normal Human Oral Fibroblast

log(inhibitor) vs. normalized response -- Variable slope			
Best-fit values			
LogIC50	2.544	1.707	1.200
HillSlope	-2.031	-0.6813	-1.128
IC50	349.9	50.93	15.86
Std. Error			
LogIC50	0.05113	0.1102	0.03710
HillSlope	0.4720	0.1136	0.09794
95% Confidence Intervals			
LogIC50	2.437 to 2.651	1.476 to 1.938	1.123 to 1.278
HillSlope	-3.018 to -1.043	-0.9190 to -0.4436	-1.333 to -0.9234
IC50	273.4 to 447.6	29.95 to 86.62	13.26 to 18.97
Goodness of Fit			
Degrees of Freedom	19	19	19
R²	0.8924	0.8493	0.9772
Absolute Sum of Squares	2328	3529	683.3
Sy.x	11.07	13.63	5.997
log(agonist) vs. normalized response -- Variable slope			
Best-fit values			
LogEC50	2.544	1.707	1.200
HillSlope	-2.031	-0.6813	-1.128
EC50	349.9	50.93	15.86 ←
Std. Error			
LogEC50	0.05113	0.1102	0.03710
HillSlope	0.4720	0.1136	0.09794
95% Confidence Intervals			
LogEC50	2.437 to 2.651	1.476 to 1.938	1.123 to 1.278
HillSlope	-3.018 to -1.043	-0.9190 to -0.4436	-1.333 to -0.9234
EC50	273.4 to 447.6	29.95 to 86.62	13.26 to 18.97
Goodness of Fit			
Degrees of Freedom	19	19	19
R²	0.8924	0.8493	0.9772
Absolute Sum of Squares	2328	3529	683.3
Sy.x	11.07	13.63	5.997
Number of points			
Analyzed	21	21	21

OKF 6/TERT 2 cell lines

Nonlin fit		A	B	C
		24 hours	48 hours	72 hours
		Y	Y	Y
1	log(inhibitor) vs. normalized response -- Variable sl			
2	Best-fit values			
3	LogIC50	0.9990	1.093	-0.001961
4	HillSlope	-0.5059	-0.4297	-0.7456
5	IC50	9.978	12.38	0.9955
6	Std. Error			
7	LogIC50	0.1054	0.2319	0.1079
8	HillSlope	0.06441	0.1097	0.1270
9	95% Confidence Intervals			
10	LogIC50	0.7804 to 1.218	0.6116 to 1.573	-0.2258 to 0.2219
11	HillSlope	-0.6394 to -0.3723	-0.6571 to -0.2022	-1.009 to -0.4821
12	IC50	6.031 to 16.51	4.089 to 37.45	0.5945 to 1.667
13	Goodness of Fit			
14	Degrees of Freedom	22	22	22
15	R²	0.8910	0.6247	0.8792
16	Absolute Sum of Squares	2593	10326	2957
17	Sy.x	10.86	21.66	11.59
18	Number of points			
19	Analyzed	24	24	24

Appendix B 6: Epithelial Thickness Analysis

Raw Data

Non-Treated (µm)	Positive Control (µm)	12µM (µm)
27.91	4.48	10.61
14.29	7.46	11.92
21.75	4.31	20.42
9.37	12.32	11.14
12.46	6.22	18.53
29.17	10.46	11.94
22.99	23.55	18.08
23.06	14.89	18.69
34.11	13.54	12.41
21.85	9.91	8.66
31.83	11.23	22.22
27.87	3.64	16.66

Statistical Analysis

	Data Set-A	Data Set-B	Data Set-C	Data Set-D	Data Set-E
Table Analyzed	Epithelial thickness				
One-way analysis of variance					
P value	< 0.0001				
P value summary	***				
Are means signif. different? (P < 0.05)	Yes				
Number of groups	3				
F	16.45				
R squared	0.4918				
Bartlett's test for equal variances					
Bartlett's statistic (corrected)	5.013				
P value	0.0815				
P value summary	ns				
Do the variances differ signif. (P < 0.05)	No				
ANOVA Table	SS	df	MS		
Treatment (between columns)	1028	2	514.0		
Residual (within columns)	1062	34	31.25		
Total	2090	36			
Tukey's Multiple Comparison Test	Mean Diff.	q	Significant? P < 0.05?	Summary	95% CI of diff
CTL vs 5 aza CDR	12.66	8.000	Yes	***	7.171 to 18.15
CTL vs 12uM	7.936	5.015	Yes	**	2.448 to 13.42
5 aza CDR vs 12uM	-4.723	2.926	No	ns	-10.32 to 0.8745

Appendix B 7: Analysis of ELISA

Standard curve for each cytokines (IL-8 and MMP-3) was generated by plotting the log of concentration versus log of O.D value on linear scale, and best fit line was determined by regression analysis. All samples were duplicated. One way ANNOVA statistical analyses was performed.

(pg/ml)	O.D value		Average	Corrected
0	0.0097	0.0097	0.0097	0
31.25	0.0637	0.0515	0.0576	0.0479
62.5	0.0979	0.1028	0.10035	0.09065
125	0.2372	0.2368	0.237	0.2273
250	0.2779	0.3312	0.30455	0.29485
500	0.8072	0.6991	0.75315	0.74345
1000	1.3327	1.0185	1.1756	1.1659
2000	1.7704	1.7513	1.76085	1.75115

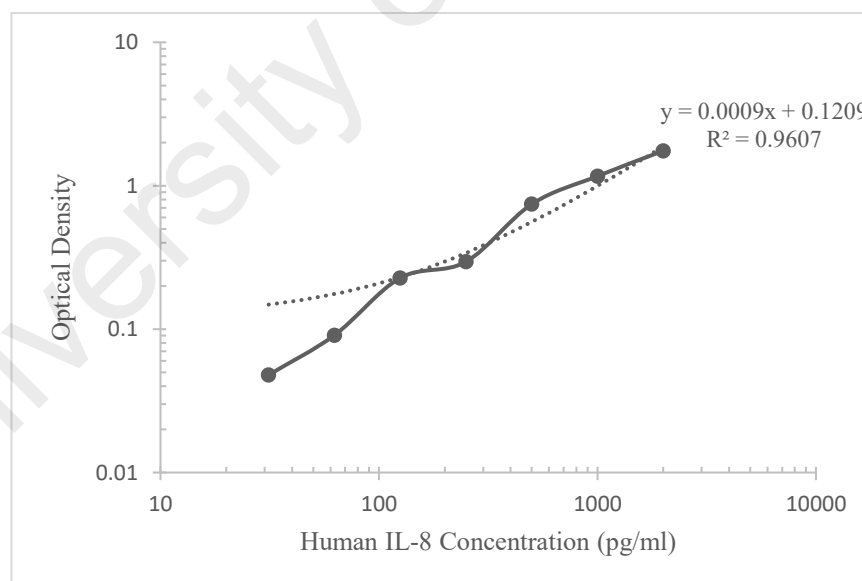$y = 0.0009x + 0.1209$
$R^2 = 0.9607$

Figure 6.2: A standard curve generated for IL-8 with R-squared value 96.07% with raw data tabulated above. Value are corrected by subtract the average zero standard optical density.

ng/ml	OD		Average	Corrected
0	0.0104	0.0104	0.0104	0
0.156	0.0083	0.011	0.00965	-0.00075
0.313	0.0119	0.0146	0.01325	0.00285
0.625	0.0195	0.0255	0.0225	0.0121
1.25	0.0455	0.0669	0.0562	0.0458
2.5	0.1178	0.1552	0.1365	0.1261
5	0.287	0.4053	0.34615	0.33575
10	1.1571	0.7423	0.9497	0.9393
100	2.3505	3.8968	3.12365	3.11325

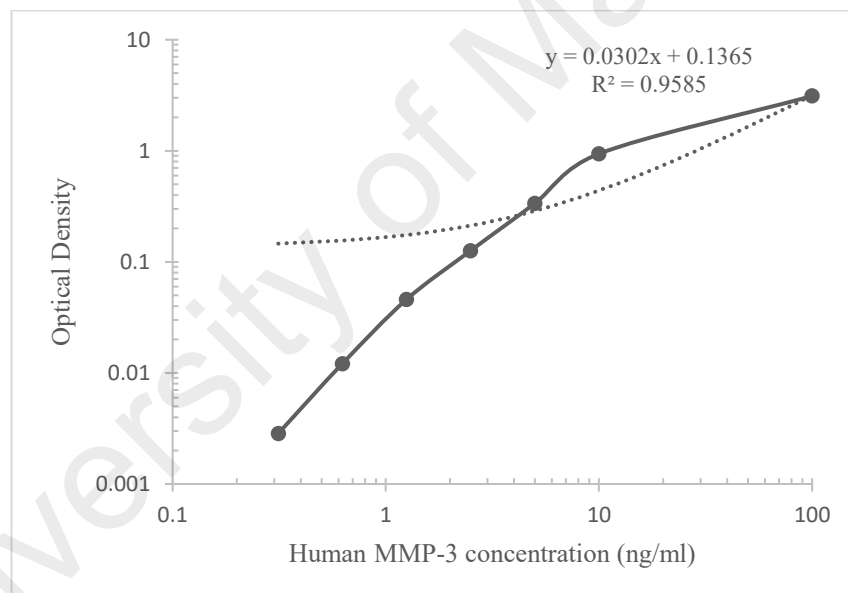$y = 0.0302x + 0.1365$
$R^2 = 0.9585$

Figure 6.3: A standard curve generated for MMP-3 with R-squared value 95.85% with raw data tabulated above. Value are corrected by subtract the average zero standard optical density.

Table 6.1: Sample data was deduced from model generated by standard curve y=0.0009x + 0.1209

Variables	Average OD value	Corrected	Concentration (pg/ml)	Standard deviation
Non-treated	2.1337	2.1337	2236.44	25.455
12 μM	3.194	3.1940	3414.56	94.28
Positive Control	3.3336	3.3336	3569.67	50.44

Table 6.2: Sample data was deduced from model generated by standard curve y=0.0302x + 0.1365

Variables	Average OD value	Corrected	Concentration (pg/ml)	Standard deviation
Non-treated	0.2780	0.2780	4.3400	0.5151
12 μM	0.3564	0.3507	7.0911	0.2693
Positive Control	0.5290	0.5290	12.8940	0.4308

Table 6.3: One way ANNOVA analysis of IL-8 cytokines

Table Analyzed	IL-8				
One-way analysis of variance					
P value	0.0004				
P value summary	***				
Are means signif. different? (P < 0.05)	Yes				
Number of groups	3				
F	264.0				
R squared	0.9944				
ANOVA Table	SS	df	MS		
Treatment (between columns)	2126000	2	1063000		
Residual (within columns)	12080	3	4027		
Total	2138000	5			
Tukey's Multiple Comparison Test	Mean Diff.	q	Significant? P < 0.05?	Summary	95% CI of diff
0uM vs 12uM	-1178	26.25	Yes	***	-1443 to -912.9
0uM vs 5 aza CDR	-1333	29.71	Yes	***	-1598 to -1068
12uM vs 5 aza CDR	-155.1	3.457	No	ns	-420.3 to 110.1

Table 6.4: One way ANNOVA analysis of MMP-3 cytokines

Table Analyzed	MMP-3				
One-way analysis of variance					
P value	0.0006				
P value summary	***				
Are means signif. different? (P < 0.05)	Yes				
Number of groups	3				
F	204.1				
R squared	0.9927				
ANOVA Table	SS	df	MS		
Treatment (between columns)	71.23	2	35.61		
Residual (within columns)	0.5234	3	0.1745		
Total	71.75	5			
Tukey's Multiple Comparison Test	Mean Diff.	q	Significant? P < 0.05?	Summary	95% CI of diff
0uM vs 12uM	-2.406	8.145	Yes	*	-4.151 to -0.6600
0uM vs 5 aza CDR	-8.209	27.79	Yes	***	-9.954 to -6.463
12uM vs 5 aza CDR	-5.803	19.65	Yes	**	-7.549 to -4.057

Appendix B 8: Repository Form